1-27-2017 12:00 AM

MT1-MMP Mediates the Migratory and Tumourigenic Potential of Breast Cancer Cells via Non-Proteolytic Mechanisms

Mario Cepeda, *The University of Western Ontario*

Supervisor: Dr. Sashko Damjanovski, *The University of Western Ontario*

A thesis submitted in partial fulfillment of the requirements for the Doctor of Philosophy degree in Biology

Abstract

Membrane Type-1 Matrix Metalloproteinase (MT1-MMP) is a multifunctional protease that affects cell function via proteolytic and non-proteolytic mechanisms such as promoting degradation of the extracellular matrix (ECM) or augmentation of cell migration and viability, respectively. MT1-MMP has been implicated in metastatic progression ostensibly due to its ability to degrade ECM components and to allow migration of cells through the basement membrane. Despite *in vitro* studies demonstrating this principle, this knowledge has not translated into the use of MMP inhibitors (MMPi) that inhibit substrate catalysis as effective cancer therapeutics, or been corroborated by evidence of *in vivo* ECM degradation mediated by MT1-MMP, suggesting that our understanding of the role of MT1-MMP in cancer progression is incomplete. To further our understanding of MT1-MMP function, MCF-7 and MDA-MB 231 breast cancer cell lines were created that stably overexpress different levels of MT1-MMP. Using 2D culture, I analyzed proMMP-2 activation (gelatin zymography), ECM degradation (fluorescent gelatin), ERK signaling (immunoblot), cell migration (transwell/scratch closure/time-lapse imaging), and viability (colorimetric substrate) to assess how different MT1-MMP levels affect these cellular parameters. Matrigel 3D cell culture and avian embryos were also utilized to examine how different levels of MT1-MMP expression affect morphological changes in 3D culture, and tumourigenicity and extravasation efficiency *in vivo.* In 2D culture, breast cancer cells expressing high levels of MT1-MMP were capable of widespread ECM degradation and TIMP-2-mediated proMMP-2 activation, but were not the most migratory. Instead, cells expressing low levels of MT1-MMP were the most migratory, and demonstrated increased viability and ERK activation. In 3D culture, MCF-7 breast cancer cells expressing low

levels of MT1-MMP demonstrated an invasive protrusive phenotype, whereas cells expressing high levels of MT1-MMP demonstrated loss of colony structure and cell fragment release. Similarly, *in vivo* analysis demonstrated increased tumourigenicity and metastatic capability for cells expressing low levels of MT1-MMP, whereas cells expressing high levels were devoid of these qualities despite the production of functional MT1-MMP protein. This study demonstrates that excessive ECM degradation mediated by high levels of MT1-MMP is not associated with cell migration and tumourigenesis, while low levels of MT1-MMP promote invasion and vascularization *in vivo*.

Keywords

Matrix Metalloproteinases, MMP-14, Cell migration, 3D culture, Breast cancer, Intravital imaging

Acknowledgments

Firstly, I would like to thank my supervisor, Dr. Sashko Damjanovski, for his unwavering support over the past 8 years. During this time, Sash was a mentor and a father figure, inside and outside of the lab. I am extremely thankful for my experience in the Sash Lab, and it will always hold a special place in my heart. I would also like to thank Dr. Hon Leong for his limitless generosity, mentorship and opportunities that he has provided me. I am truly excited of what we can accomplish in the future. I would also like to thank Dr. Greg Kelly and Dr. Robert Cumming for providing resources, guidance, and critical assessment of my work throughout my time at Western.

I would like to acknowledge and thank all the senior graduate students that mentored me, graduate students and 4999s that I was lucky enough to mentor, and work-studies that I got to boss around. I shared casual, personal, serious, hilarious, embarrassing, and touching moments with all of you that I will always cherish and that made me into a better man, friend, and teacher.

I also want to thank my parents for allowing me to embrace the opportunities I was given in this country, and I am eternally grateful for the sacrifices they made to immigrate to Canada. I would also like to thank my beautiful wife-to-be Leanne Sandieson, for being my rock, my best friend, and for all the support and love you have given me throughout this journey; and also thanks to our awesome cat, CleoPAWtra, for being amazing.

Lastly I want to thank my Grandmother, Abuelita Meme. Everything good of me is only a reflection of the love and care you gave me since I was born until I was a young man. Thank you for always watching over me, and I will continue to make you proud.

Table of Contents

List of Figures

List of Abbreviations

ADAPT	Automated detection and analysis of protrusions
ADH	Atypical ductal hyperplasia
Akt	Protein kinase B
ANOVA	Analysis of variance
APMA	Aminophenylmercuric acetate
ATP	Adenosine triphosphate
BM	Basement membrane
BSA	Bovine serum albumin
CAM	Chorioallantoic membrane
CD-44	Cluster of differentiation-44
cDNA	Complementary deoxyribonucleic acid
CM	Conditioned media
DAPI	4’,6-diamidino-2-phenylindole
DCIS	Ductal carcinoma in situ
DIC	Differential interference contrast
DMEM	Dulbecco’s Modified Eagles Medium
DMSO	Dimethyl sulfoxide
ECM	Extracellular matrix
ERK	Extracellular regulated kinase
F-actin	Filamentous actin
FBS	Fetal bovine serum
FGF	Fibroblast growth factor

FIH	Factor inhibiting HIF-1α
GAPDH	Glyceraldehyde-3-phosphate dehydrogenase
GFP	Green fluorescent protein
GPI	Glycophosphatidylinositol
HIF-1α	Hypoxia inducible factor 1 alpha
HRP	Horseradish peroxidase
IF	Immunofluorescence
IMC	Invasive mammary carcinoma
MAPK	Mitogen activated protein kinase
MCF-7	Michigan Cancer Foundation 7
MDA-MB-231	MD Anderson Metastatic Breast 231
MMP	Matrix metalloproteinase
mRNA	Messenger ribonucleic acid
MT-MMP	Membrane-type matrix metalloproteinase
PBS	Phosphate-buffered saline
pH3	Phospho-histone 3
PS	Peripodial epithelium and stalk
qPCR	Quantitative (real-time) polymerase chain reaction
SDS-PAGE	Sodium dodecyl sulphate polyacrylamide gel electrophoresis
SEM	Standard error of the mean
SF	Serum-free
ShRNA	Short hairpin RNA
TDLU	Terminal duct lobular unit

TIMP	Tissue inhibitor of metalloproteinases
ZsGreen	Zoanthus species green

Chapter 1

1 Introduction

1.1 Cancer Metastasis

Cancer, the collection of related diseases involving uncontrollable cell growth and spread of abnormal cells in the body, is still a major health problem worldwide despite the progress made towards reducing its incidence and improving the survival rates of patients [1]. Almost half of all Canadians will develop cancer in their lifetime, and as such it is the leading cause of death in Canada followed by cardiovascular disease and respiratory illness [2]. There were about 100,000 new cancer cases for both genders in 2015, with prostate cancer having the highest incidence in males (23.9%), and breast cancer in females (25.9%) [3]. Beyond the personal costs afforded by those directly and indirectly affected, cancer also poses a major economic burden on the Canadian healthcare system, by one estimate costing $3.8 billion in direct healthcare costs in 2008 [4].

Metastasis formation, which is defined as the ability of cancer cells to spread to distant organs, is responsible for more than 90% of cancer-associated deaths [5]. Metastasis progression is an extremely complex and multifunctional process whereby cancer cells separate from the primary tumours and disseminate to distant anatomical sites, via the vascular or lymphatic system, where they proliferate and form secondary tumours [6]. The progression to metastatic disease occurs in stages characterized by differential regulation of adhesive interactions and migratory events, and interactions with non-cancerous cells of the stroma and chemotactic factors [7]. The stages of metastasis include: development of new blood vessels (angiogenesis);

the ‘dissemination’ of cancer cells from the primary tumour; migration through the extracellular matrix (ECM) surrounding the epithelium; invasion of the basement membrane (BM) underlying the endothelium of local blood and/or lymphatic vessels (intravasation); transit in the blood/lymphatic system; arrest and adhesion of the circulating tumour cells to the endothelium of capillaries at the target organ site; invasion through the endothelial cell layer and surrounding BM (extravasation); and adaption and growth of secondary tumours at the target organ site **(fig 1a)** [8-10].

1.2 Traversing the ECM and the Role of Matrix Metalloproteinases

During the multiple stages of metastasis progression, particularly during intravasation and extravasation, tumour cells must physically traverse the impeding ECM to enter/exit the circulatory system [11]. The ECM is the heterogeneous non-cellular components of tissues composed of a network of proteins, glycoproteins, and proteoglycans that includes collagen, elastin, and fibronectin, amongst others [12]. The role of the ECM is to provide structural support and modulate cell-signaling cascades via cell surface receptors, predominantly the integrins [13], to properly compartmentalize tissues while regulating cell fate and function [14-17]. Structurally, the ECM can be separated into two types: the interstitial ECM found in connective tissue, and the basement membrane (BM) underlying tissue epithelia and endothelia of vessels [18]. The BM is a thin, dense and highly cross-linked ECM composed of an interwoven mixture of type IV collagen, laminins, nidogen and sulfated proteoglycans beneath the epithelia and endothelia that surrounds muscles, nerves, adipocytes and smooth muscle cells **(fig 1a, Pre-Cancer)** [19]. The ECM in animals can be a highly dynamic structure depending on developmental stage and tissue location, and as such requires active remodeling of ECM components by proteolytic degradation or deposition by local epithelial and stromal cells.

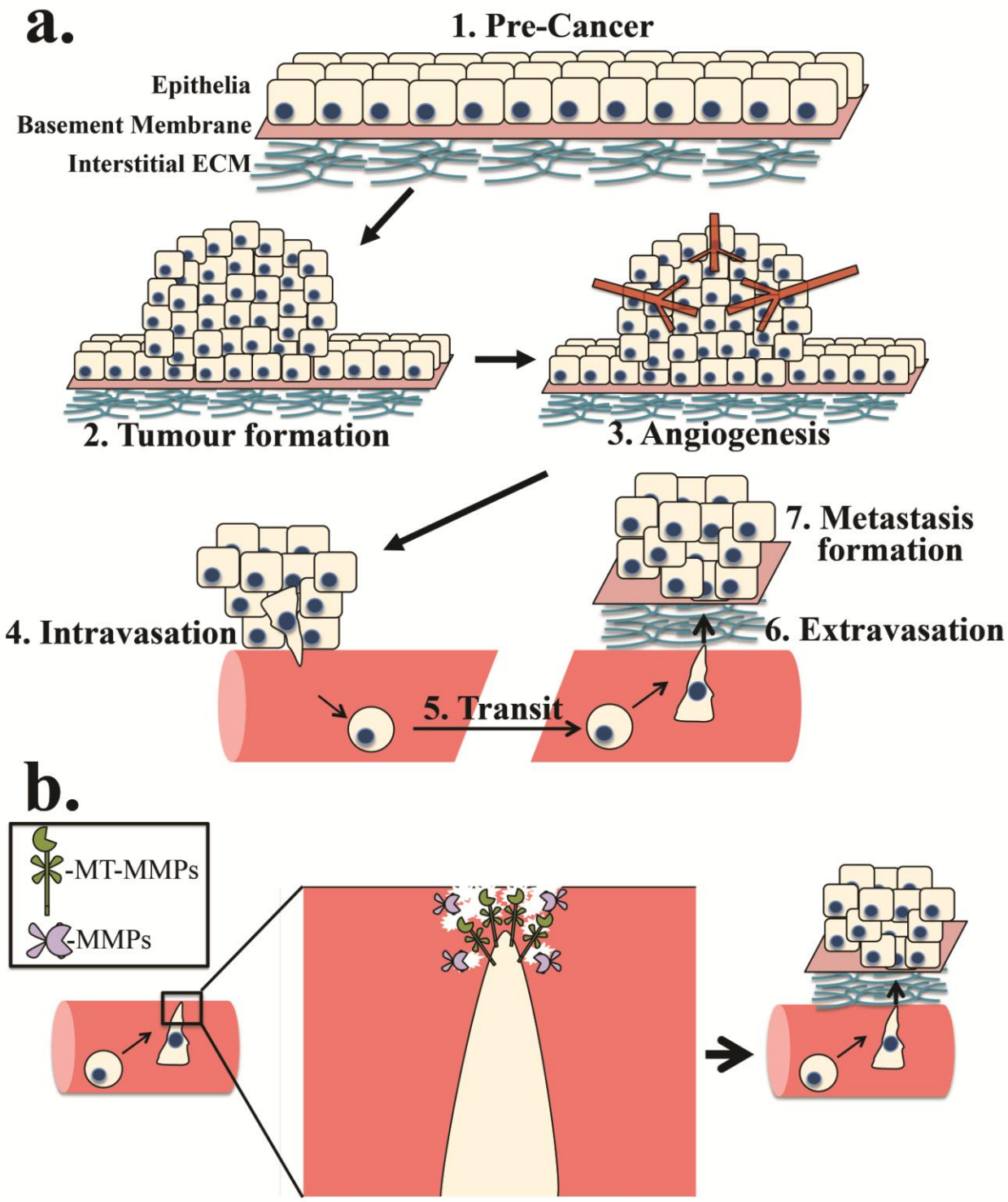
a.
1. Pre-Cancer
Epithelia
Basement Membrane
Interstitial ECM
2. Tumour formation
3. Angiogenesis
7. Metastasis formation
4. Intravasation
6. Extravasation
5. Transit
b.
-MT-MMPs
-MMPs

Figure 1. The Matrix Metalloproteinases (MMPs) are thought to function as ECM remodelers during metastasis formation.

a) Shown is a schematic depicting the process of metastasis of tumour cells derived from an epithelial cancer. During Pre-cancer (1) there is an organized layer of epithelial cells that are polarized due to their interaction with the underlying extracellular matrix (ECM). The ECM can be categorized into two types: the basement membrane (BM) that is a thin dense layer underlying epithelia/endothelia, and the interstitial ECM that can be found in connective tissue. During cancer initiation, a carcinogenic mutation occurs that leads to loss of cell cycle control, excessive proliferation and formation of a primary tumour (2) with accompanying tissue disorganization. Due to increasing energetic requirements of the tumour, angiogenesis occurs (3) that allows for vascularization of the tumour and connection to the circulatory system. A subpopulation of tumour cells will gain the ability to transverse the local ECM and BM to enter the vascular or lymphatic circulation (intravasation, 4) where they can travel to distant anatomical sites (5). Cells that survive transit in the circulation can then arrest at the capillary beds of target organs and exit the circulation (extravasation, 6), transverse the local ECM and BM, and adapt at the secondary site to eventually form a metastases (7). **b)** The Matrix Metalloproteinases (MMPs) are a family of secreted and membrane-type (MT-MMP) proteases that can collectively cleave all components of the ECM. The predominant role of MMPs during metastasis formation is thought to be as ECM remodelers, which is shown in the diagram during the process of extravasation. Excessive MMP activity of cancer cells is thought to allow them to traverse the BM of circulatory vessels and local tissue prior to metastasis formation at the secondary site.

The degradation of ECM components is predominantly mediated by the Matrix MetalloProteinases (MMPs), which are a family of zinc-dependent endopeptidases that can collectively cleave all components of the ECM [20]. Originally, the MMPs were divided into collagenases, gelatinases, stromelysins and matrilysins based on their substrate specificity for components of the ECM [21]. However, it is now known that the MMPs can cleave much more than ECM components including cell surface receptors, latent ligands, cell adhesion molecules, and intracellular proteins [22-24]. Due to the continually growing list of MMP substrates, the current classification for MMPs is rather a sequential numbering system that reflects common structural features **(fig 2)**. There are six distinct structural classes of MMPs: three are secreted (typical, gelatin binding, and minimal) and three are membrane-type MMPs (MT-MMPs – type I, type II, and GPI anchored) [25]. Structurally, the 'typical' secreted MMPs (MMP-1, -3, -8, -10, -11, -12, -13, -18, -19, -20 -22, -27, -28) are composed of: an N-terminal signal sequence that directs them for secretion; a pro-domain that inhibits catalytic activity until it is proteolytically removed (MMP activation); a catalytic domain with zinc-dependent endopeptidase activity; a flexible hinge region; and a hemopexin domain that is responsible for substrate specificity, dimerization, and protein-protein interactions. The 'minimal' type of secreted MMPs (MMP-7, -26) are distinct in that they lack a hinge and hemopexin domain, whereas the 'gelatin binding' type (MMP-2, -9) have fibronectin and collagen-like protein domain between the catalytic and hemopexin domains. In addition to the aforementioned domains, type-I MT-MMPs (MMP-14, -15, -16, -24), the most common of the MT-MMPs, contains a transmembrane and short cytoplasmic domain. Type II MT-MMPs (MMP-23) contains a cysteine array and IgG-like domain in place of the hemopexin and transmembrane domains, and GPI-anchored MT-MMPs

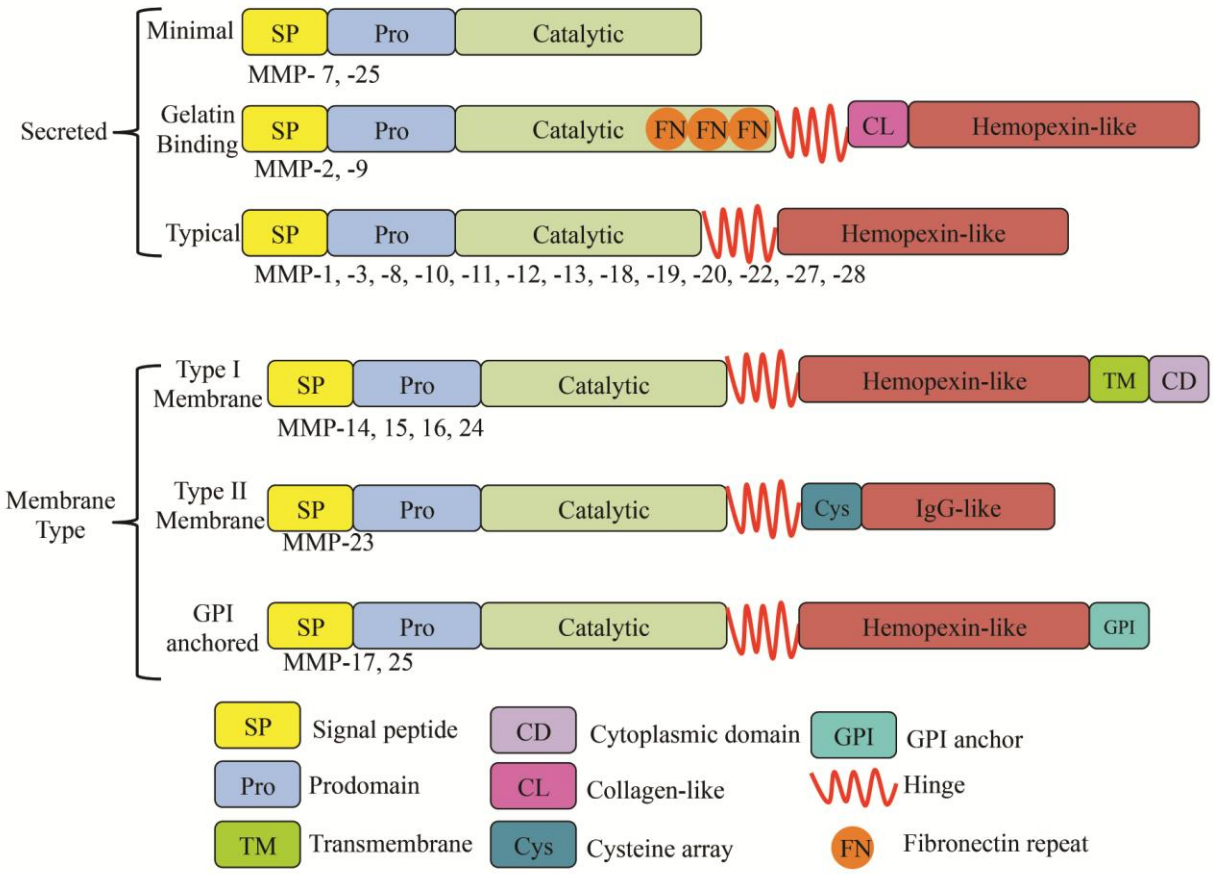
Secreted
Minimal
SP
Pro
Catalytic
MMP- 7, -25
Gelatin Binding
SP
Pro
Catalytic
FN FN FN
CL
Hemopexin-like
MMP-2, -9
Typical
SP
Pro
Catalytic
Hemopexin-like
MMP-1, -3, -8, -10, -11, -12, -13, -18, -19, -20, -22, -27, -28
Membrane Type
Type I Membrane
SP
Pro
Catalytic
Hemopexin-like
TM
CD
MMP-14, 15, 16, 24
Type II Membrane
SP
Pro
Catalytic
Cys
IgG-like
MMP-23
GPI anchored
SP
Pro
Catalytic
Hemopexin-like
GPI
MMP-17, 25
SP Signal peptide
Pro Prodomain
TM Transmembrane
CD Cytoplasmic domain
CL Collagen-like
Cys Cysteine array
GPI GPI anchor
Hinge
FN Fibronectin repeat

Figure 2. Matrix Metalloproteinases can be categorized based on domain structure.

The mammalian Matrix Metalloproteinases (MMPs) are grouped into two main classifications based on domain structure: Secreted and Membrane –type MMPs. Of the secreted MMPs, the 'minimal' types are composed of a signal peptide (SP) that directs them for secretion, a pro-domain that requires removal for proteolysis, and a catalytic domain with endopeptidase activity. In addition to the aforementioned domains, 'typical' MMPs also contain a flexible hinge region, and a hemopexin-like domain that dictates binding and substrate specificity. 'Gelatin binding' secreted MMPs also contain fibronectin-like repeats, and a collagen-like domain. 'Type I' membrane-type MMPs are directed to the cell membrane by the N-terminal signal peptide, and contain a transmembrane and short cytoplasmic domain in addition to the domains of the 'typical' MMPs. 'Type II' membrane-type MMPs possess a cysteine array and IgG-like domain in place of the hemopexin-like, and transmembrane and cytoplasmic domains. GPI anchored membrane-type MMPs are anchored into the membrane by a GPI anchor and lack a cytoplasmic domain .

(MMP-17, -25) contain a GPI-anchor, in place of the hemopexin, transmembrane and cytoplasmic domains.

Since MMPs represent a large family of potent proteolytic enzymes, their activity must be tightly regulated to properly mediate ECM remodeling and maintain homeostasis. The expression of *MMPs* is temporally and spatially regulated at the level of transcription by various growth factors, cytokines and chemokines [21], and also regulated at the post-translational level via multiple mechanisms. All MMPs are synthesized as zymogens with an inhibitory pro-domain that inserts into the catalytic site thus preventing access to substrates and ECM degradation. The proteolytic removal of this domain is necessary to activate MMPs and allow for substrate degradation, and thus represents the primary mechanism of post-translational regulation [26]. The secreted MMPs are activated by removal of the pro-peptide domain by other active proteases, including serine proteinases such as chymase and trypsin, or other already active MMPs [25, 27]. The MT-MMPs are reported to be activated intracellularly prior to membrane placement by the proprotein convertase, or furin, as they contain the conserved furin target sequences RXKR or RRKR between the pro- and catalytic domains [28, 29]. However, the mechanism of MMP activation in general is a contentious point in the literature, as the mode of activation of most MMPs is more presumed than proved, and the *in vivo* mechanism for activation of most proMMPs is unknown [30]. Evidence of our incomplete understanding of MMP activation is the proof that complete deletion of the furin target sites from MT1-MMP does not affect its activation [31], indicating the possible role of yet unknown MMP activation mechanisms.

Once the prodomain has been removed and MMPs are active, their proteolytic activity can be regulated by the secreted Tissue Inhibitors of MetalloProteinases (TIMPs) [32]. The

mammalian TIMP family contains four members (TIMPs 1-4) that are composed of an N-terminal MMP inhibitory domain, and a C-terminal domain that has distinct functions depending on the TIMP [33]. The TIMPs share the common feature that they are the endogenous inhibitors of MMPs and inhibit their proteolytic activity by forming noncovalent 1:1 stoichiometric complexes that are resistant to heat denaturation and proteolytic degradation. Although all TIMPs inhibit MMP activity, TIMPs differ in their expression pattern, solubility, and binding affinities with the different MMPs. TIMP-1, TIMP-2 and TIMP-4 can be found in soluble forms in the extracellular milieu, whereas TIMP-3 is strictly found tightly bound to ECM components [34, 35]. The expression patterns of the TIMPs is regulated at the level of transcription by various factors for the controlled inducible expression of TIMPs that results in differential temporal and spatial expression patterns, with the exception of TIMP-2 which demonstrates a constitutive expression pattern in all tissues [21]. Although TIMPs were originally characterized as MMP inhibitors, it is now known that TIMPs are multifunctional proteins that can affect different cellular processes by using their C-terminal domain to interact with cell surface receptors to induce intracellular signaling cascades that have been shown to promote cell cycle arrest and affect cell migration [36-38].

Although it has become increasingly clear that MMPs and TIMPs have other biological functions in addition to ECM homeostasis, the presumed role of these two protein families during metastasis progression continues to be as ECM remodelers **(fig 1b)**. This presumption emerges from the fact that during metastasis progression there is a requirement for tumour cells to traverse the interstitial ECM and BM during the processes of intravasation and extravasation [11], and given the fact that MMPs can degrade all ECM components, created a longstanding idea that the role of MMPs in carcinogenesis is to clear a path through the ECM so tumour cells

can spread to distant organs [30, 39]. This claim is supported by numerous studies conducted in the past two decades that demonstrate two key concepts unequivocally: there is increased expression of MMPs in primary tumour tissues [40-48], and interfering with the functions of certain MMPs results in reduced tumourigenicity [49-62]. Additionally, MMP research in the cancer field has yielded valuable insight into the cellular molecular mechanisms regarding MMPs synthesis, transport, function and dynamics [24, 28, 53, 63-77], but has generated few solid mechanisms, especially using *in vivo* models and clinical samples [19, 30, 78], regarding the true role of MMPs in tumourigenicity, and whether they actually play an important role in this process. The presumed role of MMPs in cancer progression is best exemplified by the research regarding the complex multifaceted contribution to tumourigenesis of MT1-MMP, MMP-2 and MMP-9 [23, 79].

1.3 MT1-MMP is a Multifunctional Protease Involved in Tumourigenesis

Historically, research on MMPs has predominantly focused on the gelatinases, MMP-2 (gelatinase A or GelA) and MMP-9 (GelB), as the number of studies reporting MMP-2 and -9 function are log-fold higher in number than for other MMPs [30]. However, this leads to the misconception that MMP-2 and -9 are the most biologically important MMPs, which is not the case, and rather these two MMPs are the most reported because they are measured the most frequently due to gelatin zymography. Gelatin zymography is an SDS-PAGE based technique that uses a gel copolymerized with gelatin which allows for the detection and visualization of MMP-2 and -9 protein *in situ* by virtue of their ability to degrade gelatin [80]. This became the preferred approach to detect these MMPs before the availability of antibodies that detect both

pro- and active forms of MMP-2/-9 [81]. Therefore, the sheer amount of studies of MMP-2/-9 function stems from the ease and inexpensiveness of detecting these MMPs using gelatin zymography.

As mentioned, all MMPs are synthesized as inactive zymogens that require activation via removal of the pro-domain. Since gelatin zymography allowed for accurate and inexpensive detection of the isoforms (pro- and active) of MMP-2 and -9, the mechanisms responsible for the activation of these gelatinases could be investigated. This lead to the discovery of the only *bona fide*, well-characterized and replicable activation mechanism for any MMP: the TIMP-2-assisted activation of proMMP-2 by MT1-MMP at the cell membrane [82]. MT1-MMP is a type-I MT-MMP that is anchored at the cell membrane by a hydrophobic transmembrane domain and also contains a short intracellular cytoplasmic domain [70]. TIMP-2 is the only constitutively expressed TIMP that also demonstrates the highest affinity towards MT1-MMP and MMP-2, and thus is essential to control the proteolytic activity of these two MMPs [83]. However, TIMP-2 also shares an interesting relationship with MT1-MMP and MMP-2, as instead of inhibiting these proteases, it can also act as an adapter protein critical for the activation of proMMP-2 when TIMP-2 is present at low levels. In this activation process, extracellular TIMP-2 binds the hemopexin domain of secreted proMMP-2 using the non-inhibitory C-terminal domain, thereby creating a molecular complex where the inhibited catalytic site of proMMP-2 is physically separated from the free N-terminal domain of TIMP-2 [84]. This molecular complex composed of TIMP-2:proMMP-2 can then insert itself between dimerized active MT1-MMP molecules at the cell surface due to the free N-terminal domain of TIMP-2 being able to bind to the catalytic site one of the dimerized MT1-MMP molecules thereby inhibiting it. As a result of this binding mode, the proMMP-2:TIMP-2 complex is oriented in a way that exposes the pro-domain of

proMMP-2 to the catalytic site of the uninhibited dimerized MT1-MMP that can then proteolytically cleave the pro-domain of MMP-2 releasing the active gelatinase [85]. The activation of proMMP-2 by the cooperation of TIMP-2 and MT1-MMP is the perfect example regarding the pleiotropy of MMPs and TIMPs, as it demonstrates that MMPs can cleave non-ECM components, and that TIMPs can act as promoters, as well as inhibitors, of MMP activity.

The discovery that MT1-MMP is necessary for proMMP-2 activation, and thus can exacerbate ECM degradation, along with the aforementioned presumption that the role of MMPs during cancer progression was to facilitate a path through the ECM, lead to the development of chemical agents that inhibit the catalytic activity of MMPs (MMP inhibitors – MMPi) as anti-cancer therapeutics. These therapeutic agents demonstrated value *in vitro* and in animal models but were ineffective in human clinical trials, in some cases causing serious adverse effects, and have continued to be a persistent failure as a cancer therapy for the past two decades [86-93]. The failure of these MMPis generated a call to action to appreciate and elaborate on the non-proteolytic functions of MMPs, as the immediate explanations as to why MMPis were ineffective was the functional redundancy amongst the MMPs (which to date has not been resolved), and/or that they exerted their biological function through mechanisms that do not involve proteolysis of ECM components or that are completely non-proteolytic in nature. Similar to the situation regarding MMP-2 and -9 studies, the discovery of MT1-MMP mediated proMMP-2 activation, along with the failure of MMPis, created the necessary momentum for the research community to turn its attention to the ECM independent functions of MT1-MMP [94], and as such the amount of publications devoted to MT1-MMP are disproportionate in number compared to the other MT-MMPs [95], and may not reflect the biological importance of MT1-MMP [30]. Due to research conducted in the past decade, it is now known that MT1-MMP is indeed a

multifunctional membrane protease capable of functions independent of ECM remodeling or catalytic activity, affecting varied biological processes including migration, viability, metabolism, and induction of intracellular signaling [96].

MT1-MMP has been shown to increase the migratory ability of different types of cancer cells, in some cases due to MT1-MMP overexpression alone [31, 49, 97]. Reports have shown that MT1-MMP overexpression increases the migration potential of MCF-7 breast cancer [31], MG-63 osteosarcoma [98], COS-1 [49], and COS-7 cells [97]. Currently, there is limited evidence regarding the mechanism behind MT1-MMP mediated migration augmentation, with some reports showing that co-localization and processing of the cell adhesion molecule CD-44 [98], or increased MAPK signaling via ERK1/2 [97, 99], is responsible for increased migration of MT1-MMP positive cells. In one of the latter reports, the authors showed that increased migration as a result of MAPK activation does not depend on proteolytic activity, as high levels of TIMP-2 or a proteolytically-inactive mutant of MT1-MMP can still induce ERK1/2 phosphorylation and increase migration of MCF-7 breast cancer cells [99]. In addition to migration promotion, MT1-MMP can also mediate viability of cancer cells, particularly during serum-free incubation without pro-survival signals. It has been demonstrated that overexpression of MT1-MMP in MT1-MMP deficient breast cancer cells maintains a proliferative phenotype when cultured in low-serum conditions [99], and also protects cancer cells from apoptosis via the AKT pathway when cultured in serum-free conditions [100]. Similar to migration promotion, apoptosis protection mediated by MT1-MMP did not require its proteolytic activity, as treatment with TIMP-2 was optimal to promote survivability, which could also be mediated by a catalytically inactive MT1-MMP.

A novel and unanticipated function of MT1-MMP was recently reported whereby MT1-MMP can initiate and maintain the "Warburg effect" in both macrophages and cancer cells. The "Warburg effect" or "glycolytic switch" is a hallmark of malignant tumours that is characterized by increased aerobic glycolysis during normoxia (normal oxygen tension) [101]. This effect is mediated by the transcription factor hypoxia inducible factor-1 (HIF-1), which is regulated by post-translational modifications that make this protein liable to degradation in normoxic conditions and stable in hypoxic conditions [102]. Therefore, when cells sense hypoxic conditions, HIF-1 is stable and translocates to the nucleus to increase the expression of glycolytic-related genes to meet with cellular energy requirements in low oxygen conditions. The distinction between functional HIF-1 in normal physiology and the "Warburg effect" during tumour progression is that in the Warburg effect HIF-1 is stable and functioning despite normal oxygen tension, and as such it is still incompletely understood how HIF-1 is stabilized in normoxic conditions [103]. To further understand HIF-1 function, a research group used macrophages as their cell model since these cells are an important component of the immune system and rely predominantly on aerobic glycolysis to produce ATP [104]. This group found, unexpectedly, that macrophages lacking MT1-MMP produced considerably lower levels of ATP than wild-type cells. The authors go on to demonstrate that the cytoplasmic domain of MT1-MMP can bind to FIH-1 (factor inhibiting HIF-1), which leads to its inhibition (and thus stabilization of HIF-1) by its recently identified inhibitor, Mint3/APBA3. In follow-up work, the authors used a variety of cancer cells to show that tumour cell lines that endogenously express MT1-MMP exhibited increased glycolytic activity, and that overexpression of MT1-MMP in MT1-MMP deficient cells is sufficient to induce the Warburg effect [50]. Importantly, using cancer cells, these authors demonstrated that HIF-1 stabilization by MT1-MMP is not dependent

on the its proteolytic activity, and this effect could be mediated solely by transfection with the cytoplasmic domain of MT1-MMP, again demonstrating that MT1-MMP is multifunctional and does not need proteolytic activity to exert its biological function **(fig 3)**. Additionally, the aforementioned report also demonstrated *in vivo* that treating MT1-MMP positive tumours with a MT1-MMP cytoplasmic domain (CD) peptide suppresses aerobic glycolysis and tumour growth in a dominant-negative fashion, which strongly suggests a substantial non-proteolytic role for MT1-MMP in tumourigenesis.

Although originally characterized as a potent initiator of ECM remodeling, it is now accepted that MT1-MMP has many functions beyond degradation of ECM components, for which the proteolytic activity does not seem to be necessary. However, with this mind, the role of MT1-MMP in mediating cell function and cancer progression remains unclear, and potentially more cofounding than ever since the known varied functions of MT1-MMP make it difficult to delineate the relative contributions of these functions to tumourigenicity. Recently, efforts have been made to understand the individual functions of MT1-MMP and their relation to cell invasion and tumorigenic potential. Strongin et al (2013) isolated an antibody that binds MT1-MMP in such a way that it does not sterically inhibit the catalytic site of MT1-MMP, but does interfere with TIMP-2 binding, and thus can completely inhibit TIMP-2-assisted proMMP-2 activation [105]. Although this antibody is effective at inhibiting proMMP-2 activation, it is not effective at decreasing migratory potential of MT1-MMP positive breast cancer cells, and to date has not been applied to *in vivo* models or used in clinical trials.

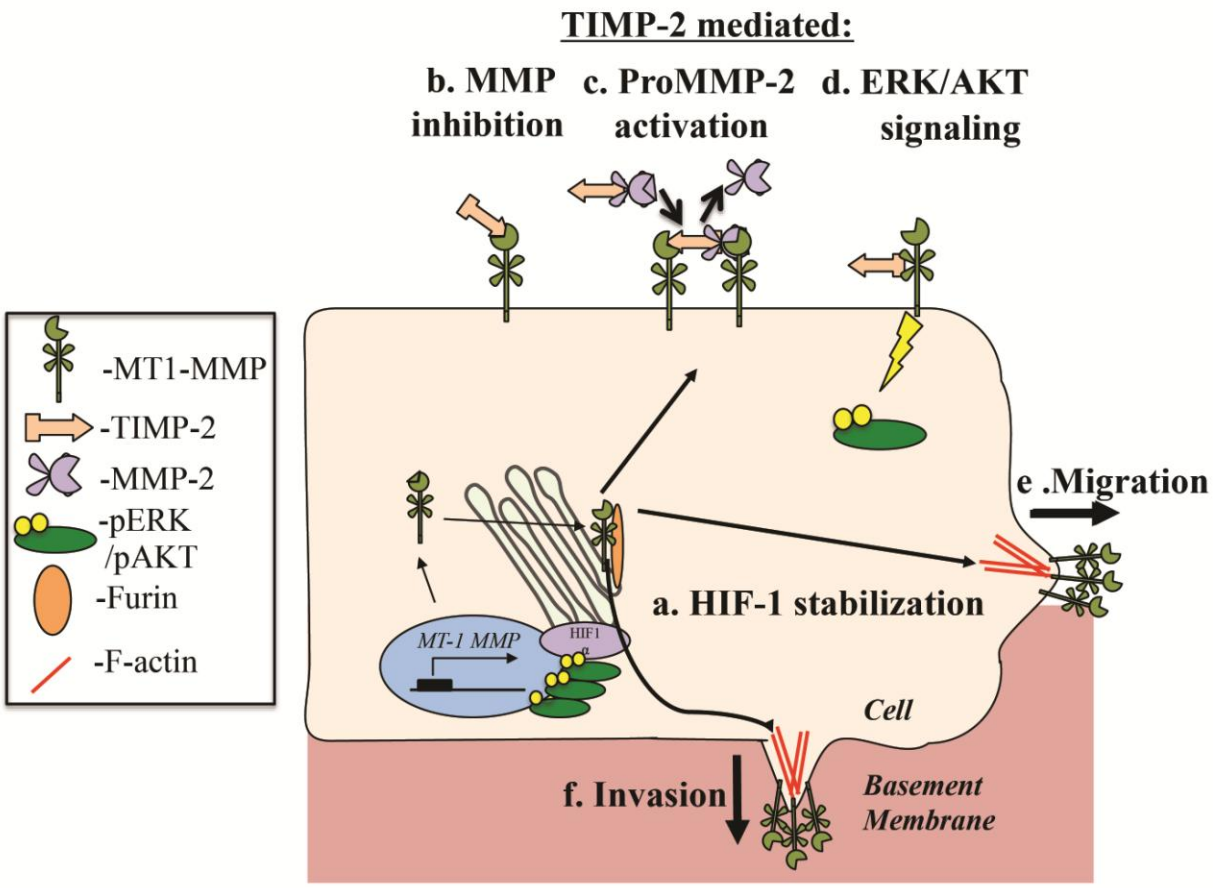
TIMP-2 mediated:
b. MMP inhibition
c. ProMMP-2 activation
d. ERK/AKT signaling
-MT1-MMP
-TIMP-2
-MMP-2
-pERK /pAKT
-Furin
-F-actin
e .Migration
a. HIF-1 stabilization
MT-1 MMP
HIF1 α
Cell
f. Invasion
Basement Membrane

Figure 3. MT1-MMP is a multifunctional protease that can affect different processes in distinct cellular compartments.

MT1-MMP is synthesized in the nucleus, translated in the cytoplasm, and presumably activated intracellularly at the golgi by the proprotein convertase Furin that removes the pro-domain of MT1-MMP. During intracellular processing, MT1-MMP can induce stabilization of transcription factor HIF-1 (a) thereby increasing expression of glycolytic genes and mediating the Warburg effect. Active MT1-MMP is then anchored in the plasma membrane where it can degrade its respective substrates, and where it can be inhibited by the TIMPs, particularly TIMP-2 which can binds its catalytic domain and block access to substrates (b). In addition to MT1-MMP inhibition, TIMP-2 can also act as an adapter protein to proMMP-2, which aids in its activation at the cell surface by dimerized MT1-MMP (c), and exacerbates ECM remodeling. TIMP-2 has also been shown to interact with MT1-MMP at the hemopexin domain where it can induce ERK and AKT intracellular signaling cascades that have been shown mediate increased migration and apoptosis protection, respectively. MT1-MMP has also been shown to affect cell motility by localizing to cellular structures marked by cytoskeletal protrusions, such as lamellopodia or filopodia that are crucial for lateral cell migration (e), or invadopodia which are necessary for ventral cell invasion through an impeding ECM barrier (f).

1.4 Research Project

Despite what is known about the individual functions of MT1-MMP, how these different functions integrate to mediate cell behavior and tumourigenesis remains poorly understood. The goal of my PhD research project was to understand the role of MT1-MMP in tumourigenicity by overexpressing MT1-MMP and analyzing appropriate cellular parameters to determine their contribution to a metastatic phenotype. To accomplish this goal I used three different experimental platforms: 2D culture, 3D Matrigel culture, and *in vivo ex-ovo* avian embryos, and two cell models: MCF-7 and MDA-MB 231 breast cancer cells.

MCF-7 cells are breast cancer cells that are MT1-MMP deficient, non-migratory and non-tumorigenic [40, 106]. In contrast, MDA-MB 231 breast cancer cells endogenously produce MT1-MMP, and are migratory and tumorigenic [41, 66]. Using these two different cell lines, I created three different clonal cell lines of each that express different levels of MT1-MMP. In 2D culture, I examined how different levels of MT1-MMP expression alter proMMP-2 activation, ECM degradation, ERK signaling, cell migration and viability. Using 3D Matrigel culture [107], I analyzed how different levels of MT1-MMP affected morphological changes associated with an invasive phenotype. Lastly, I conducted *in vivo* assays using avian embryos to examine the potential of the MT1-MMP expressing cell lines to form vascularized tumours [108] and extravasate out of the vasculature [109], two parameters related to tumourigenicity and metastasis, respectively.

1.5 Hypothesis

I hypothesize that in 2D culture, the different functions of MT1-MMP will correlate with the expression level of MT1-MMP in breast cancer cells. Therefore, I expect cells that express

the highest level of MT1-MMP to demonstrate the highest increase in proMMP-2 activation, ECM degradation, ERK signaling, cell migration, and viability, in contrast to MT1-MMP deficient cells that will demonstrate baseline activation of these cellular activities. Furthermore, I hypothesize that breast cancer cells demonstrating excessive ECM degradation, and increased migration and viability will display an invasive metastatic phenotype in 3D culture and *in vivo.* I expect breast cancer cells expressing the highest levels of MT1-MMP to demonstrate a protrusive phenotype in 3D culture, indicative of an invasive phenotype, and increased ability to form vascularized tumours and extravasate out of the vasculature *in vivo*.

Chapter 2

2 Materials and Methods

2.1 Cell culture

MCF-7, MDA-MB 231 and HS578t human breast cancer cell lines were obtained from the American Type Culture Collection (Manassas, VA). Cells were maintained in DMEM/F-12 media (Thermo Fisher) supplemented with 10% FBS, 100 IU/ml penicillin, 100 μg/ml streptomycin, and incubated at 37^{o}C and 5 % CO_2.

2.2 cDNA clones and reagents

Human MT1-MMP (sc116990), TIMP-2 (sc118083) and MMP-2 (sc321560) cDNA clones were purchased from Origene and subcloned into the vector pcDNA 3.3 (Thermo Fisher). The generation of the ALA+TIMP-2 cDNA construct in pcDNA 3.3 is described in Walsh et al., 2012 [110]. The following reagents were used: Recombinant human TIMP-2 and 4-aminophenylmercuric acetate (APMA) (Sigma-Aldrich), BB-94 (Batimastat), U-0126, and AKT inhibitor IV (Santa Cruz), and Furin inhibitor II (Millipore).

2.3 Antibodies

For immunoblot analysis, the following primary antibodies were used: MT1-MMP (1:1000, AB6004, Millipore); MT1-MMP (1:1000, AB51074, Abcam); Phospho-ERK1/2 (1:2000, D13.14.4E), ERK1/2 (1:2000, 137F5) (Cell Signaling Technology); TIMP-2 (1:1000, 3A4), β-Actin (1:1000, C4), and phospho-histone-3 (PH3) (1:5000, C1513) (Santa Cruz). Goat anti-mouse IgG (H+L) (Bio-Rad) and goat anti-rabbit IgG (H+L) (Thermo Fisher) HRP

conjugates were used as secondary antibodies (1:10000). For immunofluorescence analysis, the anti-MT1-MMP antibody AB6004 (1:200) was used, along with anti-rabbit-IgG-Alexa488 or Alexa594 (Thermo Fisher) as secondary antibodies (1:400).

2.4 Transfection and generation of stable cell lines

MCF-7 and MDA-MB 231 cells were seeded at a density of $5x10^5$ cells/ml and incubated for 24 hours in DMEM/F-12 with 10% FBS. Following incubation, cells were transfected with Lipofectamine 2000 (Thermo Fisher) according to the manufacturers instructions. For transient transfection experiments, cells were incubated for 24 hours after transfection and then utilized for experiments.

Stable cell lines were generated by transfection of cells with the respective cDNAs in the vector pcDNA 3.3, which contains a neomycin mammalian selection marker. Following transfection, cells were split 1:1000 and incubated in media containing 1 mg/ml G-418 (VWR). Individual colonies were selected after four weeks of incubation in selection media and expanded to assay for the levels of MT1-MMP by qPCR and immunoblotting. Stable cells lines expressing an shRNA sequence targeting MT1-MMP in the vector pRS (TR311445, Origene) were generated in the same manner except using puromycin (2 μg/ml) as the selection antibiotic.

For zsGreen infection, cells were seeded at ~ 40% density in a 6-well cell culture dish in 3 ml of media with a final concentration of 8 μg/ml polybrene and infected with 250 μL of virus. For virus production, the pLVX-ZsGreen1-N1 lentiviral plasmid was used. Twenty-four hours post-infection, the media containing virus was removed and replaced with puromycin selection media (2 μg/ml) for three days of incubation to select for infected cells.

2.5 Generation of MMP-2, TIMP-2 and ALA+TIMP-2 conditioned media (CM)

Conditioned media (CM) containing high levels of MMP-2, TIMP-2, and ALA+TIMP-2 protein were created by transfecting MCF-7 cells with cDNA constructs coding for the respective proteins. Following a 24-hour incubation post-transfection, transfected cells were washed with phosphate buffered saline (PBS) and incubated in DMEM/F12 media without FBS for 24 hours. The serum-free CM were then collected, aliquoted and stored for later use. Conditioned media from mock-transfected cells were used as a control.

2.6 Quantitative Real-Time PCR

RNA was collected from cells using the RNeasy Kit (Qiagen) and cDNA was synthesized from 1 μg of RNA using qScript cDNA supermix (Quanta). MT1-MMP mRNA levels were assayed by qPCR using PerfeCta SYBR Green Supermix (Quanta) and a CXF connect real time system with CFX manager software (Bio-Rad). mRNA levels were quantified by the ΔΔCT method and are displayed as fold change relative to parental MCF-7 or MDA-MB 231 cells in control conditions as indicated in the figure legends. The level of GAPDH mRNA was used as the internal control. Primers (5'-3') are as follows: MT1-MMP; F: gcagaagttttacggcttgca, R: tcgaacattggccttgatctc, MMP-2; F: agctcccggaaaagattgatg, R: cagggtgctggctgagtagat, MMP-9; F: cctggagacctgagaaccaatc, R: gatttcgactctccacgcatct, GAPDH; F: acccactcctccacctttga, R: ctgttgctgtagccaaattcgt [40].

2.7 Immunoblotting

Post-incubation cells were washed 3X with PBS (pH=7.2) and disrupted using lysis buffer (150 mM NaCl, 1% NP-40, 0.5% NaDC, 0.1% SDS, 50 mM Tris pH 8.0) supplemented with protease/phosphate inhibitor (Thermo Scientific). Cell lysates were homogenized by sonication and 15 μg aliquots were analyzed by immunoblotting with MT1-MMP, TIMP-2, pH-3, β-actin, pERK1/2 or ERK1/2 primary antibodies, followed by incubation with the appropriate secondary HRP-conjugated antibody and detection using SuperSignal West Pico chemiluminescent substrate (Thermo Fisher). Protein lysate from human 21T cell lines was acquired as previously described [111].

2.8 Gelatin zymography and reverse zymography

Gelatin zymography and reverse zymography were done using samples of serum-free media (15 μl) as described previously [80]. To assess the proMMP-2 activation ability of MCF-7 cells, which endogenously express very low levels of MMP-2 [41], proMMP-2 CM was added to cells at a dilution of 30 μl proMMP-2 CM/mL SF media. For reverse zymography, serum-free medium conditioned for 24 hours by HS578t cells was used as the source of active MMP-2 within the gel, as these cells naturally express high levels of MMP-2 [40].

2.9 Immunofluorescence

Samples for fluorescent gelatin degradation and 3D culture experiments were fixed and prepared for immunofluorescence according to their respective protocols (see below). MT1-MMP primary antibody (AB6004) was detected using anti-rabbit IgG Alexa594 or Alexa488 for Oregon green-488 gelatin degradation or 3D culture experiments respectively. F-actin was stained with Alexa633 phalloidin (1:100, Thermo Fisher) and nuclei with 4',6-diamidino-2-

phenylindole (1 µg/ml, BioShop Canada). Samples were imaged using a Nikon A1R+ confocal microscope (1.2 au) with a 20x dry or 60x oil-immersion lens and presented using NIS Elements software.

2.10 Transwell assays

The migratory potential of cells was measured using 24-well 8 µm pore transwell inserts (Corning Costar). Cells ($2x10^4$) were seeded on the upper chamber of the transwell in serum-free medium and allowed to migrate towards the bottom chamber which was placed in DMEM/F-12 medium supplemented with 10% FBS. Migration assays were done with uncoated transwell inserts, whereas invasion assays were done with inserts coated with 20% Matrigel. Cells that migrated to the lower chamber of the transwell insert were quantified as described previously [112]. Migrated cells were normalized to MCF-7/MDA-MB 231 parental cells in control conditions and are presented as a mean percentage ± SEM.

2.11 Scratch closure migration assay

Cells were seeded at a density of $5x10^5$/mL cells in a 35 mm cell culture dish and allowed to form a monolayer for 24 hours. Following incubation, medium was removed and a scratch (an area clear of cells) was made down the middle of the cell culture dish with a 100 µl pipette tip. Cells were washed 3x with PBS (pH 7.2) to remove cell debris and then incubated with fresh medium. After 2 hours, 10 images were captured down the length of the scratch that represent the 'initial' size of the scratch for that sample. Every 24 hours for 3 days, the same area of the scratch was imaged to examine how cells migrated to close the scratch. Scratch closure was quantified using ImageJ 2.0.0 software by measuring the width of the scratch each day and

normalizing it to the initial size of the scratch. Scratch closure is presented as a mean percentage of the initial scratch size ± SEM.

2.12 Celltiter96® proliferation assay

Cell viability was inferred by measuring metabolically active cells using Celltiter96® AQueous One Solution (Promega). Cells were seeded in triplicate (5000 cells/well) onto a 96-well cell culture dish in medium supplemented with 10% FBS or serum-free medium. Immediately after seeding, 20 uL of Celltiter96® AQueous One Solution was added in triplicate to each sample to obtain an initial reading and ensure that the different cell lines were seeded equally. The OD at 490 nm was measured using a Bio-Rad model 3550-UV microplate reader after incubating the cells with the substrate for 2 hours. The substrate was added at the indicated day intervals and measured in the same way as the initial measurement to create a growth curve over that span, or to compare the effect of chemical inhibitors on cell viability during prolonged serum-free incubation.

2.13 Fluorescent gelatin degradation assay

Coverslips were coated with either Oregon Green-488 gelatin (for immunofluorescence analysis) or gelatin labeled using an Alexa594 protein labeling kit (for live imaging analysis) (Thermo Fisher) and used to analyze ECM degradation as per Martin et al., 2012 [113]. Immunofluorescence conditions are as described above.

2.14 Three-dimensional (3D) cell culture

Cells ($2.5x10^4$) were embedded in 50% Matrigel (Corning Costar) and processed for immunofluorescence as per Cvetkovic et al., 2014 [107]. To quantify colony morphologies

observed in 3D culture, five random 50 μm Z-stacks (2 μm step size) were acquired using DIC microscopy at 10x magnification every day for 5 days post-embedding. For each individual Z-stack, invasive features (disseminations and protrusions, see text) were blindly counted and normalized to the number of circular colonies per field of view. Immunofluorescence procedure was done as described above using 3% BSA/PBS as the blocking buffer. Single cells (marked by DAPI), F-actin disseminations, F-actin protrusions and zsGreen protrusions were blindly counted from 20x 3D volumes and normalized to the number of circular colonies per field of view.

2.15 Live-imaging and timelapse movies

Cells were embedded in Matrigel or seeded on Alexa594 gelatin coverslips as described above and placed in a live imaging chamber mounted on the stage of a Leica DM16000 B fluorescent microscope. To analyze the relationship between ECM degradation and migration, cells stably expressing zsGreen were incubated on Alexa594 gelatin coverslips and imaged at the same stage position at 10x magnification every 10 minutes for 20 hours. These images were then compiled into timelapse movies using ImageJ. The zsGreen channel timelapse movies were used to quantify the migration of individual cells in an automated manner using the ADAPT plugin for ImageJ [114]. The ADAPT plugin (v1.146) was used with default conditions and the trajectory visualization output was used to group cells according to the distance migrated. The Alexa594 gelatin channel was used to manually quantify the percentage of cells that had degraded the underlying gelatin at different time points. To visualize the dynamics of cells in 3D culture, cells were embedded in Matrigel and z-stacks (100 μm, 5 μm step size) were acquired at 20x magnification every 30 minutes for 72 hours. Focal panels showing colony features with the greatest clarity were isolated and compiled into timelapse movies using ImageJ.

2.16 Avian embryo CAM implantation and extravasation efficiency assay

For implantation experiments, the superficial layer of the CAM of day 9 chicken embryos was removed to expose the underlying capillaries [115]. MDA-MB 231, MCF-7 or MCF-7 MT1-MMP cell lines stably expressing zsGreen were then resuspended in Matrigel and pipetted onto the exposed capillaries ($5x10^5$ cells in 10 µl Matrigel/embryo). Eight days post-implantation the resulting tumour was imaged using a fluorescent stereoscope to examine vascularization of the tumour shown by the presence of non-fluorescent CAM vessels within the zsGreen tumour.

MCF-7 and MCF-7 MT1-MMP cell lines stably expressing zsGreen were used for intravenous injection into the CAM vasculature of day 14 chicken embryos and extravasation efficiency was quantified 24 hours post-injection as per Kim et al., 2016 [109].

2.17 Densitometry analysis

Quantitative analysis of immunoblots was done using QuantityOne software (Bio-Rad). Band intensity was obtained for the pERK and total ERK signal of each sample from three independent experiments. ERK activation is presented as a ratio between the pERK and the total ERK band intensity within each sample normalized to MCF-7 cells under control conditions.

2.18 Statistics

Experimental data consists of three biological replicates and is presented as mean ± SEM. Statistical analysis and graphing was performed using GraphPad Prism version 6.0 (GraphPad software, La Jolla, CA, USA). One-way ANOVA followed by Tukey's post-hoc test was used unless otherwise indicated in the figure legend. Significant differences denoted by asterisks are

shown versus MCF-7 or MDA-MB 231 parental cells in control conditions unless otherwise shown in figure. Different levels of statistical significance are denoted by a different number of asterisks and are as follows: ****$p \leq 0.0001$, ***$p \leq 0.001$, **$p \leq 0.01$, *$p \leq 0.05$.

Chapter 3

3 Results

3.1 Transient Overexpression of Functional MT1-MMP did not Result in Increased Motility

To begin assessing how MT1-MMP affects the motility of breast cancer cells, I transiently overexpressed wild-type MT1-MMP in MT1-MMP-deficient MCF-7 breast cancer cells. Twenty-four hours following transient transfection, MT1-MMP mRNA and protein levels were analyzed via qPCR and immunoblot, respectively, and proMMP-2 activation ability of transfected cells via gelatin zymography **(fig 4).** qPCR and immunoblot analysis showed that MT1-MMP transfected cells synthesized very high levels of MT1-MMP mRNA (~17,000 fold relative to mock transfected cells) and produced predominantly the pro- (63 kDa) but also active isoform (60 kDa), along with degradation forms (44 kDa), of MT1-MMP protein. Gelatin zymography analysis demonstrated that MT1-MMP transfected cells were capable of proMMP-2 activation, shown by transition from the pro- (72 kDa) to the intermediate (68 kDa) and active forms (62 kDa) of MMP-2 after transfection. In contrast, mock transfected MCF-7 cells did not produce any MT1-MMP protein and concurrently were not able to activate proMMP-2, shown by the presence of only proMMP-2 (control) in the gelatin zymography analysis. To further verify the functionality of transiently produced MT1-MMP protein, I performed an additional gelatin zymography analysis after treating transfected cells with of low levels (100 ng/ml) of recombinant TIMP-2 which was expected to enhance activation of proMMP-2 mediated by MT1-MMP **(fig 5a)**. Parental MCF-7 cells, which do not secrete endogenous proMMP-2, did not

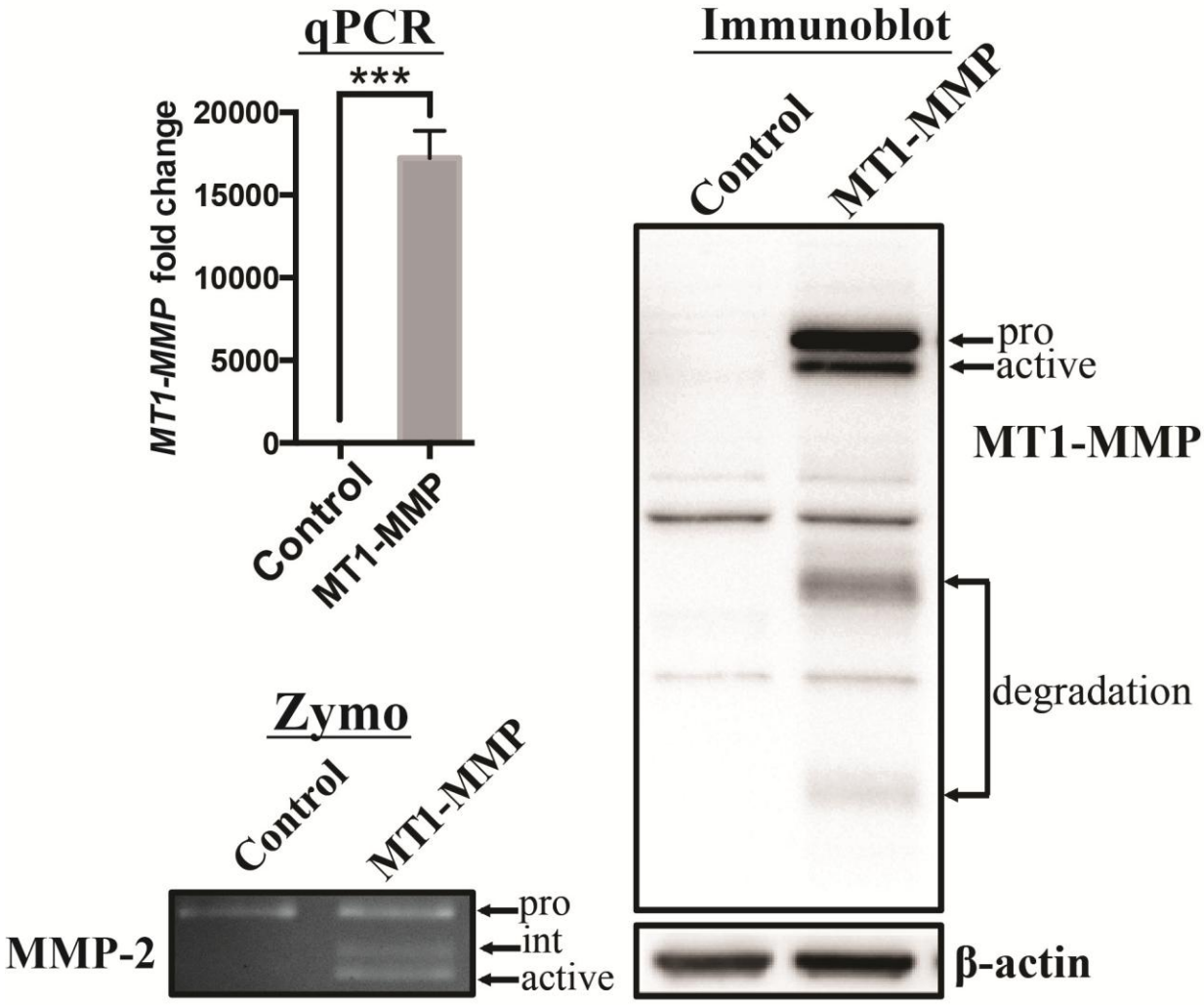
qPCR
***
MT1-MMP fold change
20000
15000
10000
5000
0
Control
MT1-MMP
Immunoblot
Control
MT1-MMP
pro
active
MT1-MMP
degradation
β-actin
Zymo
Control
MT1-MMP
MMP-2
pro
int
active

Figure 4. Transient transfection of *MT1-MMP* in MCF-7 breast cancer cells resulted in high levels of functional MT1-MMP protein.

qPCR, immunoblot, and gelatin zymography (zymo) analysis of MT1-MMP mRNA, protein levels, and proMMP-2 activation ability, respectively, of MCF-7 breast cancer cells transiently transfected with MT1-MMP compared to mock transfected cells (control). Immunoblot analysis (AB6004) showed pro- (63 kDa), active (60 kDa), and degradation forms (44 kDa) of MT1-MMP protein in MT1-MMP transfected MCF-7 cells. β-actin was used as a loading control. Gelatin zymography analysis showed that MCF-7 cells transiently transfected with MT1-MMP were capable of activating proMMP-2 after 24 hours of incubation as shown by intermediate and active forms of MMP-2.

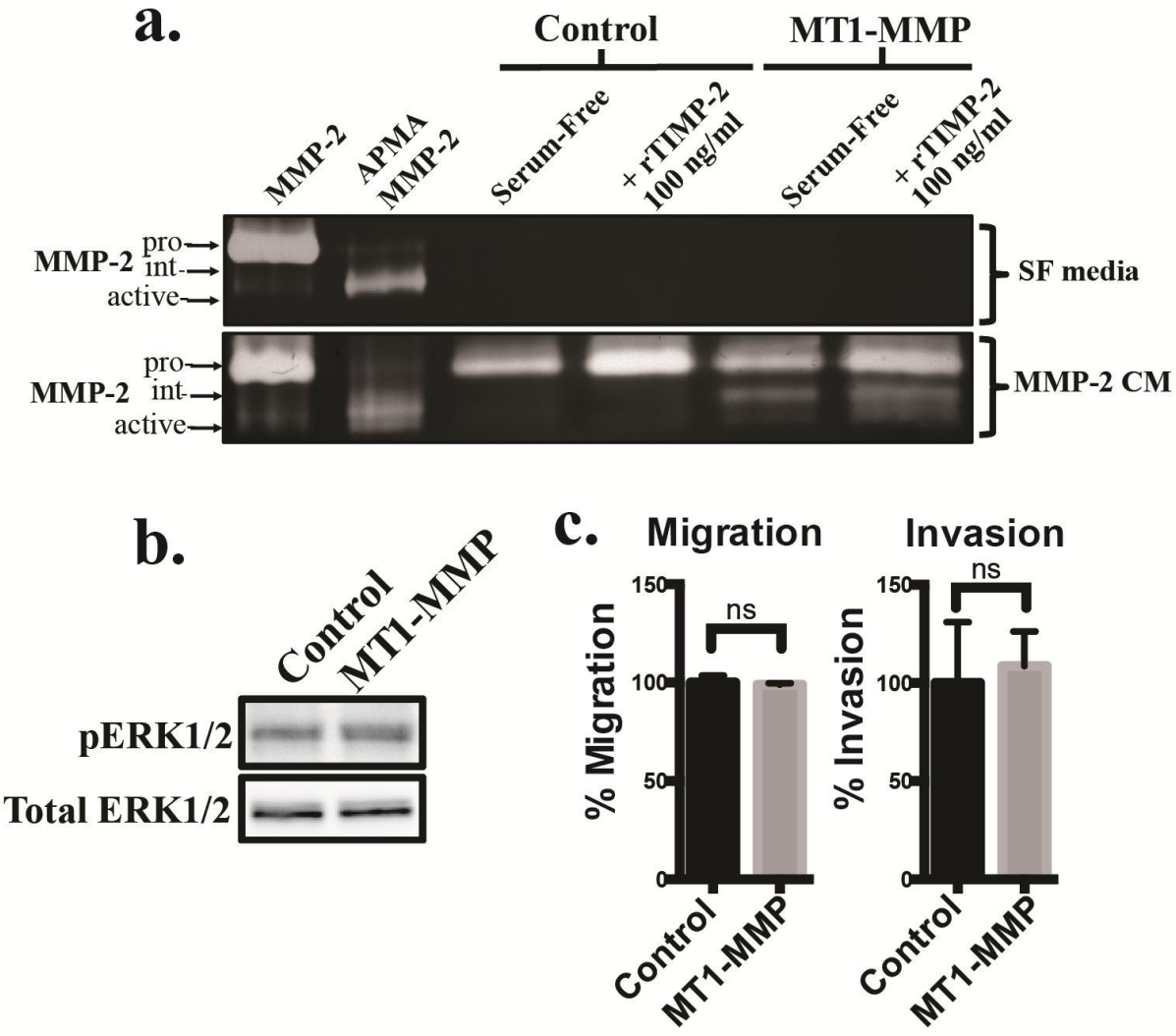
a.
Control
MT1-MMP
MMP-2
APMA MMP-2
Serum-Free
+ rTIMP-2 100 ng/ml
Serum-Free
+ rTIMP-2 100 ng/ml
MMP-2
pro
int
active
SF media
MMP-2
pro
int
active
MMP-2 CM
b.
Control
MT1-MMP
pERK1/2
Total ERK1/2
c.
Migration
Invasion
% Migration
% Invasion
150
100
50
0
ns
ns
Control
MT1-MMP
Control
MT1-MMP

Figure 5. Transient transfection of *MT1-MMP* in MCF-7 cells resulted in TIMP-2-mediated proMMP-2 activation, but not increased ERK signaling or cell motility.

(a) Gelatin zymography analysis of MCF-7 cells transiently transfected with MT1-MMP and incubated for 12 hours with serum-free media (SF, top gel) or MMP-2 conditioned media (CM, bottom gel). Lanes 1 and 2: Controls showing proMMP-2 chemically activated by APMA. Lanes 4 and 6: Recombinant TIMP-2 (rTIMP-2) was added at 100 ng/ml to enhance MT1-MMP-mediated proMMP-2 activation. **(b)** Immunoblot analysis of MT1-MMP transfected cells showing pERK1/2 levels. Total ERK1/2 was used as a loading control. **(c)** Transwell migration and invasion assays of MCF-7 cells transiently transfected with MT1-MMP. Number of migrated/invaded cells were normalized to control MCF-7 cells and expressed as a mean percentage ± SEM (ns, $p > 0.05$ by student's t-test).

increase MMP-2 production after transfection with MT1-MMP, as determined by gelatin zymography **(fig5a, top gel)**.

To analyze the ability of MCF-7 cells to activate proMMP-2, diluted proMMP-2 conditioned medium (CM) was added that was generated by transfection of MCF-7 cells with a construct coding for constitutively expressed MMP-2. Since MCF-7 cells are MT1-MMP deficient, they are not capable of activating proMMP-2 and thus MMP-2 protein in this CM is predominantly present in the pro- form **(fig 5, lane 1)**, which was confirmed by chemical activation with 4-aminophenylmercuric acetate (APMA) that completely activates proMMP-2 in the CM, as shown by the presence of only the active form after treatment **(fig 5, lane 2)**. Addition of proMMP-2 conditioned media to transfected cells demonstrated that MT1-MMP overexpression activated proMMP-2 after 12 hours of incubation, shown by the presence of an intermediate band, and this activation was enhanced by the addition of low levels of recombinant TIMP-2 that resulted in the presence of more active MMP-2 isoform **(fig 5a, bottom gel**). Following confirmation of the functionality of transfected MT1-MMP protein, it was then examined if MCF-7 cells transiently transfected with functional MT1-MMP demonstrated increased ERK activation and a corresponding increased in motility. To examine ERK activation, ERK1/2 phosphorylation was analyzed by immunoblot, whereas migration and invasion were measured using transwell assays where the transwell insert was uncoated (migration) or coated with 20% Matrigel which acts as an impeding ECM barrier (invasion). Differing from published reports [31, 49, 99] there was no difference in ERK activation, **(fig 5b)** or migration and invasion **(fig 5c, ns > 0.05)** in MCF-7 cells that produced functional MT1-MMP protein after transient transfection.

To test whether the very high (~17000 fold) levels of MT1-MMP expression achieved using transient transfection was a factor behind the discrepancies between my observation and other reports, I created clonal MCF-7 cell lines that stably express significantly different levels of MT1-MMP by neomycin selection and expansion of resistant colonies after transfection **(fig 6)**. These cell lines, MCF-7 MT1-MMP C1, C2, and C3 cells (hereby referred to as C1, C2 or C3 cells), significantly differ in their stable expression of MT1-MMP transcript from **high** (**C1**, ~2,500 fold compared to MCF-7 parental cells), **medium** (**C2**, ~1,100 fold) to **low** (**C3**, ~11 fold) as determined by qPCR analysis **(fig 6a)**. Immunoblot analysis of these MCF-7 MT1-MMP cell lines showed that both pro- and active- isoforms of MT1-MMP protein were detected in C1 cells, whereas the active isoform was predominantly detected in C2 cells and no MT1-MMP protein could be detected by immunoblot in C3 cells **(fig 6b)**. To confirm the functionality of MT1-MMP protein produced by MCF-7 stable cell lines, I incubated these cells with proMMP-2 CM alone, or in combination with recombinant TIMP-2 (rTIMP-2, 100 ng/ml), or rTIMP-2 and the panMMP inhibitor BB94 (10 μM), and assessed proMMP-2 activation via gelatin zymography after 6 or 12 hours of incubation **(fig 6c)**. Cell lines where active MT1-MMP was detected via immunoblot (C1 and C2 cells) were capable of activating proMMP-2 in a time-dependent manner, as there were higher levels of intermediate and active MMP-2 after 12 hours of incubation compared to 6 hours for these cell lines. As expected, proMMP-2 activation was enhanced by low levels of recombinant TIMP-2, shown by higher levels of intermediate and active MMP-2 when TIMP-2 was added. Additionally, proMMP-2 activation was completely inhibited by addition of BB94, which taken together, confirms production of functional MT1-MMP protein in MCF-7 MT1-MMP cell lines.

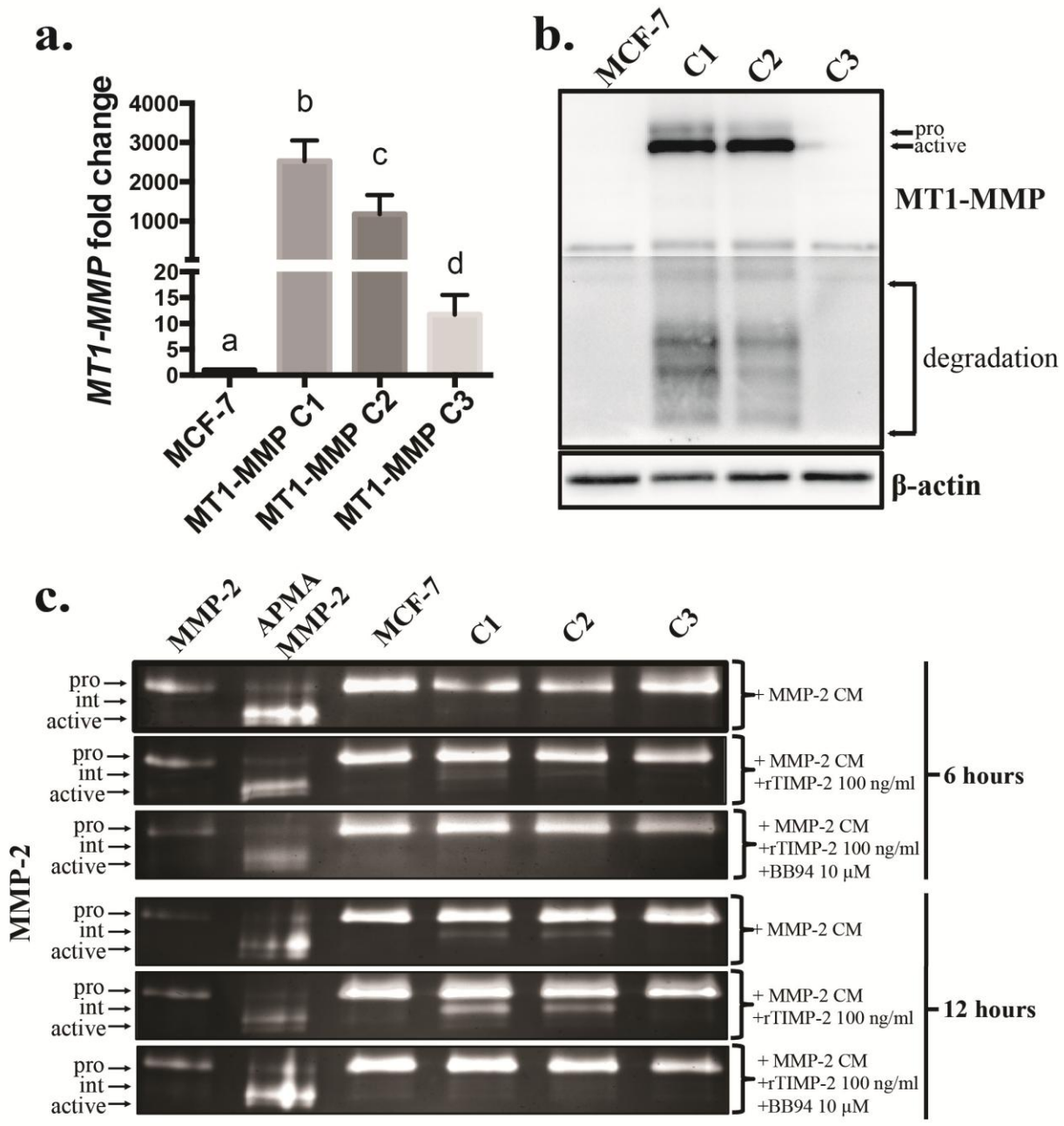
a.
MT1-MMP fold change
4000
3000
2000
1000
20
15
10
5
0
a
b
c
d
MCF-7
MT1-MMP C1
MT1-MMP C2
MT1-MMP C3
b.
MCF-7
C1
C2
C3
pro
active
MT1-MMP
degradation
β-actin
c.
MMP-2
APMA MMP-2
MCF-7
C1
C2
C3
MMP-2
pro
int
active
+ MMP-2 CM
+ MMP-2 CM +rTIMP-2 100 ng/ml
+ MMP-2 CM +rTIMP-2 100 ng/ml +BB94 10 μM
6 hours
12 hours

Figure 6. Three MCF-7 cell lines, C1, C2 and C3, stably produce different levels of MT1-MMP.

(a) qPCR analysis of MT1-MMP mRNA from MCF-7 MT1-MMP cells lines (C1, C2, and C3) that stably express different levels of MT1-MMP. Different letters indicate significant differences at $p \leq 0.05$ by one-way ANOVA, Tukey's post-hoc test. **(b)** Immunoblot analysis (AB51074) showing pro- (63 kDa), active (60 kDa), and degradation forms (44 kDa) of MT1-MMP protein in MCF-7 MT1-MMP cell lines. β-actin was used as a loading control. Lower half of blot is digitally transformed to clearly shown degradation bands. **(c)** Gelatin zymography analysis of MCF-7 MT1-MMP cell lines incubated for 6 or 12 hours with either MMP-2 CM alone, or in combination with rTIMP-2 at 100 ng/ml, or rTIMP-2 and BB94 (10 μm).

To confirm that C3 cells produced MT1-MMP protein (poorly detectable by immunoblot) I used an imaging approach whereby cells were seeded on poly-L-lysine **(fig 7)** or Oregon-green 488 gelatin coated coverslips **(fig 8)** and examined using immunofluorescence for MT1-MMP protein presence, and degradation of the underlying ECM when plated on fluorescent gelatin [113]. Immunofluorescence analysis on poly-L-lysine coverslips demonstrated that MCF-7 cell lines overexpressing MT1-MMP contain cytoplasmic MT1-MMP protein, including C3 cells which show punctate MT1-MMP signal localized at the cell periphery **(fig 7)**. MDA-MB 231 breast cancer cells were also used in this analysis to compare MCF-7, C1, C2 and C3 cells to a cell line demonstrated to express naturally increased levels of MT1-MMP **(fig 8)**. Quantification of fields of view acquired at 20x magnification demonstrated no detectable cytoplasmic MT1-MMP immunological signal nor gelatin degradation in parental MCF-7 cells. In contrast, 84% and 60% of C1 and C2 cells displayed ECM degradation (gelatin -), respectively, with approximately 20% of these cells also displaying punctate cytoplasmic immunological signal for MT1-MMP protein **(fig 8b)**. A low percentage of MT1-MMP C3 cells (~1.5%) showed ECM degradation, and a higher percentage (~3%) showed a cytoplasmic MT1-MMP signal, although these increases were non-significantly different than parental MCF-7 cells. MDA-MB 231 breast cancer cells (which endogenously produce MT1-MMP, see fig 12c below) were not capable of widespread cell-associated ECM degradation, and only ~6% of cells displayed cytoplasmic MT1-MMP signal. Analysis of these samples at 60x magnification clearly demonstrated cell associated ECM degradation mediated by MT1-MMP, as MT1-MMP protein can be detected overlaying degraded ECM, and co-localized with F-actin puncta **(fig 9, orange arrows)**. This observation is consistent with the role of invadopodia in ECM degradation as invadopodia are defined as ventral structures where F-actin and MT1-MMP are concentrated to mediate substrate

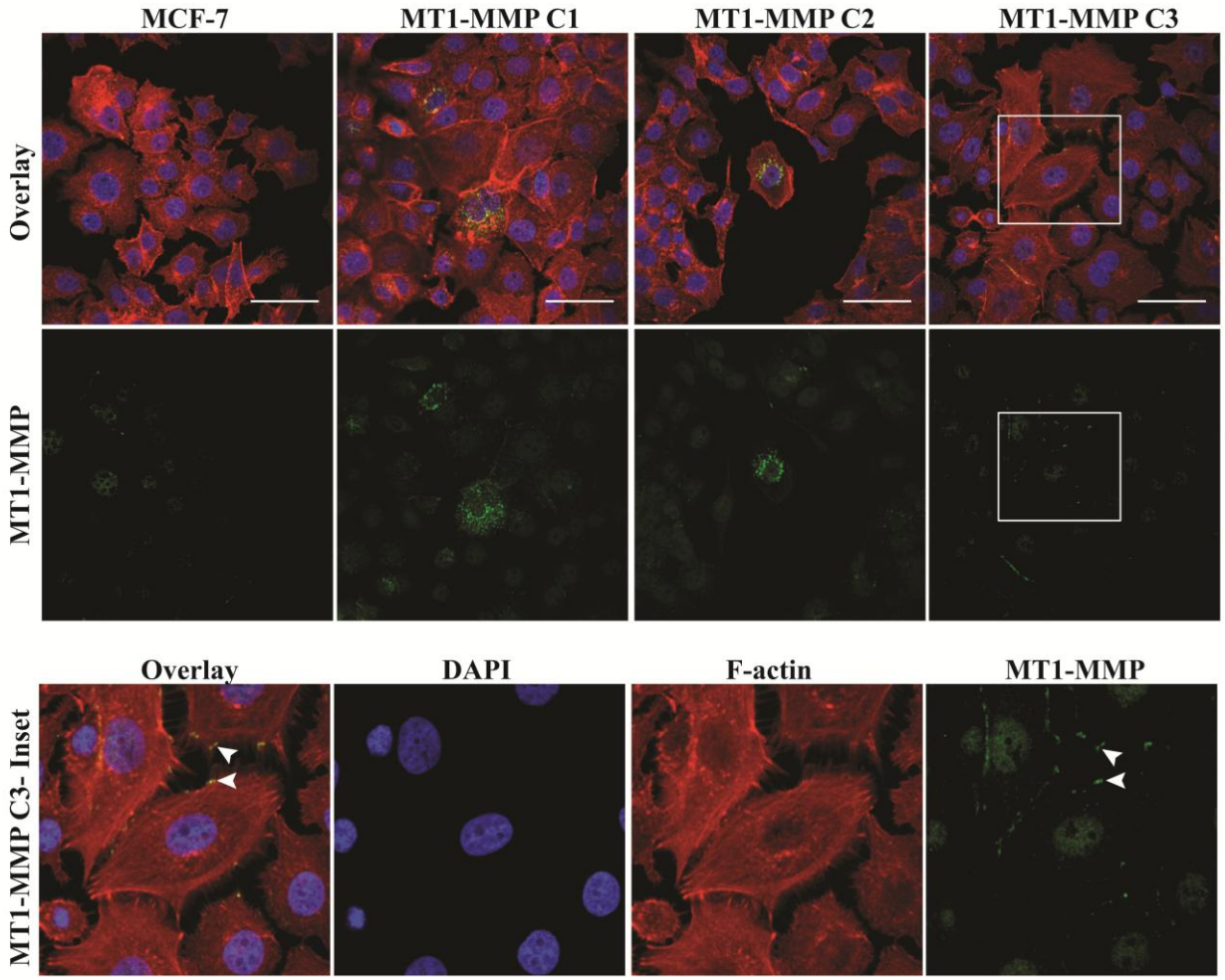
MCF-7
MT1-MMP C1
MT1-MMP C2
MT1-MMP C3
Overlay
MT1-MMP
Overlay
DAPI
F-actin
MT1-MMP
MT1-MMP C3- Inset

Figure 7. Cytoplasmic MT1-MMP protein is detectable in all MCF-7 MT1-MMP cell lines

MCF-7 MT1-MMP cell lines were incubated on poly-L-lysine coverslips for 24 hours and processed for immunofluorescence to examine cytoplasmic MT1-MMP. Representative fields of view are shown at 60x magnification. Panels are composed of an overlay showing the nuclei (blue), F-actin (red), and MT1-MMP (green), and the MT1-MMP channel below. Inset shows C3 cells that demonstrate punctate signal pertaining to MT1-MMP protein (white arrows). Scale bars = 100 μm.

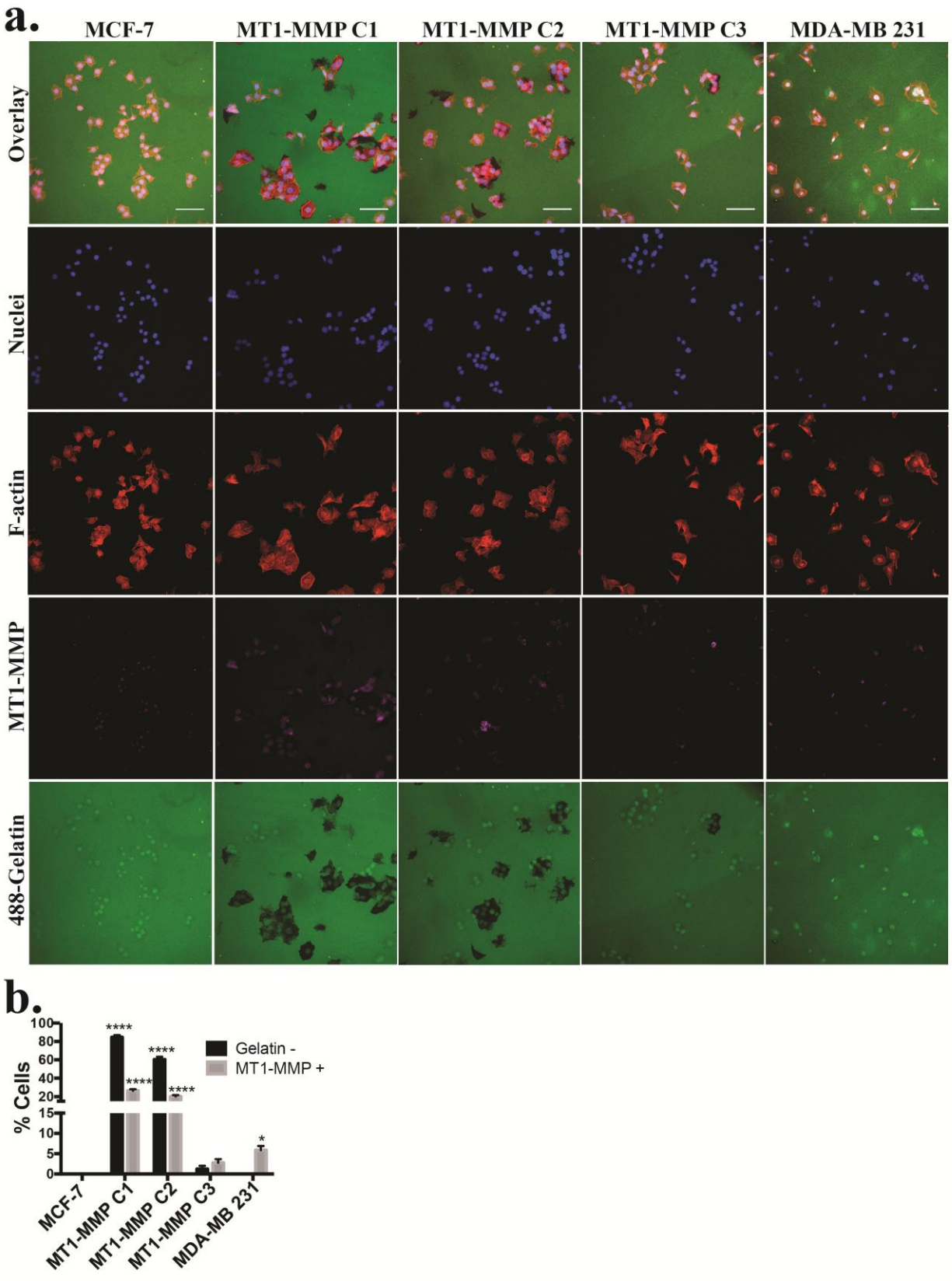
a.
MCF-7
MT1-MMP C1
MT1-MMP C2
MT1-MMP C3
MDA-MB 231
Overlay
Nuclei
F-actin
MT1-MMP
488-Gelatin
b.
% Cells
Gelatin -
MT1-MMP +
****
*
MCF-7
MT1-MMP C1
MT1-MMP C2
MT1-MMP C3
MDA-MB 231

Figure 8. MCF-7 cell lines that express high levels of MT1-MMP demonstrated widespread ECM degradation.

(a) MCF-7, MT1-MMP cell lines, and MDA-MB 231 breast cancer cells were incubated on Alexa488 gelatin-coated coverslips for 24 hours and processed for immunofluorescence to examine cytoplasmic MT1-MMP protein and ECM degradation. Representative fields of view are shown at 20x magnification. Panels are composed of an overlay showing the nuclei (blue), F-actin (red), MT1-MMP (violet), and Alexa488 gelatin (green) signal (top), and the respective individual channels below. Scale bars = 100 μm. **(b)** Cells in each sample positive for cytoplasmic MT1-MMP protein signal (MT1-MMP +) or that demonstrate gelatin degradation (Gelatin -) were quantified per 20x fields of view and are shown as mean percentage of total cells per field of view ± SEM.

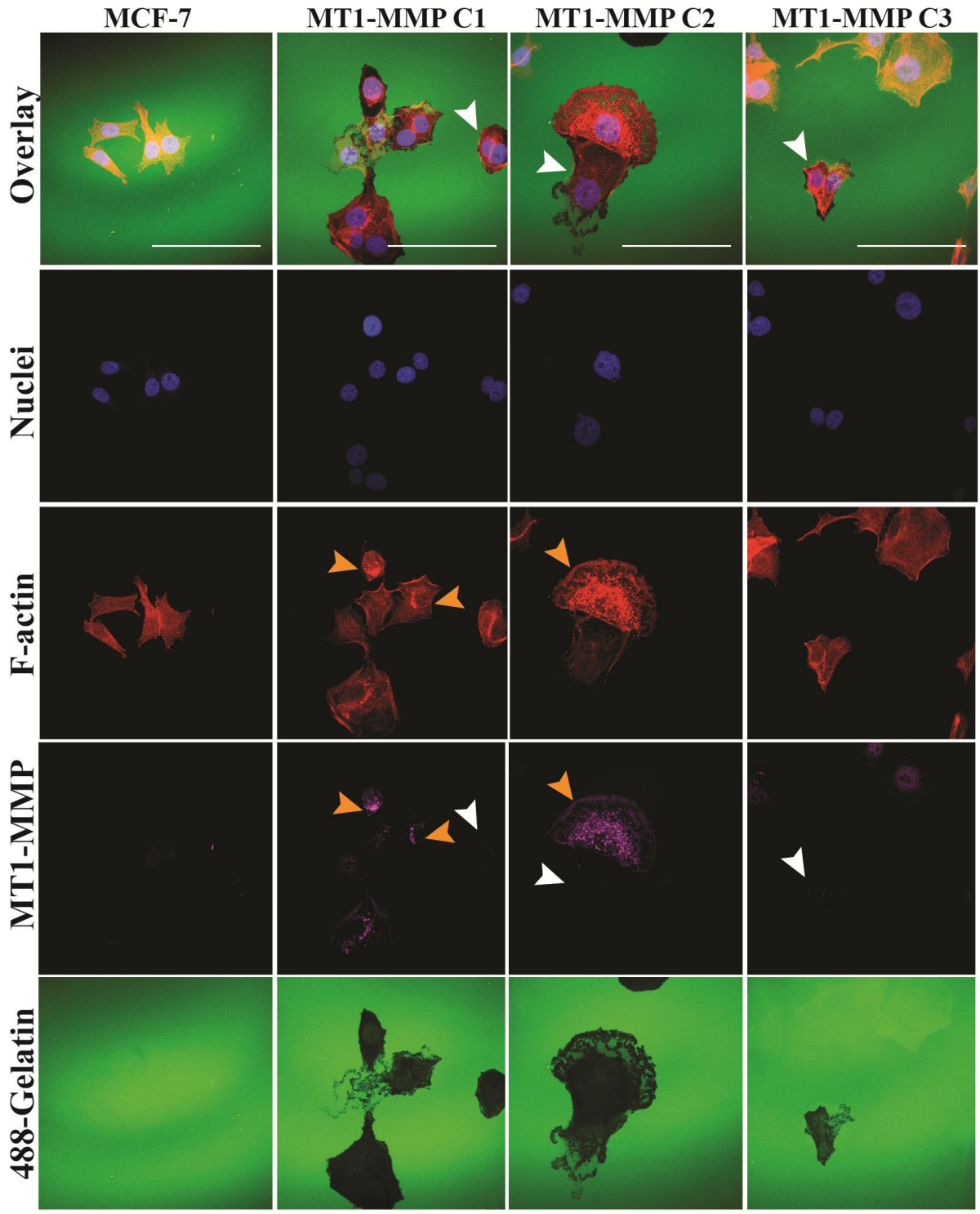
MCF-7
MT1-MMP C1
MT1-MMP C2
MT1-MMP C3
Overlay
Nuclei
F-actin
MT1-MMP
488-Gelatin

Figure 9. MCF-7 cells producing high levels of MT1-MMP formed degradative structures marked by F-actin puncta.

MCF-7 MT1-MMP cell lines were incubated on Alexa488 gelatin-coated coverslips for 24 hours and processed for immunofluorescence to examine cytoplasmic MT1-MMP protein and ECM degradation. Representative fields of view are shown at 60x magnification. Panels are composed of an overlay showing the nuclei (blue), F-actin (red), MT1-MMP (violet), and Alexa488 gelatin (green) signal (top), and the respective individual channels below. Orange arrows indicate cells that have formed cellular structures that have degraded the underlying fluorescent ECM and are marked by co-localized MT1-MMP/F-actin signal. White arrows indicate cells that have degraded the underlying gelatin but are devoid of MT1-MMP signal. Scale bars = 100 μm.

degradation [66]. Interestingly, in all experiments where MT1-MMP was overexpressed, there were cells that had degraded the underlying ECM that, paradoxically, were devoid of MT1-MMP protein signal **(fig 9, white arrows)**.

3.2 Low levels of MT1-MMP expression combined with high levels of TIMP-2 increased the migratory potential of MCF-7 cells via the ERK pathway

As assays using transient transfection of MT1-MMP demonstrated no change in cell migration or invasion, I wanted to further examine this migratory effect as well as the potential role of ERK activation using the stable cell lines that express lower levels of MT1-MMP than transiently transfected cells. As others have previously shown that TIMP-2 can modulate rapid (within 15 minutes) ERK activation by MT1-MMP expressing breast cancer cells [99, 116], I utilized conditioned media (CM) that contained high levels of TIMP-2, or ALA+TIMP-2. These CMs were generated by transiently transfecting MCF-7 cells with constructs coding for these secreted proteins and then collecting the CM after incubating transfected cells in serum-free media. ALA+TIMP-2 is a TIMP-2 mutant that cannot inhibit the enzymatic activity of MMPs as it contains a non-functional N-terminal domain due to addition of a terminal alanine (hence ALA+), but which has been shown to still bind cell surface MT1-MMP with the C-terminal domain and upregulate ERK activation [99, 117]. ALA+TIMP-2 is a useful reagent to analyze ERK activation mediated by MT1-MMP/TIMP-2 as this mutant TIMP-2 cannot be sequestered by other active MMPs and thus strongly induces ERK activation by MT1-MMP positive cells. Analysis of TIMP-2 and ALA+ TIMP-2 protein levels in the CMs via immunoblot showed that high but equal levels of TIMP-2 and ALA+TIMP-2 are present in the media after transfection,

whereas reverse zymography analysis demonstrated that only TIMP-2 was capable of inhibiting MMPs as the TIMP-2 protein was able to inhibit MMPs within the gel (shown by dark bands), whereas ALA+TIMP-2 protein was not (white bands, indicative of MMP activity) **(fig 10a)**.

Using these CMs, the ability of MCF-7 MT1-MMP cell lines to sequester TIMP-2 protein from the media was examined by treating these cells with diluted CMs. TIMP-2 levels remained equal after 15 minutes, but after 12 hours of incubation TIMP-2 levels in the media decreased corresponding to the level of MT1-MMP expression of the cell line **(fig 10b)**, further confirming that these cells produced differing levels of functional cell surface MT1-MMP that binds TIMP-2. Quantification of TIMP-2 protein in the CMs was performed via immunoblot which demonstrated that undiluted TIMP-2 CM contains approximately 10 μg/ml TIMP-2 protein **(fig 10c).** The proMMP-2 activation ability of MCF-7 MT1-MMP cells was also tested by gelatin zymography and reverse zymography in the presence of increasing levels of TIMP-2 or ALA+TIMP-2 CM **(fig 10d)**. Only C1 and C2 cells were capable of activating proMMP-2, and this was enhanced by addition of low levels of TIMP-2 (~ 100 ng/ml, red arrows), but inhibited by high levels of TIMP-2 (> ~1 μg/ml, blue arrows) [83, 116, 118], consistent with the observations of others that TIMP-2 at 100 ng/ml is optimal for proMMP-2 activation by MT1-MMP expressing cells [119]. ALA+TIMP-2 did not enhance proMMP-2 activation in these cells consistent with the requirement for both the N- and C-terminal domains of TIMP-2 to act as an adapter for proMMP-2 during its activation process [85]. Taken together, this analysis confirmed the functionality of TIMP-2/ALA+TIMP-2 CMs and demonstrated how MCF-7 cells producing high levels of MT1-MMP protein follow the well-defined mechanism described for MT1-MMP/TIMP2 mediated activation of proMMP-2.

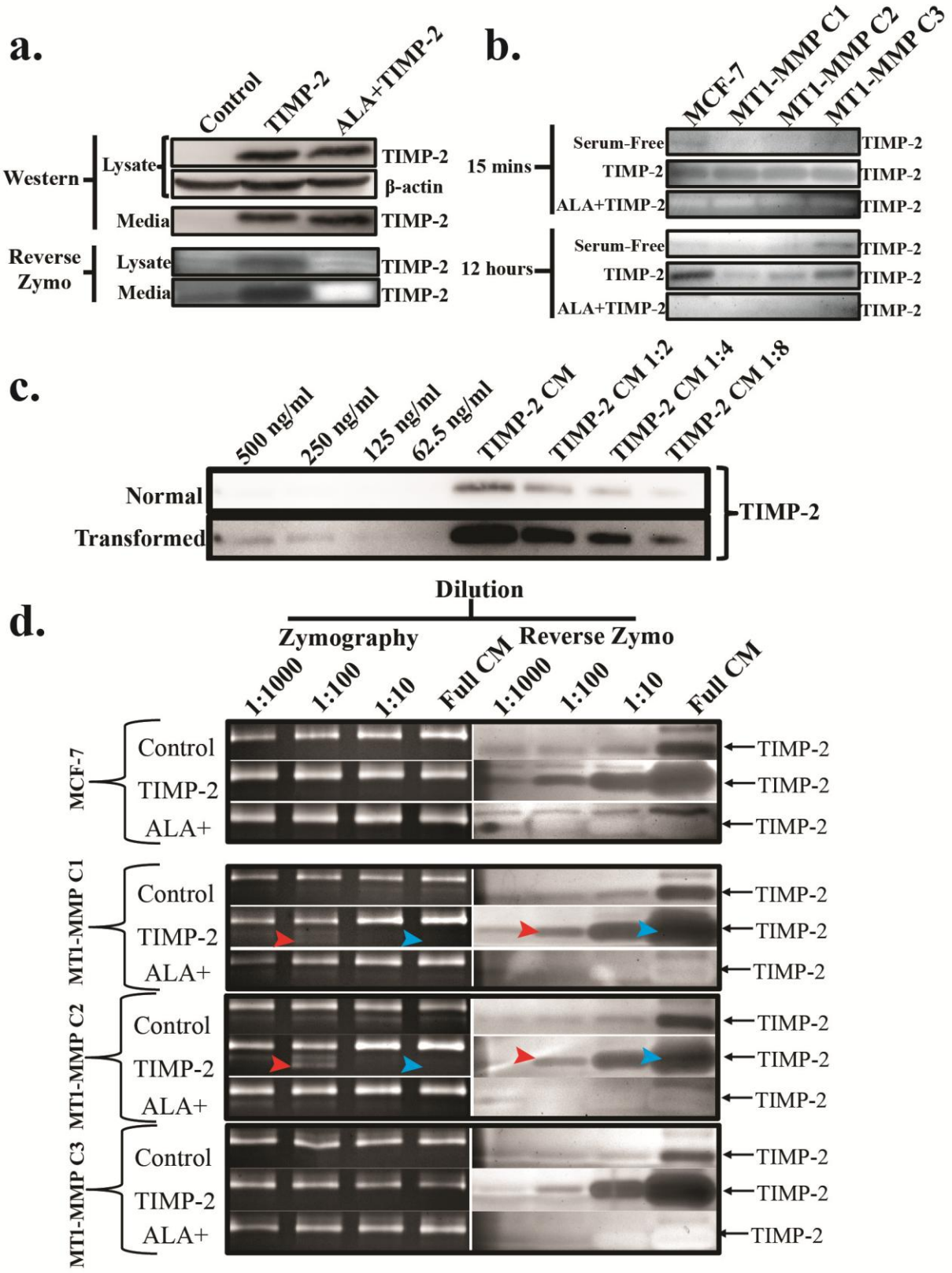
a.
Control
TIMP-2
ALA+TIMP-2
Western
Lysate
TIMP-2
β-actin
Media
TIMP-2
Reverse Zymo
Lysate
TIMP-2
Media
TIMP-2
b.
MCF-7
MT1-MMP C1
MT1-MMP C2
MT1-MMP C3
15 mins
Serum-Free
TIMP-2
TIMP-2
ALA+TIMP-2
TIMP-2
12 hours
Serum-Free
TIMP-2
TIMP-2
ALA+TIMP-2
TIMP-2
c.
500 ng/ml
250 ng/ml
125 ng/ml
62.5 ng/ml
TIMP-2 CM
TIMP-2 CM 1:2
TIMP-2 CM 1:4
TIMP-2 CM 1:8
Normal
Transformed
TIMP-2
d.
Dilution
Zymography
Reverse Zymo
1:1000
1:100
1:10
Full CM
1:1000
1:100
1:10
Full CM
MCF-7
Control
TIMP-2
ALA+
MT1-MMP C1
Control
TIMP-2
ALA+
MT1-MMP C2
Control
TIMP-2
ALA+
MT1-MMP C3
Control
TIMP-2
ALA+
TIMP-2

Figure 10. MCF-7 breast cancer cells expressing high levels of MT1-MMP displayed the well-characterized relationship of TIMP-2-mediated proMMP-2 activation.

(a) To generate TIMP-2 conditioned media MCF-7 cells were transiently transfected with TIMP-2 or ALA+TIMP-2 cDNA, and the protein lysate and media were subsequently collected for analysis using immunoblot (top) and reverse zymography (bottom) to examine TIMP-2 protein levels. β-actin was used as a loading control. Reverse zymography analysis shows that TIMP-2 inhibits MMP activity (dark bands), whereas ALA+TIMP-2 is devoid of this function (light bands) due to the non-functional N-terminal domain. **(b)** Reverse zymography of MCF-7 and MT1-MMP cell lines incubated for 15 minutes or 12 hours with TIMP-2 or ALA+TIMP-2 CM diluted 1:100 to measure TIMP-2 levels remaining in the media post-incubation with MT1-MMP expressing MCF-7 cells. Serum free medium with CM diluted from mock-transfected cells was used as a control. **(c)** Immunoblot analysis of serially diluted recombinant TIMP-2 and TIMP-2 CM. The image of the bottom blot is a visually transformed version of the top blot to enhance the banding pattern for the recombinant TIMP-2 samples. Based on densitometry analysis (not shown), the concentration of TIMP-2 protein in TIMP-2 CM is estimated to be approximately 10 μg/ml. **(d)** MCF-7 and MT1-MMP cell lines, C1, C2, and C3, were incubated for 12 hours with proMMP-2 CM supplemented with increasing dilutions of TIMP-2 or ALA+TIMP-2 CM (1:100; 1 part CM, 100 parts SF media) and then this medium was assayed using zymography and reverse zymography to assess proMMP-2 activation and TIMP-2 levels, respectively. Low levels (1:100) of TIMP-2 enhance activation of proMMP-2 by MCF-7 cells expressing high levels of MT1-MMP (red arrows), whereas high levels of TIMP-2 (Full CM; undiluted) inhibit this activation process (blue arrows).

To then examine the level of ERK activation by MCF-7 MT1-MMP cell lines and the role of TIMP-2 in mediating this process, cells were incubated in media containing either 10% FBS or in serum-free (SF) media containing different dilutions of TIMP-2 or ALA+TIMP-2 CM. Phospho-ERK levels were then examined using immunoblotting **(fig 9, left)** and quantified via densitometry **(fig 11, right)**. In media containing 10% FBS, only C2 cells had a significantly higher level of pERK (~8 fold) compared to parental MCF-7 cells. A 12-hour incubation with TIMP-2 or ALA+TIMP-2 CM demonstrated a significant decrease in ERK activation in C2 cells. In contrast, a short 15 minute incubation period with CMs demonstrated a significant increase in ERK activation of C2 and C3 cells, but not C1 cells, particularly with ALA+TIMP-2 treatment. Additionally, short incubation periods with dilutions of ALA+TIMP-2 CM showed that ERK activation in C2 and C3 cells, but not C1 cells, is significantly upregulated by high levels of ALA+TIMP-2 protein. Overall, analysis of pERK levels demonstrated that cells expressing medium (C2) and low (C3) levels of MT1-MMP demonstrate increased ERK activation that is upregulated by high levels of TIMP-2 (> ~ 200 ng/ml) and independent of MMP inhibition as shown by ALA+TIMP-2 treatment.

Since phosphorylated ERK is an active transcription factor, I assayed for changes in gene expression in MCF-7 MT1-MMP stable cell lines that may correlate with activation of ERK. I analyzed the mRNA of TIMP-2, MMP-2, and MMP-9 to assess if ERK phosphorylation correlated with altered expression of these genes, and found that activation of ERK did correlate with increased expression of MMP-2 and -9. MCF-7 C2 cells, which demonstrated the highest level of ERK phosphorylation, also demonstrated significantly higher MMP-2 and -9 mRNA levels than parental MCF-7 cells as determined by qPCR **(fig 12a).** To better define the role of elevated pERK levels in C1, C2, and C3 cells, a MEK inhibitor was used (U0126) that inhibits

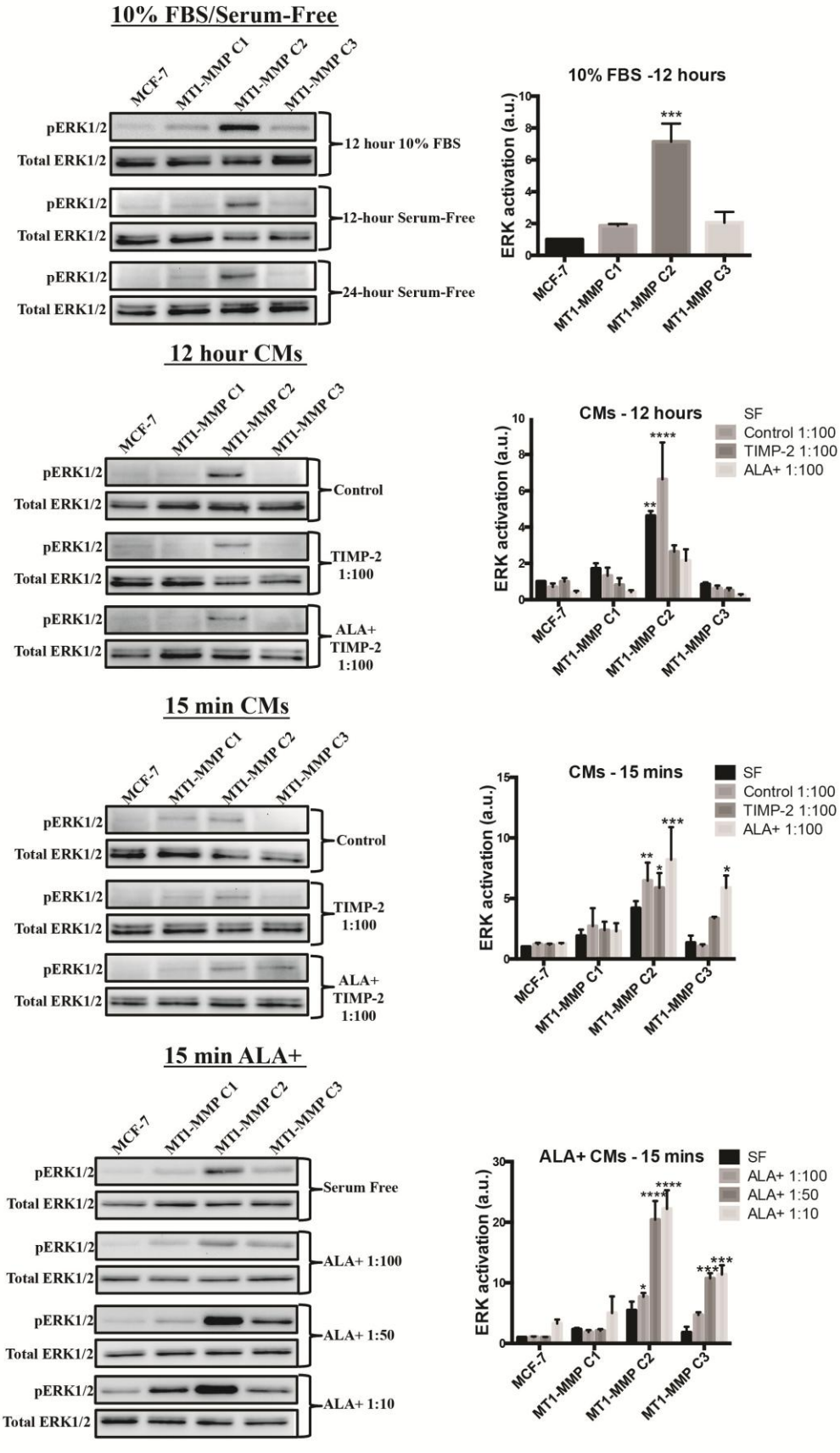
10% FBS/Serum-Free
MCF-7
MT1-MMP C1
MT1-MMP C2
MT1-MMP C3
pERK1/2
Total ERK1/2
12 hour 10% FBS
12-hour Serum-Free
24-hour Serum-Free
10% FBS -12 hours
ERK activation (a.u.)
12 hour CMs
Control
TIMP-2 1:100
ALA+ TIMP-2 1:100
CMs - 12 hours
SF
Control 1:100
TIMP-2 1:100
ALA+ 1:100
15 min CMs
CMs - 15 mins
15 min ALA+
Serum Free
ALA+ 1:100
ALA+ 1:50
ALA+ 1:10
ALA+ CMs - 15 mins

Figure 11. MCF-7 cells producing active MT1-MMP and exposed to high levels of TIMP-2 showed rapid activation of the ERK pathway.

Representative immunoblot analysis (left) of ERK1/2 activation after MCF-7 and MT1-MMP expressing cell lines, C1, C2, and C3, were seeded and incubated for 12 hours or 15 minutes with media containing 10% FBS or SF media supplemented with different dilutions of TIMP-2 or ALA+TIMP-2 CM (1:100=1 part CM:100 parts SF media). Total ERK1/2 was used as a loading control. ERK activation was measured (respective bar graphs on the right) by densitometry quantification of the pERK1/2 signal and normalization to the total ERK1/2 signal for each sample. ERK activation is displayed as mean arbitrary units (a.u.) ± SEM.

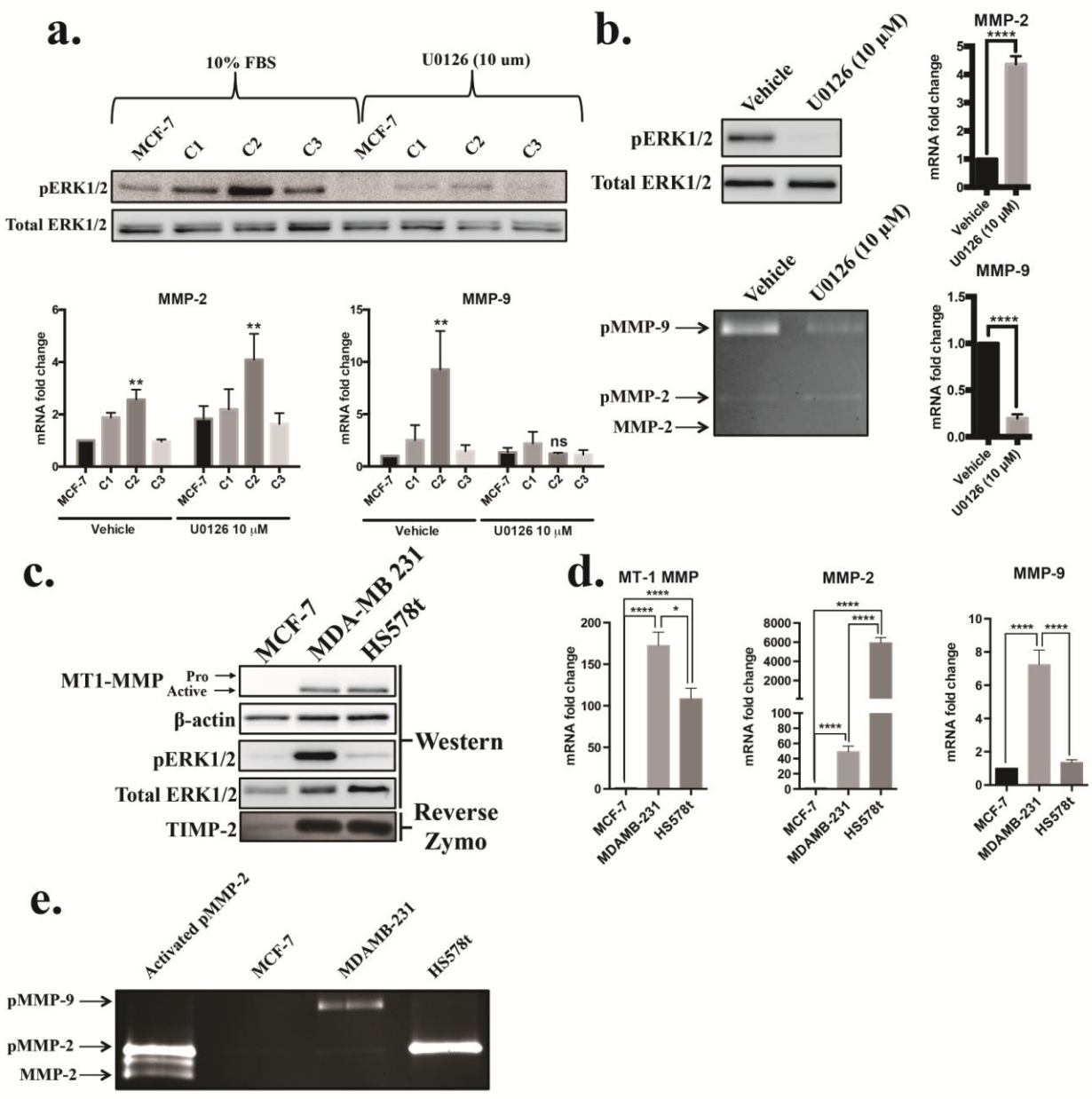
a.
10% FBS
U0126 (10 um)
MCF-7
C1
C2
C3
pERK1/2
Total ERK1/2
MMP-2
MMP-9
mRNA fold change
Vehicle
U0126 10 μM
b.
Vehicle
U0126 (10 μM)
pERK1/2
Total ERK1/2
pMMP-9
pMMP-2
MMP-2
MMP-2
MMP-9
mRNA fold change
c.
MCF-7
MDA-MB 231
HS578t
MT1-MMP
Pro
Active
β-actin
pERK1/2
Total ERK1/2
TIMP-2
Western
Reverse Zymo
d.
MT-1 MMP
MMP-2
MMP-9
mRNA fold change
MCF-7
MDAMB-231
HS578t
e.
Activated pMMP-2
MCF-7
MDAMB-231
HS578t
pMMP-9
pMMP-2
MMP-2

Figure 12. MT1-MMP-mediated ERK activation regulates an inverse transcriptional relationship between *MMP-2* and *MMP-9* in breast cancer cells.

(a) (Top) Immunoblot analysis of pERK1/2 levels after MCF-7 and MT1-MMP cell lines were incubated for 24 hours in media containing 10% FBS and supplemented with a vehicle control (0.1% DMSO) or the MAPK inhibitor U0126 (10 μM). Total ERK1/2 was used as a loading control. (Bottom) Following incubation, MMP-2 and MMP-9 mRNA levels were quantified via qPCR and displayed as mean fold change relative to vehicle treated MCF-7 cells ± SEM. **(b)** MDA-MB 231 cells were incubated for 24 hours in media containing 10% FBS and supplemented with a vehicle control (0.1% DMSO) or the MAPK inhibitor U0126 (10 μM). Following incubation, pERK1/2 and MMP-2/9 protein levels were measured via immunoblot and gelatin zymography, respectively (left), and MMP-2 and MMP-9 mRNA levels were quantified via qPCR (right) and displayed as mean fold change relative to vehicle treated MDA-MB 231 cells ± SEM. **(c)** Immunoblot (AB51074) and reverse zymography analysis comparing MT1-MMP, pERK and TIMP-2 protein levels between MCF-7, MDA-MB 231, and HS578t breast cancer cells. β-actin and total ERK1/2 were used as loading controls. **(d)** qPCR analysis of endogenous MT1-MMP, MMP-2, and MMP-9 mRNA levels from MCF-7, MDA-MB 231 and HS578t breast cancer cells. mRNA levels are displayed as mean fold change relative to MCF-7 cells ± SEM. **(e)** Gelatin zymography analysis of MCF-7, MDA-MB 231, and HS578t breast cancer cells incubated in SF media for 12 hours. Lane 1 shows proMMP-2 CM activated by MCF-7 C2 cells treated with TIMP-2 CM diluted 1:100 to show proMMP-2 activation as a result of TIMP-2/MT1-MMP.

phosphorylation of ERK1/2, with the expectation that expression of these genes would be decreased following treatment with U0126. Inhibition of ERK phosphorylation by U-0126 (10 μM) demonstrated that ERK activation was indeed responsible for altered transcription of these genes; however only MMP-9 transcription was decreased to parental levels in C2 cells, whereas MMP-2 expression actually increased in C2 cells after U-0126 treatment. To confirm that this "transcriptional switch" of MMP-2/-9 mediated by ERK activation in MT1-MMP positive cells is not an anomaly related to MT1-MMP overexpression in MCF-7 cells, MDA-MB 231 cells were also used to perform a similar analysis whereby ERK activation was inhibited and MMP-2 and -9 levels were then examined **(fig 12b)**. MDA-MB 231 cells endogenously produce high levels of phosphorylated ERK that can be successfully inhibited by incubation with U-0126, as shown by immunoblot **(fig 12b, top left)**. After incubating MDA-MB 231 cells with U-0126, MMP-2 and -9 levels were examined via gelatin zymography **(fig 12b, bottom left)** and qPCR **(fig 12b, right)**, which demonstrated that ERK inhibition increased MMP-2 and decreased MMP-9 at the protein and mRNA level, respectively. To further establish this transcriptional relationship between MMP-2 and -9 in MT1-MMP positive breast cancer cells, the levels of endogenous MMP-2 and -9 mRNA were examined between MT1-MMP deficient MCF-7 cells and MT1-MMP positive MDA-MB 231 and HS578t cells. Immunoblot analysis demonstrated that MDA-MB 231 and HS578t cells produce active MT1-MMP protein in contrast to MCF-7 cells, and that MDA-MB 231 cells produce significantly higher pERK than both MCF-7 and HS578t cells, although some pERK could be detected from HS578t cells **(fig 12c)**. Reverse zymography analysis demonstrated that MDA-MB 231 and HS578t cells produce higher and relatively equal levels of TIMP-2 compared to MCF-7 cells. qPCR analysis confirmed that both MDA-MB 231 and HS578t cells express significantly higher levels of MT1-MMP than MCF-7

cells, with HS578t cells expressing significantly lower levels of MT1-MMP compared to MDA-MB 231 cells (~100 vs ~170 fold, respectively) **(fig 12d)**. Comparing the levels of MMP-2 and -9 transcripts from MDA-MB 231 and HS578t cells demonstrated that MDA-MB 231 cells express higher levels of MMP-9, and lower levels of MMP-2, which correlated with the level of pERK between these cell lines and is consistent with the previous observations. Furthermore, MMP-2 and -9 protein levels were compared between the three breast cancer cell lines using gelatin zymography **(fig 12e)**, which demonstrated that MDA-MB 231 cells produce high levels of MMP-9 protein, and HS578t produce high levels of MMP-2 protein. Importantly, endogenous MMP-2 and -9 protein secreted by these cells is predominantly found in the pro-form, indicating that activation of these secreted MMPs does not occur in these cell lines despite production of active MT1-MMP protein.

After demonstrating that MT1-MMP overexpression does result in activation of functional ERK in MCF-7 C2 and C3 cell lines, I then examined how TIMP-2-mediated ERK activation related to the migratory potential of these cell lines. A scratch closure assay was performed over a span of 3 days which demonstrated that only C3 cells closed the scratch significantly faster than parental MCF-7 cells, indicating increased migratory ability of C3 cells **(fig 13)**. Migration was then examined using transwell assays where the cells were incubated in SF media containing TIMP-2 and ALA+TIMP-2 CMs in the upper compartment and allowed to migrate towards the lower compartment containing 10% FBS **(fig 14a)**. TIMP-2 CM caused a significant increase in the number of migrated C2 and C3 cells, while ALA+TIMP-2 CM also caused a significant increase in the number migrated C3 cells **(fig 14a, top)**. Higher dilutions of ALA+TIMP-2 CM showed a similar trend whereby only C2 and C3 cells demonstrated a significant increase in the number of migrated cells **(fig 14a, bottom)**. C1 cells, which express

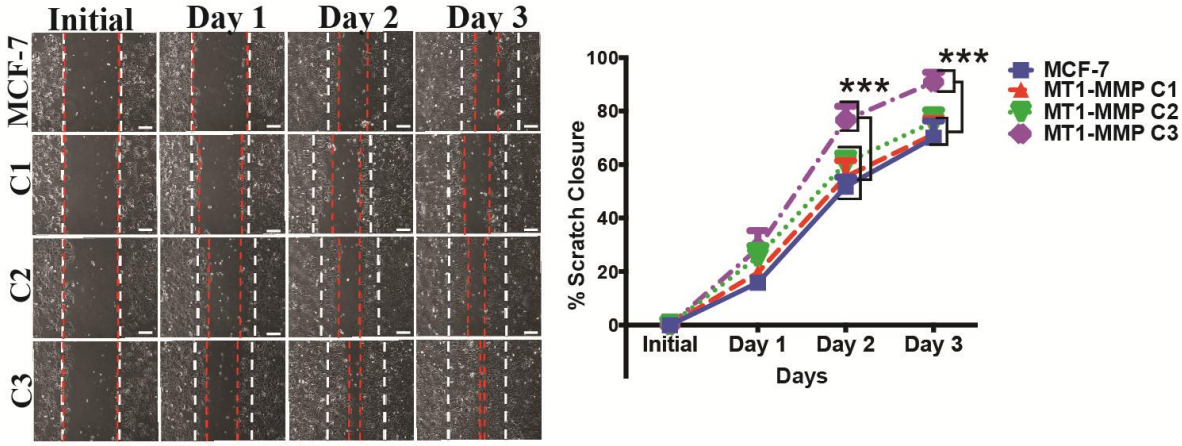
Initial
Day 1
Day 2
Day 3
MCF-7
C1
C2
C3
% Scratch Closure
100
80
60
40
20
0
***
***
Initial
Day 1
Day 2
Day 3
Days
MCF-7
MT1-MMP C1
MT1-MMP C2
MT1-MMP C3

Figure 13. MCF-7 cells expressing low levels of MT1-MMP demonstrated increased migratory potential.

Scratch closure migration assay of MCF-7 MT1-MMP cell lines, C1, C2, and C3, monitored for 3 days. Shown are representative 10x fields of view. The white dotted lines indicate the initial scratch size; red dotted lines indicate the scratch size at the respective day. Scale bars = 100 μm. Line graph on the right shows scratch closure quantification that demonstrates significantly increased migratory potential of C3 cells. Scratch closure is shown as percent closure relative to initial scratch size ± SEM.

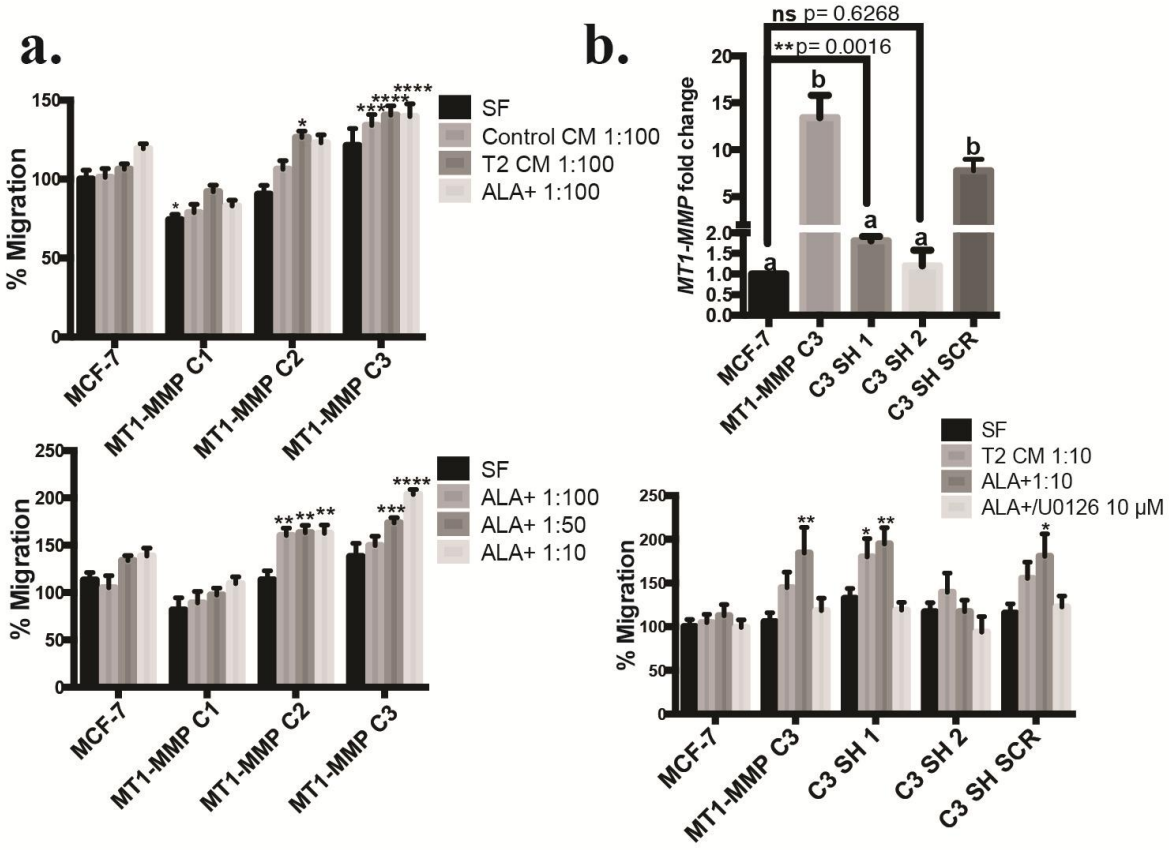
a.
% Migration
SF
Control CM 1:100
T2 CM 1:100
ALA+ 1:100
MCF-7
MT1-MMP C1
MT1-MMP C2
MT1-MMP C3
SF
ALA+ 1:100
ALA+ 1:50
ALA+ 1:10
b.
ns p= 0.6268
**p= 0.0016
MT1-MMP fold change
MCF-7
MT1-MMP C3
C3 SH 1
C3 SH 2
C3 SH SCR
SF
T2 CM 1:10
ALA+1:10
ALA+/U0126 10 µM

Figure 14. Low MT1-MMP/high TIMP-2 was optimal to promote migration of MCF-7 cells via ERK activation.

(a) Transwell migration assays of MCF-7 MT1-MMP cell lines incubated for 48 hours in TIMP-2, or ALA+TIMP-2 CM diluted 1:100 (top), or ALA+TIMP-2 CM in increasing dilutions (bottom). Migration is shown as the percentage of migrated cells relative to MCF-7 cells incubated in SF media ± SEM. **(b)** (top) qPCR analysis showing MT1-MMP mRNA from two cell lines derived from MT1-MMP C3 cells that stably express an shRNA construct targeting MT1-MMP, and one cell line stably expressing a control scrambled shRNA construct. Different letters indicate significant differences at $p \leq 0.05$ by one-way ANOVA, Tukey's post-hoc test. Individual student's t-tests comparing MCF-7 cells against the C3 SH 1 cell line is also shown. MT1-MMP transcripts levels are shown as fold change relative to MCF-7 cells ± SEM. (bottom) Transwell migration assay of MT1-MMP C3 cell lines incubated for 48 hours in either TIMP-2 or ALA+TIMP-2 CM diluted 1:10, or ALA+TIMP2 /U0126 (10 μm). Migration is shown as the percentage of migrated cells relative to MCF-7 cells incubated in SF media ± SEM.

the highest level of MT1-MMP, demonstrated an inability to increase migration potential when incubated with TIMP-2 CMs, and this was consistent with the lack of ERK activation upon TIMP-2 treatment in these cells. To determine if the enhanced migratory ability of C3 cells was a result of the relatively low (11 fold) increase in MT1-MMP expression, these cells were transfected with a construct expressing an shRNA targeting MT1-MMP, and two cell lines were selected: C3 SH 1, a partial knockdown which displayed a small but significant increase in MT1-MMP mRNA level (1.8 fold change $p \leq 0.01$) as compared to parental MCF-7 cells, and C3 SH 2, a complete knockdown with 1.1 fold change (ns p=0.62) **(fig 14b, top)**. A cell line was also derived from C3 cells stably expressing a scrambled control shRNA (C3 SH SCR). Migration of these C3 cell line variants were assayed during incubation in SF media containing TIMP-2 or ALA+TIMP-2 CM, or ALA+TIMP-2 CM along with the ERK inhibitor U0126 (10 μM). Consistent with the previous transwell assays, C3 and control C3 SH SCR cells were significantly more migratory than parental MCF-7 cells when exposed to high levels of TIMP-2 (> ~1 μg/ml), and this correlated with ERK activation as ALA+TIMP-2/U0126 incubation attenuated this migration **(fig 14b, bottom)**. This analysis also showed that complete knockdown of MT1-MMP expression (C3 SH 2) inhibited the TIMP-2-mediated increase in migration, indicating that MT1-MMP is needed for enhancement of migratory potential via TIMP-2. Surprisingly, C3 SH 1 cells, which express a small but significant (1.8 fold) increase in MT1-MMP transcript levels, demonstrated a similar TIMP-2-mediated increase in migration via ERK activation. Additionally, I attempted to knockdown MT1-MMP expression in C1 and C2 cells to rescue migratory potential using the same approach, however, this was unsuccessful using transfection of shRNA (not shown) presumably because of the excessively high expression of MT1-MMP in these cells. Taken together, these data demonstrated that TIMP-2 enhancement of

migratory potential is indeed dependent on MT1-MMP and ERK activation, but low levels (1.8 - 11 fold) of MT1-MMP expression appear to be optimal to increase migratory ability, whereas high (> ~1000 fold) MT1-MMP expression does not result in augmented cell migration.

3.3 Low levels of MT1-MMP expression and activity were optimal for cell viability in serum free conditions

To analyze how MT1-MMP overexpression mediated viability and how this might explain the different migratory potential of MCF-7 MT1-MMP cell lines, cell viability was inferred by measuring metabolically active cells using CellTiter 96® AQueous One Solution each day for 7 days during incubation in media containing 10% FBS or SF media **(fig 15)**, which represents the two compartments in the transwell assay. In 10% FBS, C1 cells (high MT1-MMP level) showed a significantly lower viability throughout the 7 days. Conversely C3 cells (low MT1-MMP level) were significantly more viable from seeding until day 3 **(fig 15, top)**. Similarly, in SF media C1 cells were less viable than parental MCF-7 cells from seeding until day 5, whereas C3 cells were significantly more viable during this time **(fig 15, bottom)**. After 6 days of incubation in SF media, all MT1-MMP expressing cells were significantly more viable than MCF-7 cells indicating that MT1- MMP has an essential role in mediating viability during prolonged absence of growth factors. To confirm that MT1-MMP was responsible for this increased viability during SF incubation, the previous analysis was repeated using the C3 knockdown variants **(fig 16)**. Consistent with the previous analysis, only C3 cells had significantly higher viability at day 3, but by day 6 and 9 all MT1-MMP expressing cell lines were significantly more viable than MCF-7 cells **(fig 16a)**. Viability measurements of the C3 knockdown variants demonstrated that MT1-MMP is responsible for enhanced viability during

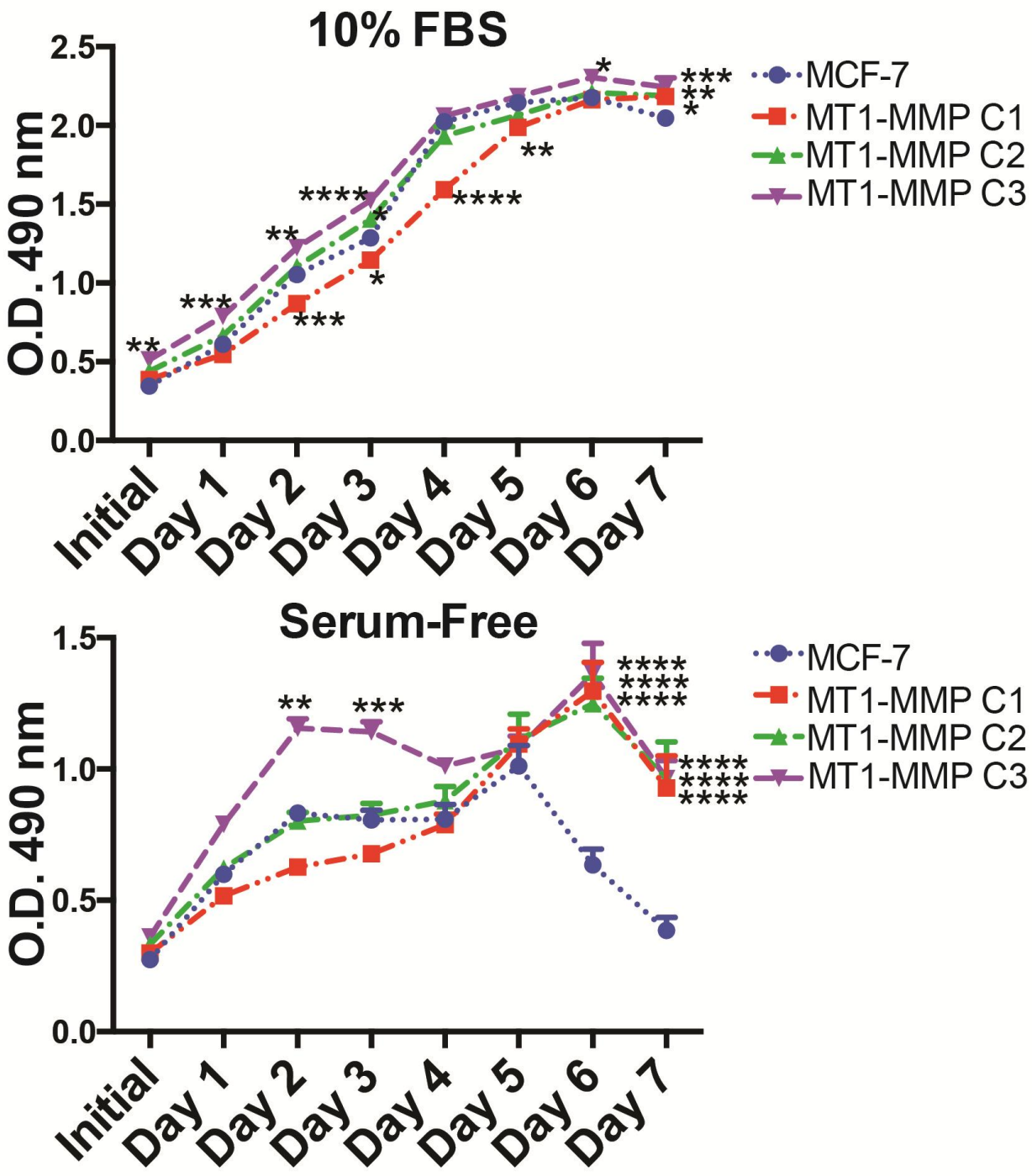
10% FBS
O.D. 490 nm
2.5
2.0
1.5
1.0
0.5
0.0
Initial
Day 1
Day 2
Day 3
Day 4
Day 5
Day 6
Day 7
MCF-7
MT1-MMP C1
MT1-MMP C2
MT1-MMP C3
Serum-Free
O.D. 490 nm
1.5
1.0
0.5
0.0
Initial
Day 1
Day 2
Day 3
Day 4
Day 5
Day 6
Day 7
MCF-7
MT1-MMP C1
MT1-MMP C2
MT1-MMP C3

Figure 15. MCF-7 cells expressing MT1-MMP demonstrated increased viability during incubation in serum-free conditions.

MCF-7 cells and MT1-MMP cell lines were seeded in 96-well cell culture plates and their viability was measured every day for seven days using Celltiter96® during incubation in media containing 10% FBS (top) or serum-free media (bottom). Viability is displayed as mean optical density (O.D) at 490 nm ± SEM.

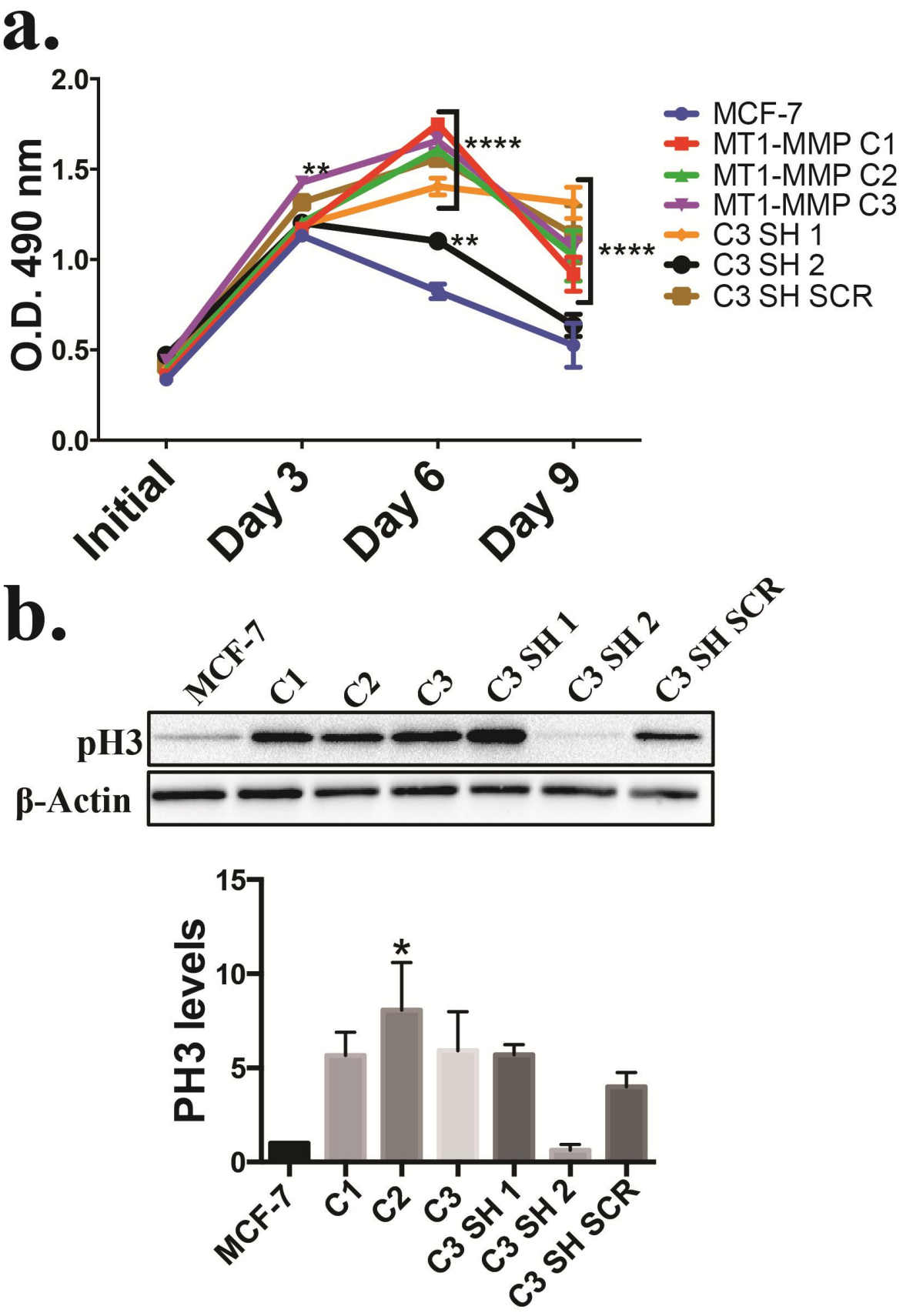
a.
O.D. 490 nm
2.0
1.5
1.0
0.5
0.0
Initial
Day 3
Day 6
Day 9
**
****
**
****
MCF-7
MT1-MMP C1
MT1-MMP C2
MT1-MMP C3
C3 SH 1
C3 SH 2
C3 SH SCR
b.
MCF-7
C1
C2
C3
C3 SH 1
C3 SH 2
C3 SH SCR
pH3
β-Actin
PH3 levels
15
10
5
0
*
MCF-7
C1
C2
C3
C3 SH 1
C3 SH 2
C3 SH SCR

Figure 16. Low levels of MT1-MMP were necessary and optimal for increased survivability of MCF-7 breast cancer cells to serum-free stress.

(a) Viability of MCF-7 MT1-MMP cell lines, C1, C2, and C2, and C3 SH cell line variants during incubation in SF media measured every 3 days for 9 days using Celltiter96®. Viability is displayed as mean optical density (O.D) at 490 nm ± SEM. **(b)** Immunoblot analysis showing PH3 protein levels collected from MCF-7 MT1-MMP cell lines and C3 cell line variants incubated in SF media for 6 days. β-actin was used as a loading control. Bar graph below shows densitometry analysis of PH3 levels relative to β-actin and normalized to MCF-7 cells ± SEM.

SF incubation as C3 SH 2 cells, which are MT1-MMP deficient similar to parental MCF-7 cells, are less viable than other cell lines at day 6, and show the same viability as MCF-7 cells at day 9. To corroborate these results, cell lysates from MCF-7 MT1-MMP cell lines that were incubated in SF media for 6 days were analyzed via immunoblot **(fig 16b)** for the cell proliferation marker phospho-histone 3 (PH3), and quantified using densitometry **(fig 16b, bar graph)**. All MCF-7 cell lines that expressed significantly higher levels of MT1-MMP than MCF-7 cells showed higher levels of PH3 after incubation in SF media, particularly C2 cells, which accumulated high levels of active MT1-MMP protein, and showed significantly higher levels of PH3 than MCF-7 cells.

It was then examined how inhibition of select signaling pathways affected the viability of MCF-7 MT1-MMP cell lines during prolonged SF incubation to gain insight into the mechanism behind MT1-MMP-mediated survivability. The chemical inhibitors U0126, BB94, furin inhibitor II, and AKT inhibitor IV were used to examine their effect on the viability of MCF-7 MT1-MMP cell lines after 6 days of SF incubation **(fig 17)**. ERK inhibition and AKT inhibition significantly decreased the viability of all MT1-MMP expressing cells consistent with the observations of others [99, 100]. Furin inhibitor (which would inhibit intracellular activation of MT1-MMP) showed a non-significant dose dependent decrease in the viability of cells expressing MT1-MMP, a trend not seen in MCF-7 parental cells, indicating that high levels of pro-MT1-MMP likely negatively mediated viability. Unlike all the other inhibitors that generally decreased viability, low concentrations of BB94 trended to increase the viability of all MT1-MMP expressing cells, especially C1 cells which displayed a significant increase in viability after 6 days of SF incubation with 2.5 μM BB94. Taken together, these data demonstrated that MT1-MMP mediated survivability to serum-free stress, but that excessive MT1-MMP proteolytic

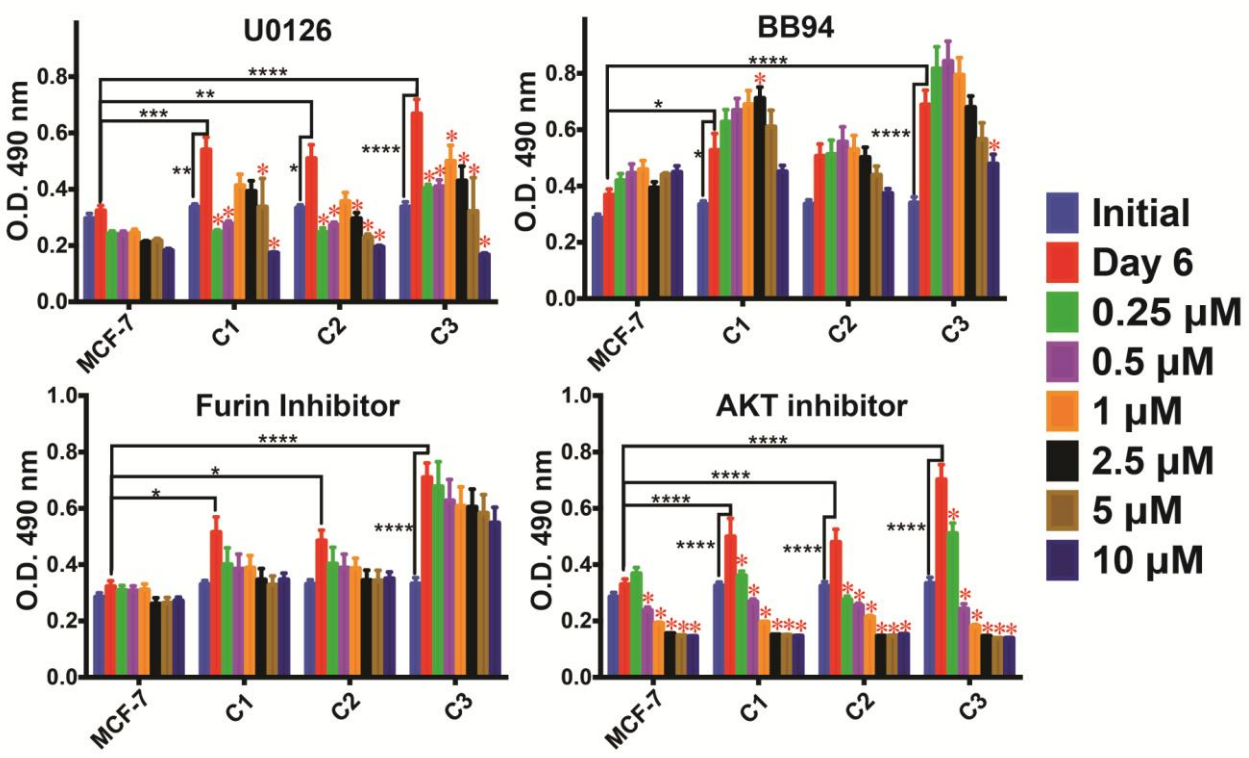
U0126
BB94
Furin Inhibitor
AKT inhibitor
O.D. 490 nm
MCF-7
C1
C2
C3
Initial
Day 6
0.25 µM
0.5 µM
1 µM
2.5 µM
5 µM
10 µM

Figure 17. Low level of MMP activity was optimal for increased viability of MCF-7 breast cancer cells to serum-free stress.

Viability of MCF-7 MT1-MMP cell lines was measured after incubation for 6 days in SF media containing increasing concentrations of U0126, BB94, a furin inhibitor or an AKT inhibitor. Black asterisks show statistically significant differences between the initial and day 6 viability within cell lines, and also differences between the day 6 viability of MCF-7 cells compared to MT1-MMP expressing cell lines. Red asterisks indicate significant differences ($p \leq 0.05$) within cell lines between the day 6 viability in SF media compared to the viability after 6 days of incubation with the different concentrations of the inhibitors. Viability is displayed as mean optical density (O.D) at 490 nm ± SEM.

activity may be counterproductive to increased viability. Furthermore, this analysis also demonstrated that cell viability has to be considered as a component to the pattern of migration seen in transwell assays, as C3 cells which were the most migratory are also the most viable, whereas in contrast C1 cells were the least viable and migratory. Therefore, it is difficult to delineate the relative contribution of changes in cell proliferation or changes in migratory capability to the difference in the number of cells quantified in the bottom compartment of a transwell at the endpoint of the assay.

3.4 MT1-MMP levels did not correlate with migratory potential of breast cancer cells

Here I present evidence that high MT1-MMP levels (transient transfectants, C1 and C2 cells) did not correlate with the migration of MCF-7 breast cancer cells, as seen using the transwell migration assay, which I showed also included a substantial cell viability component. Increased MT1-MMP-mediated viability may have yielded a higher number of cells in the transwell compartments, which may have resulted in incorrect conclusions about migratory potential if viability were not considered. To confirm that high MT1-MMP overexpression (> 1000 fold compared to MCF-7 cells) does not result in increased migration, a live imaging approach was used with automated migration quantification of MCF-7 MT1-MMP cells that were stably expressing fluorescent zsGreen protein and incubated on Alexa594 gelatin coated coverslips in control conditions (0.1% DMSO) **(fig 18, videos 1-4)** and with BB94 (10 μM) (data not shown). Automated quantification using the ADAPT plugin for ImageJ software [114] allowed me to track the migration of all individual cells in three independent experiments, which were then grouped according to their distance migrated **(fig 18b, video 5)**. This analysis showed

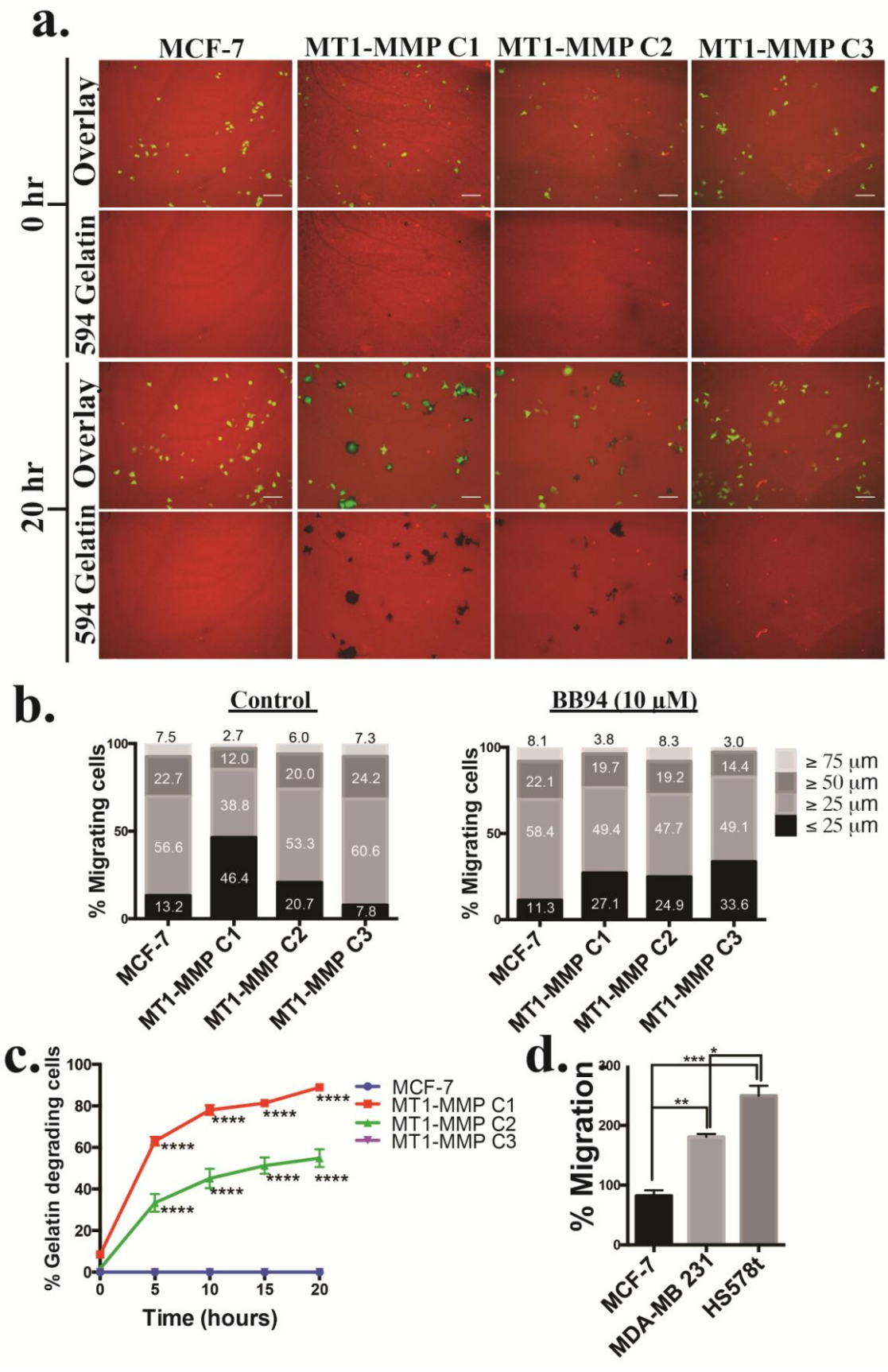
a.
MCF-7
MT1-MMP C1
MT1-MMP C2
MT1-MMP C3
0 hr
Overlay
594 Gelatin
20 hr
Overlay
594 Gelatin
b.
Control
BB94 (10 µM)
% Migrating cells
7.5
2.7
6.0
7.3
22.7
12.0
20.0
24.2
56.6
38.8
53.3
60.6
13.2
46.4
20.7
7.8
8.1
3.8
8.3
3.0
22.1
19.7
19.2
14.4
58.4
49.4
47.7
49.1
11.3
27.1
24.9
33.6
≥ 75 µm
≥ 50 µm
≥ 25 µm
≤ 25 µm
MCF-7
MT1-MMP C1
MT1-MMP C2
MT1-MMP C3
c.
% Gelatin degrading cells
Time (hours)
MCF-7
MT1-MMP C1
MT1-MMP C2
MT1-MMP C3
****
d.
% Migration
***
*
**
MCF-7
MDA-MB 231
HS578t

Figure 18. MT1-MMP levels were inversely correlated to the migratory potential of breast cancer cells.

(a) MCF-7 MT1-MMP cell lines stably expressing zsGreen were seeded on Alexa594-gelatin (red) coated coverlips in media containing 0.1% DMSO (control) or 10 μm BB94 and incubated in a live imaging chamber. Each sample was imaged at the same five stage positions every 10 mins for 20 hours to visualize zsGreen cell movement and associated ECM degradation, shown as black holes devoid of Alexa594 signal (Videos 1-4). Shown are stills of the Alexa594 gelatin channel and an overlay including the zsGreen cells at time 0 and 20 hours post-seeding of the control sample (BB94 not shown). Scale bars = 100 μm. **(b)** Time-lapse videos from (a) were analyzed using the ADAPT plugin for ImageJ and all individual cells tracked from each cell line were examined and grouped according to their migration distance from initial point of tracking. **(c)** Percentage of cells per field of view from each cell line that degraded the underlying AlexaFluour594-gelatin at five different time points. MCF-7 and MT1-MMP C3 cells did not demonstrate degradation of the underlying fluorescent gelatin. **(d)** Transwell migration assay of MCF-7, MDA-MB 231, and HS578t breast cancer cells incubated in SF media for 24 hours. Migration is shown as the percentage of migrated cells relative to MCF-7 cells ± SEM.

that high MT1-MMP overexpression inhibited migration of MCF-7 cells as a higher proportion of C1 and C2 cells migrated a shorter distance from the initial point of tracking compared to parental MCF-7 cells, as 53% and 79% of C1 and C2 cells, respectively, migrated more than 25 μm, compared to 86% of parental MCF-7 cells that migrated the same distance. In contrast, C3 cells did have increased migration ability compared to MCF-7 cells, as 92% of C3 cells migrated more than 25 μm. Importantly, this 6% increase in migratory ability between MCF-7 and C3 cells does not reflect the increase seen using the transwell assays (20-100% increase), confirming that there is a cell viability component underlying the number of cells that transgressed to the bottom transwell compartment. BB94 incubation did not affect the migration of MCF-7 cells or C2 cells, but did alter the migratory patterns of C1 and C3 cells. Inhibition of MMP activity by BB94 decreased the migratory ability of C3 cells as 92% of cells migrated more than 25 μm in control conditions compared to 66% during BB94 incubation. C1 cells, which express the highest level of MT1-MMP and are the least migratory under control conditions, markedly improved their migratory potential during BB94 incubation as 73% of cells migrated more than 25 μm (compared to 53% in control conditions). This migration data is consistent with the cell viability assay during BB94 incubation, as C1 cells saw an augmentation rather than decrease in viability and migration when MMPs were inhibited, suggesting that excessive MMP activity is counterproductive to those cellular processes. Analysis of the percentage of cells that degraded the underlying ECM demonstrated a time-dependent increase in ECM degradation correlated to high MT1-MMP expression in C1 and C2 cells **(fig 18c**), confirming functional MT1-MMP protein production in these cells during the course of this assay. As expected, incubation with BB94 (10 μM) did not allow for degradation of the fluorescent gelatin by MT1-MMP expressing cells (not shown). Taken together, this analysis demonstrated that low levels of MT1-MMP

expression (11 fold compared to parental cells) are optimal for increased migratory ability of MCF-7 breast cancer cells, whereas high MT1-MMP overexpression (> 1000 fold) does not increase migration but allows for widespread ECM degradation. To further investigate the correlation between MT1-MMP expression levels and the migratory potential of cells, I extended my observations to MDA-MB 231 and HS578T breast cancer cells. Transwell migration assays demonstrated that MDA-MB 231 and HS578t were significantly more migratory than MCF-7 cells **(fig 18d)**. Importantly, HS578t cells were significantly more migratory than MDA-MB 231 cells even though they express lower levels of MT1-MMP **(fig 12)**.

Having examined MT1-MMP overexpression in MT1-MMP deficient MCF-7 cells, I then tested how overexpression of MT1-MMP in MDA-MB 231 cells affects the migration of cells that natively express MT1-MMP and have endogenous migratory ability. MDA-MB 231 MT1-MMP stable cell lines were created in the same manner as the MCF-7 cell lines, and three were selected which produce the isoforms of MT1-MMP shown via immunoblot **(fig 19a)**. MDA-MB 231 C1 cells produce pro- and active- MT1-MMP, whereas MDA-MB 231 C2 and C3 produce predominantly active MT1-MMP at higher levels than parental MDA-MB 231 cells. Transwell migration analysis of these MDA-MB 231 MT1-MMP cell lines showed that overexpression of MT1-MMP significantly decreased their migratory potential compared to parental MDA-MB 231 cells **(fig 19b)**. Viability of these cell lines was analyzed in 10% FBS (top) and SF media (bottom) in the same manner as MCF-7 cell lines to show that MT1-MMP overexpression significantly inhibited viability, particularly of MDA-MB 231 C1 and C3 cells **(fig 19c)**. Further, MDA-MB 231 C2 cells, which accumulate high levels of active MT1-MMP protein, exhibited increased viability in SF media and during prolonged incubation in 10% FBS, which was consistent with both the PH3 analysis of MCF-7 C2 cells that predominantly produce

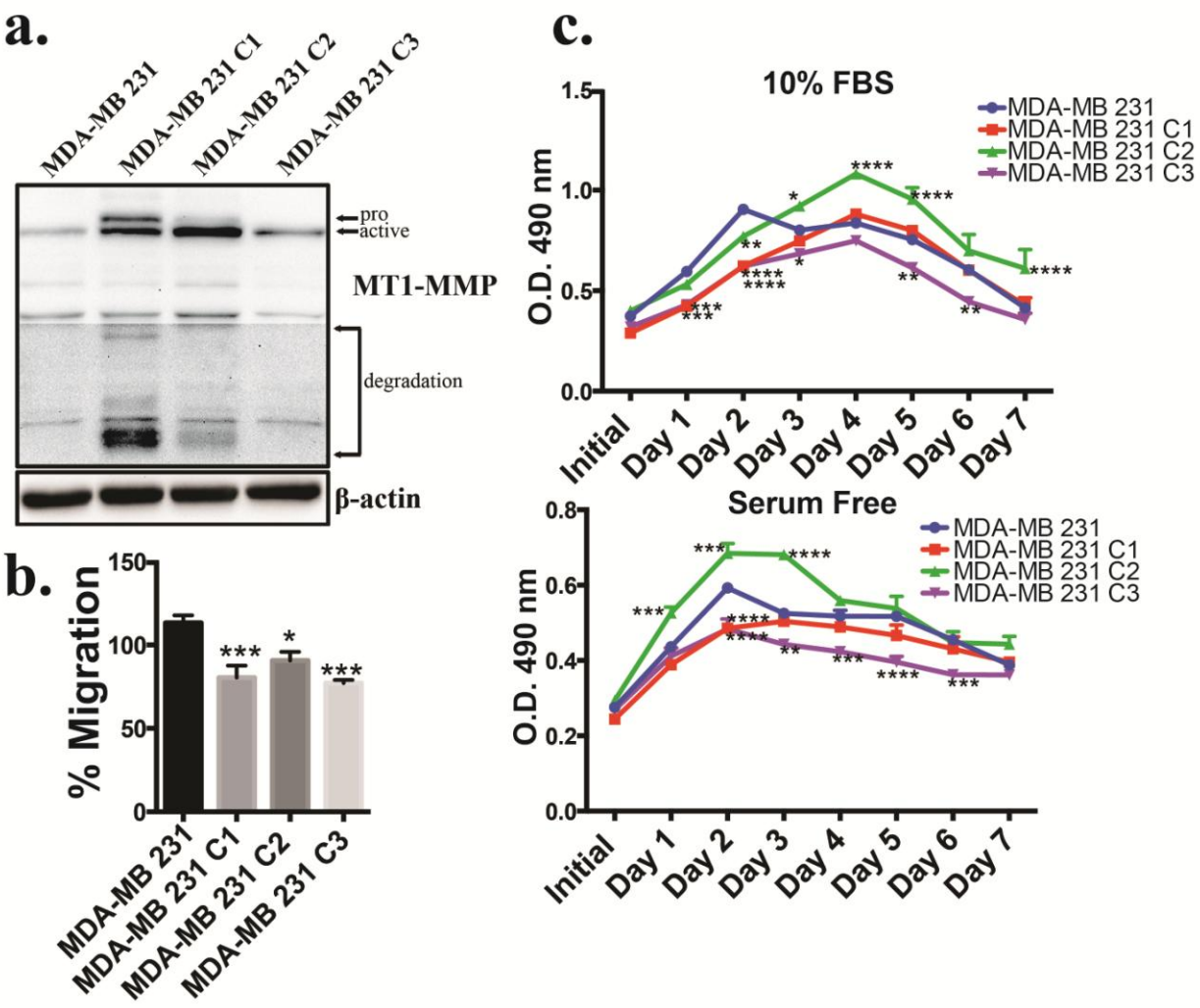
a.
MDA-MB 231
MDA-MB 231 C1
MDA-MB 231 C2
MDA-MB 231 C3
pro
active
MT1-MMP
degradation
β-actin
b.
% Migration
150
100
50
0
***
*
***
MDA-MB 231
MDA-MB 231 C1
MDA-MB 231 C2
MDA-MB 231 C3
c.
10% FBS
MDA-MB 231
MDA-MB 231 C1
MDA-MB 231 C2
MDA-MB 231 C3
O.D. 490 nm
1.5
1.0
0.5
0.0
Initial
Day 1
Day 2
Day 3
Day 4
Day 5
Day 6
Day 7
Serum Free
MDA-MB 231
MDA-MB 231 C1
MDA-MB 231 C2
MDA-MB 231 C3
O.D. 490 nm
0.8
0.6
0.4
0.2
0.0
Initial
Day 1
Day 2
Day 3
Day 4
Day 5
Day 6
Day 7

Figure 19. Overexpression of MT1-MMP in MDA-MB 231 cells negatively affected migration and viability

(a) Immunoblot analysis (AB6004) showing pro- (63 kDA), active (60 kDa), and degradation forms (44 kDa) of MT1-MMP in MDA-MB 231 breast cancer cells and three MDA-MB 231 cell lines expressing different levels of MT1-MMP. β-actin was used as a loading control. Lower half of blot is digitally transformed to clearly shown degradation bands. **(b)** Transwell migration assay of MDA-MB 231 MT1-MMP cells incubated in SF media for 12 hours. Migration is shown as the percentage of migrated cells relative to MDA-MB 231 cells ± SEM. **(c)** Viability of MDA-MB 231 MT1-MMP cell lines during incubation in media containing 10% FBS (top) or serum free media (bottom) measured daily for 7 days using Celltiter96®. Viability is displayed as mean optical density (O.D) at 490 nm ± SEM.

active MT1-MMP, and with their higher migration levels relative to the other MDA-MB 231 MT1-MMP cell lines. Taken together these analyses show that naturally increased MT1-MMP expression in transformed cancer cells (MDAMB-231, HS578t cells) does result in enhanced migration, but this is not the case for experimental MT1-MMP overexpression (MCF-7 MT1-MMP cell lines), as increasing overexpression of MT1-MMP decreases rather than enhances the migratory potential of breast cancer cells.

Furthermore, the levels of MMP-2 and -9 produced by MDA-MB 231 cells were analyzed via gelatin zymography and qPCR to determine if MT1-MMP overexpression affected the expression of these genes **(fig 20).** Gelatin zymography analysis was conducted to assay MMP-2 and -9 protein levels after MT1-MMP MDA-MB 231 cell lines were incubated with serum-free media or MMP-2 CM for 12 hours. This analysis demonstrated that MT1-MMP MDA-MB 231 cell lines were capable of activating proMMP-2, particularly C1 and C2 MDA-MB 231 cells that facilitated the transition to the intermediate and active forms of proMMP-2 **(fig 20a).** Interestingly, MDA-MB 231 C1 cells, which express the highest level of MT1-MMP and demonstrated the highest ability to activate proMMP-2, were completely devoid of MMP-9 protein production **(fig 20a, red asterisk)**. This observation was confirmed at the mRNA level using qPCR analysis, which demonstrated a significant change in MMP-2 and -9 levels in C1 and C2 MDA-MB 231 cells, particularly C1 cells which demonstrated a significant decrease in MMP-9 expression and concurrent increase in MMP-2 expression **(fig 20b),** consistent with my previous observations regarding MMP-2/-9 levels and MT1-MMP-mediated ERK activation **(figs 11,12)**.

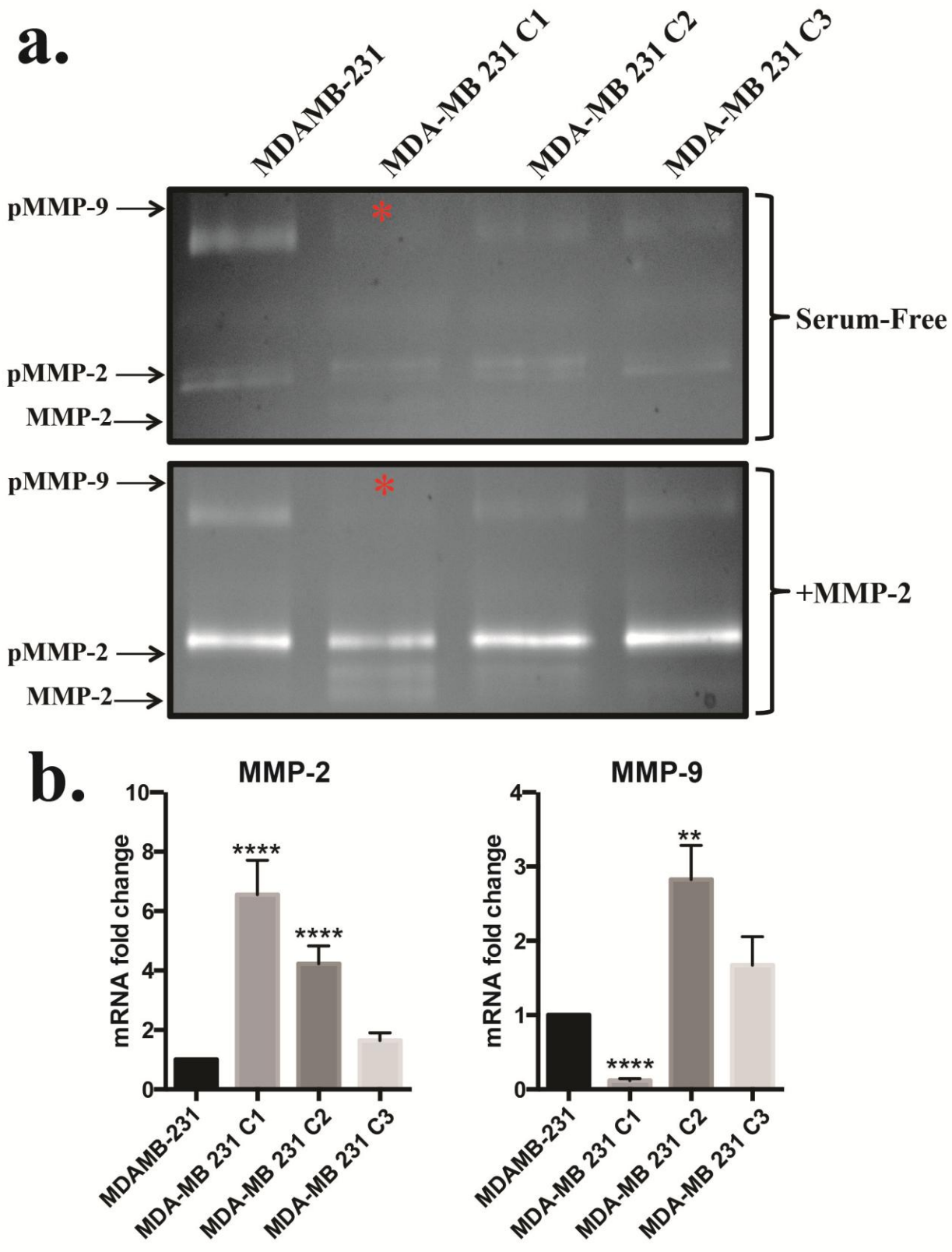
a.
MDAMB-231
MDA-MB 231 C1
MDA-MB 231 C2
MDA-MB 231 C3
pMMP-9
pMMP-2
MMP-2
Serum-Free
pMMP-9
pMMP-2
MMP-2
+MMP-2
b.
MMP-2
mRNA fold change
10
8
6
4
2
0
****
****
MDAMB-231
MDA-MB 231 C1
MDA-MB 231 C2
MDA-MB 231 C3
MMP-9
mRNA fold change
4
3
2
1
0
**
****
MDAMB-231
MDA-MB 231 C1
MDA-MB 231 C2
MDA-MB 231 C3

Figure 20. Overexpression of MT1-MMP in MDA-MB 231 cells permitted proMMP-2 activation and reciprocally affected *MMP-2/-9* levels.

(a) Gelatin zymography analysis of MDA-MB 231 MT1-MMP cell lines after being incubated for 24 hours in serum-free media (top) or serum-free media containing MMP-2 CM (bottom). Red asterisks show a clear deficiency in MMP-9 protein from MDA-MB 231 C1 cells that express the highest level of MT1-MMP. **(b)** qPCR analysis of MMP-2 and MMP-9 mRNA levels from MDA-MB 231 MT1-MMP cell lines. mRNA levels are displayed as mean fold change relative to MDA-MB 231 cells ± SEM.

3.5 Low level of MT1-MMP expression mediated a protrusive phenotype in 3D culture

As my work using *in vitro* 2D culture demonstrated that increased, but relatively low levels of MT1-MMP expression were optimal for enhanced viability and migration, I subsequently examined how these observations translated to *ex vivo* 3D culture. In this culture system breast cancer cells are embedded in Matrigel, whose composition resembles the components of a natural BM, and as such mimics a more physiologically relevant 3D environment [107]. MCF-7 MT1-MMP cell lines were embedded in Matrigel and cultured for 5 days in media containing 10% FBS. During this time, cell morphology was monitored using DIC microscopy to examine how MT1-MMP expression affected cell behavior during 3D culture. Non-invasive MCF-7 cells have been shown to form and remain in circular colonies during 3D culture [120] **(see fig 22, white arrow)**, which resemble the acini-like structures that normal breast cells form that are representative of the terminal ductal lobular unit (TDLU) in the human breast [121]. In contrast, invasive cells, such as MDA-MB 231 cells lose this circular morphology and develop into an interconnected network within the Matrigel **(see fig 25, red arrow)**.

During 3D culture, C1, C2 and C3 cells do not form an interconnect network as seen with MDA-MB 231 cells. Instead, their colonies remained circular but displayed two distinct phenotypes; disseminations - distinct particles being released from circular colonies **(fig 21, green arrow)**, and short dynamic protrusions emerging from colonies **(fig 21, red arrows)**, which were confirmed using time-lapse microscopy **(videos 6-9).** Comparison of the morphological features between cell lines was performed by quantifying the number of disseminations and protrusions over a span of 5 days per 10x magnification fields of view and

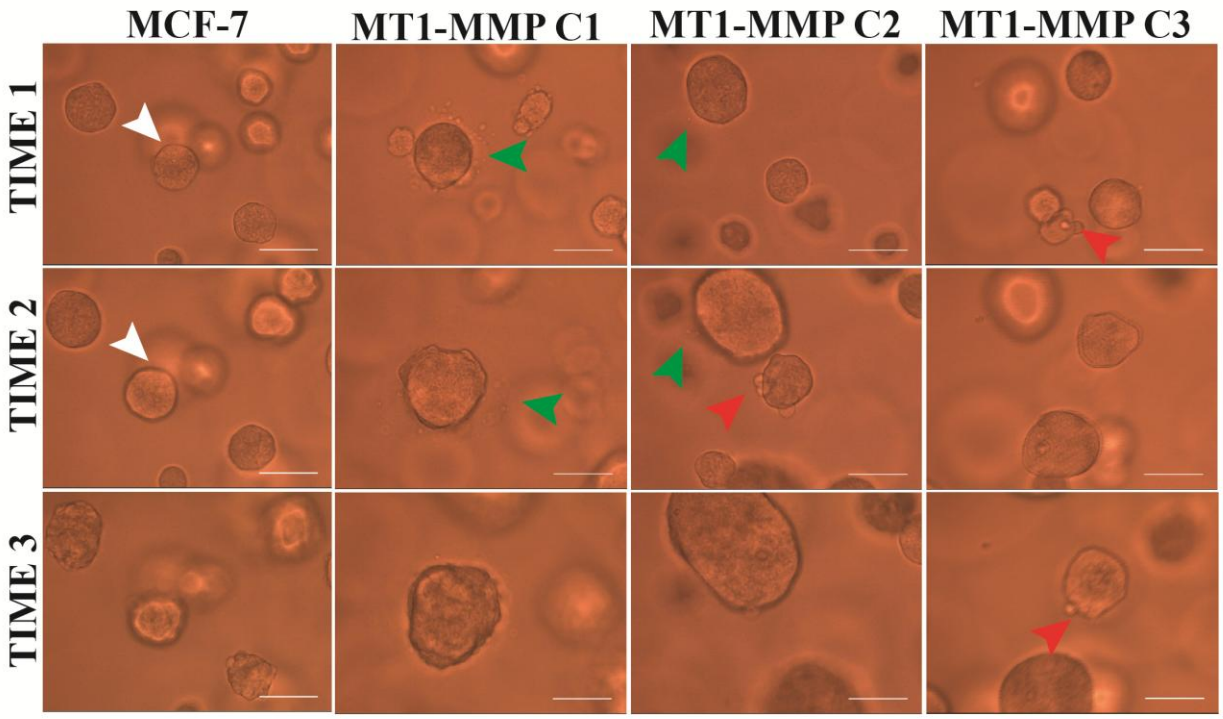
MCF-7
MT1-MMP C1
MT1-MMP C2
MT1-MMP C3
TIME 1
TIME 2
TIME 3

Figure 21. MCF-7 MT1-MMP cell lines demonstrated two distinct morphologies during Matrigel 3D culture.

MCF-7 and MT1-MMP cell lines were embedded in 50% Matrigel and incubated for 5 days in media containing 10% FBS. Between days 2 and 5, samples were placed in a live imaging chamber and imaged at 20x magnification at the same stage position every 30 minutes for 72 hours to make timelapse movies showing cell dynamics in 3D culture (See videos 6-9). Shown are stills at three different time points for each sample that demonstrate two distinct morphologies of MT1-MMP expressing cells during 3D culture. White arrows show a non-invasive circular morphology of MCF-7 cells, green arrows show a dissemination morphology whereby there is a release of cell fragments from circular colonies, and red arrows display dynamic protrusions emerging from colonies. Scale bars = 100 μm.

normalizing it to the number of circular colonies per field of view **(fig 22)**. This quantification demonstrated that MCF-7 cells expressing high levels of MT1-MMP (C1 and C2) had significantly higher number of disseminations per colony than parental MCF-7 and C3 cells, particularly C1 cells which showed a time-dependent release of particles **(video 7)**. In contrast, the number of protrusions per colony at day 5 was inversely proportional to MT1-MMP levels, as C2, and especially C3 cells had significantly more protrusions per colony, whereas C1 cells had a significantly lower number of protrusions than MCF-7 cells. Immunofluorescence analysis of these MCF-7 MT1-MMP cell lines **(fig 23)**, confirmed that while MCF-7 colonies retained circularity during 3D culture (white arrows), C1 and C2 cells had clear disorganization of colony structure with released cell fragments (disseminations) containing MT1-MMP protein (green arrows). In contrast, C3 cells demonstrated long F-actin protrusions emerging from circular colonies (red arrows), consistent with the protrusive phenotype.

To further characterize this novel dissemination phenotype mediated by MT1-MMP, the cellular composition of released fragments was examined by repeating the immunofluorescence analysis with the MCF-7 zsGreen tagged cells **(fig 24)**. The fluorescently tagged variants were used to provide information about the origin of morphological structures as zsGreen accumulated in the cytoplasm and could be used to better visualize the origins of disseminations or protrusions. The number of single cells (marked by DAPI), F-actin disseminations, F-actin protrusions, and zsGreen protrusions were quantified per colony from 20x magnification 3D volume views **(fig 24a)**. This quantification demonstrated that the disseminations are likely enucleated cells, as C1 cells show significantly higher levels of single cells (0.18/colony) and F-actin disseminations (0.67/colony) **(fig 24b)**, which added together represented a density of ~0.85/colony, similar to the ~1 dissemination/colony seen by day 5 in the DIC microscopy

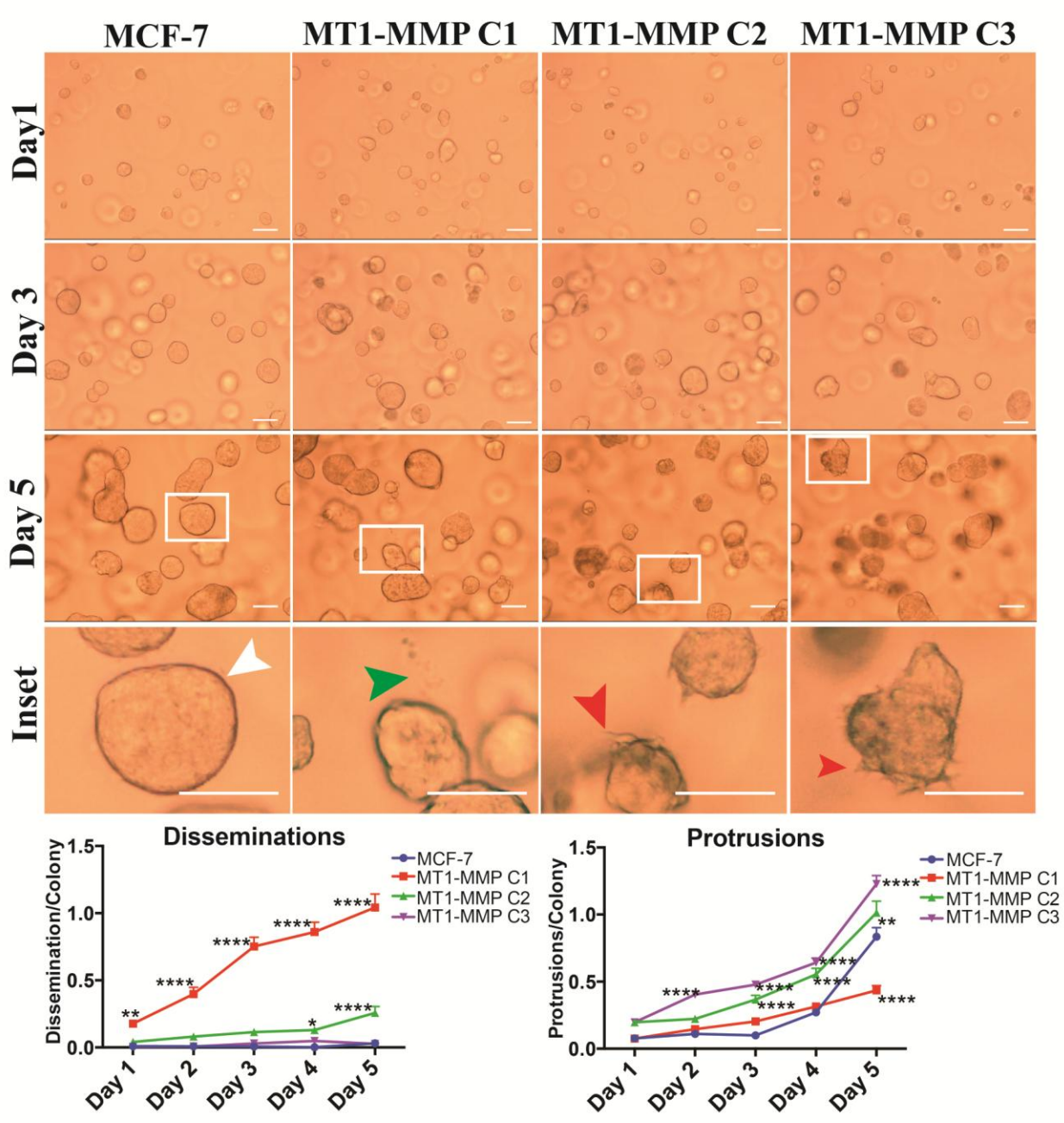
MCF-7
MT1-MMP C1
MT1-MMP C2
MT1-MMP C3
Day1
Day 3
Day 5
Inset
Disseminations
Dissemination/Colony
MCF-7
MT1-MMP C1
MT1-MMP C2
MT1-MMP C3
Day 1
Day 2
Day 3
Day 4
Day 5
Protrusions
Protrusions/Colony

Figure 22. MT1-MMP levels in MCF-7 cells correlated with a dissemination morphology and were inversely correlated with a protrusive morphology in 3D culture.

(top) MCF-7 MT1-MMP cells were embedded in Matrigel and imaged every day for 5 days at 10x magnification. Shown is a representative field of view of each cell line at days 1, 3 and 5, and indicated inset images at day 5 which show the cell features quantified: Circular colonies (white arrow), disseminations around colonies (green arrow), or protrusions emanating from colonies (red arrows). Scale bars = 100 μm. (Bottom line graphs) Five z-stacks per cell line were acquired every day for 5 days and disseminations and protrusions were quantified per colony for each cell line. Morphologies are displayed as mean dissemination/protrusion per colony ± SEM.

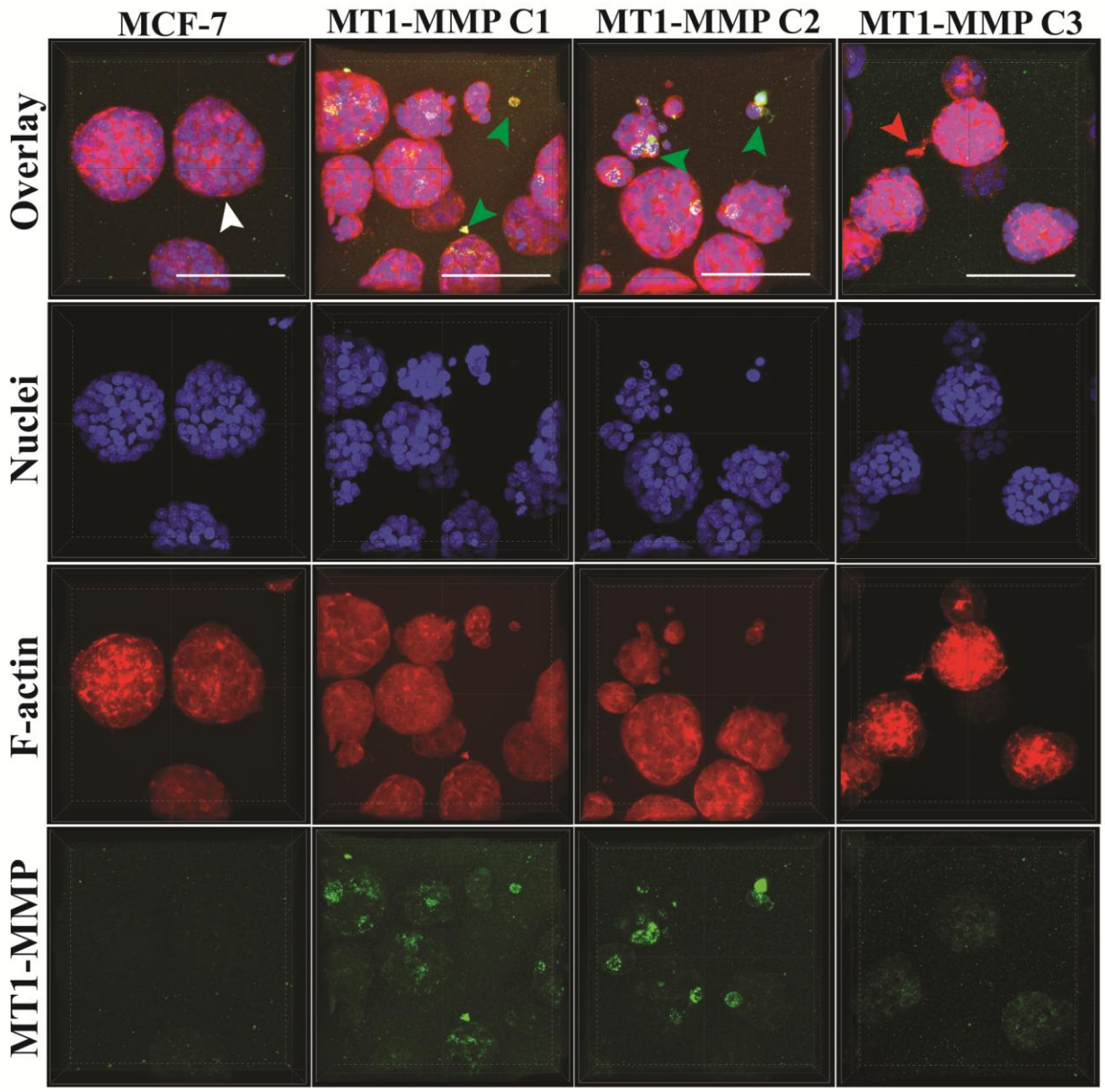
MCF-7
MT1-MMP C1
MT1-MMP C2
MT1-MMP C3
Overlay
Nuclei
F-actin
MT1-MMP

Figure 23. High level of MT1-MMP expression causes loss of colony organization and dissemination release in MCF-7 cells during 3D culture.

Representative 3D volume views of immunofluorescence analysis after MCF-7 MT1-MMP cells were embedded in Matrigel for 5 days. Samples were imaged using confocal microscopy at 60x and are displayed as an overlay (top) showing nuclei (blue), F-actin (red), and MT1-MMP signal (green), and the respective individual channels below. Scale bars = 100 μm. White arrow show circular colonies. Green arrows identify single cells that disseminated from the nearby colonies and show MT1-MMP protein. Red arrow indicates an F-actin protrusion emanating from a circular colony of MCF-7 cells expressing low levels of MT1-MMP.

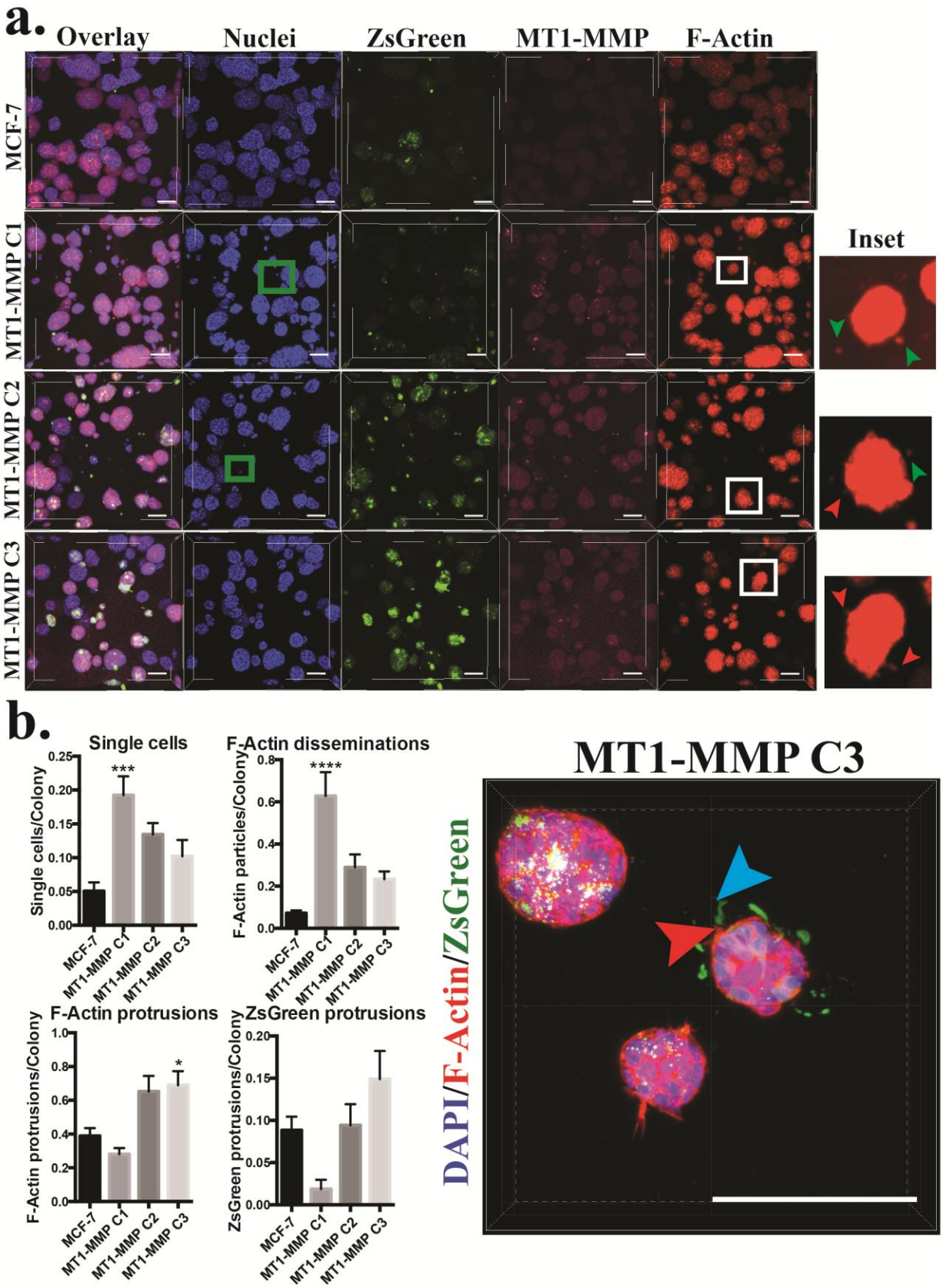
a.
Overlay
Nuclei
ZsGreen
MT1-MMP
F-Actin
MCF-7
MT1-MMP C1
MT1-MMP C2
MT1-MMP C3
Inset
b.
Single cells
Single cells/Colony
F-Actin disseminations
F-Actin particles/Colony
F-Actin protrusions
F-Actin protrusions/Colony
ZsGreen protrusions
ZsGreen protrusions/Colony
MCF-7
MT1-MMP C1
MT1-MMP C2
MT1-MMP C3
MT1-MMP C3
DAPI/F-Actin/ZsGreen

Figure 24. High levels of MT1-MMP correlated with a dissemination phenotype while low levels of MT1-MMP correlated with a protrusive morphology in zsGreen MCF-7 cells during 3D culture.

(a) MCF-7 and MT1-MMP cell lines stably expressing zsGreen were embedded in 50% Matrigel for 5 days and processed for immunofluorescence to visualize nuclei, zsGreen protein, MT1-MMP protein and F-actin distribution. Samples were imaged using confocal microscopy at 20x magnification and displayed as a 3D volume overlay and the individual channels. Green boxes indicate single cells adjacent to a colony, white boxes highlight the magnified insets on the right showing F-actin disseminations (green arrows) and F-actin protrusions (red arrows). Scale bars = 100 μm. **(b)** Single cells, F-actin disseminations, F-actin protrusions, and zsGreen protrusions were quantified from 20x magnification 3D volumes acquired after MCF-7 MT1-MMP cell lines stably expressing zsGreen were embedded in Matrigel for 5 days. The representative 60x magnification 3D volume of MT1-MMP C3 cells on the right shows both F-actin (red arrow) and zsGreen (blue arrow) protrusions emerging from a colony. Scale bars = 100 μm.

analysis **(fig 22)**. In contrast, C3 cells demonstrate higher density of F-actin (0.65/colony) and zsGreen protrusions (0.15/colony), which when added together represent a density of ~0.8/colony similar to the ~1 protrusion/colony seen by day 5 in the DIC analysis, confirming that these cells demonstrate a protrusive morphology in 3D culture. Volume views at 60x magnification also showed C3 colonies (**fig 24b, right**) that demonstrated many zsGreen protrusions (blue arrow) that emerged distal to existing F-actin protrusions (red arrow). These protrusions are indicative of invadopodia, which are characterized by extension of the cell body due to F-actin polymerization, and subsequent F-actin retraction to result in a protrusion devoid of F-actin [66].

To corroborate my 3D observations with the MCF-7, C1, C2 and C3 cell lines, I performed a similar analysis with MDA-MB 231 MT1-MMP cell lines **(fig 25)**. Parental MDA-MB 231 cells progressively lost circular morphology and developed into an interconnecting network of cells within the Matrigel **(fig 25, red arrow)**, represented by a significantly higher number of protrusions per colony (~25) than MCF-7 cells. In contrast, all MDA-MB 231 cells with elevated levels of MT1-MMP showed a significant inhibition to form networks in 3D culture and instead retained a large proportion of circular colonies **(fig 25, white arrows)**. As well, MDA-MB 231 MT1-MMP cells demonstrated a nonsignificant increase in the number of disseminations (~0.4 dissemination/colony), although it was comparatively lower than in MCF-7 MT1-MMP cells. Immunofluorescence analysis of F-actin and nuclear structures in 3D culture confirmed these observations and showed that parental MDA-MB 231 cells formed an extensive cellular network, whereas MDA-MB 231 MT1-MMP cells retained circular colonies marked by MT1-MMP protein **(fig 26)**. Taken together, this *ex vivo* analysis demonstrated that low MT1-MMP expression mediated a protrusive phenotype in 3D culture, shown by MCF-7 C3 **(fig 22)**

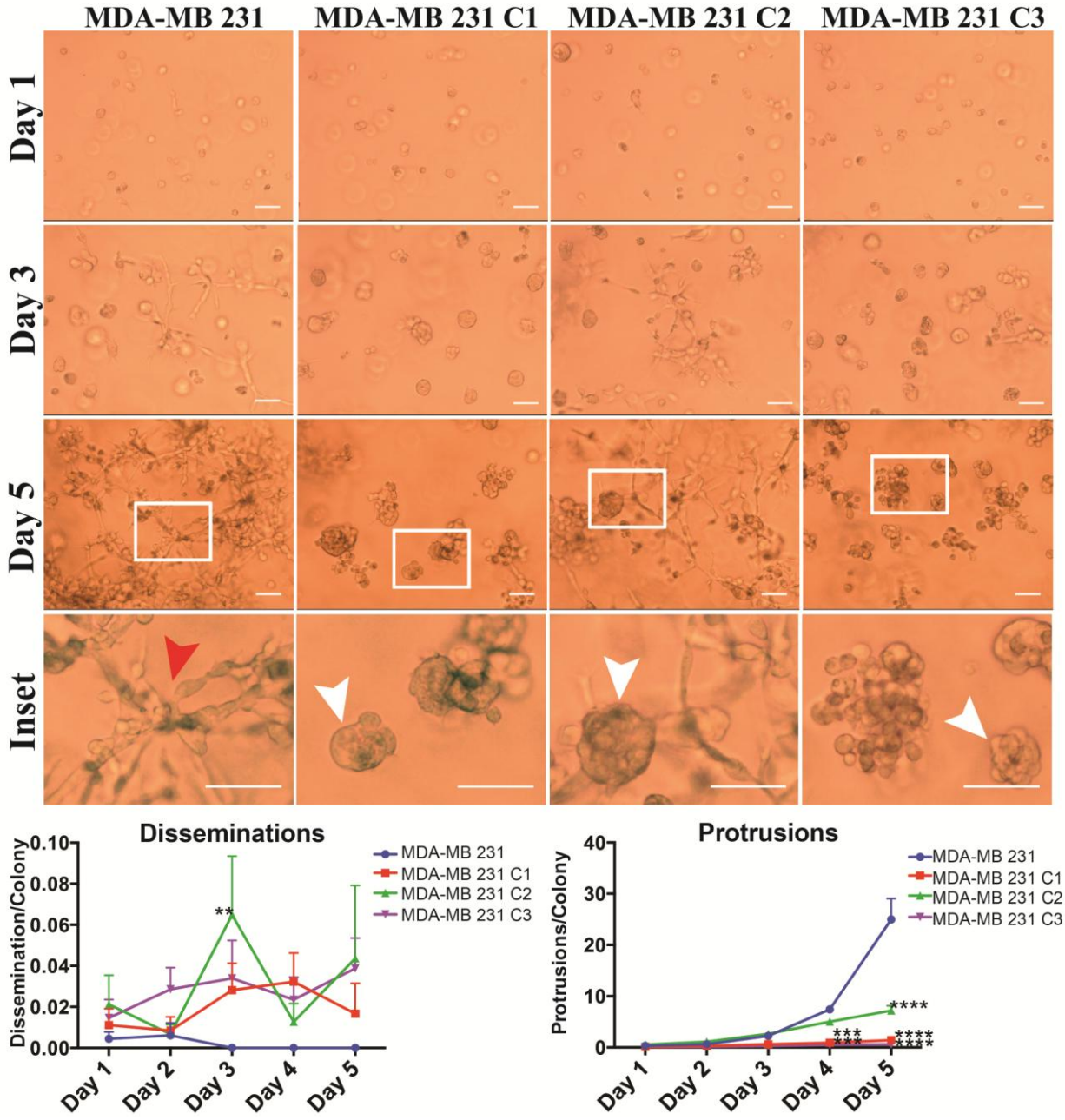
MDA-MB 231
MDA-MB 231 C1
MDA-MB 231 C2
MDA-MB 231 C3
Day 1
Day 3
Day 5
Inset
Disseminations
Dissemination/Colony
0.10
0.08
0.06
0.04
0.02
0.00
**
Day 1
Day 2
Day 3
Day 4
Day 5
MDA-MB 231
MDA-MB 231 C1
MDA-MB 231 C2
MDA-MB 231 C3
Protrusions
Protrusions/Colony
40
30
20
10
0
***
****
****
****
Day 1
Day 2
Day 3
Day 4
Day 5
MDA-MB 231
MDA-MB 231 C1
MDA-MB 231 C2
MDA-MB 231 C3

Figure 25. MT1-MMP overexpression inhibited the protrusive morphology of MDA-MB 231 breast cancer cells in 3D culture.

(a) (top) MDA-MB 231 MT1-MMP cells were embedded in Matrigel and imaged every day for 5 days at 10x magnification. Shown are representative fields of view of each cell line at days 1,3, and 5 and a respective inset at day 5. Red arrow shows a portion of the protrusive network MDA-MB 231 cells form in 3D culture. White arrows show MDA-MB 231 MT1-MMP cell colonies that have retained circularity after 5 days in 3D culture. Scale bars = 100 μm. (Bottom line graphs) Five z-stacks per cell line were acquired every day for 5 days and disseminations and protrusions were quantified per colony for each cell line. Morphologies are displayed as mean dissemination/protrusion per colony ± SEM.

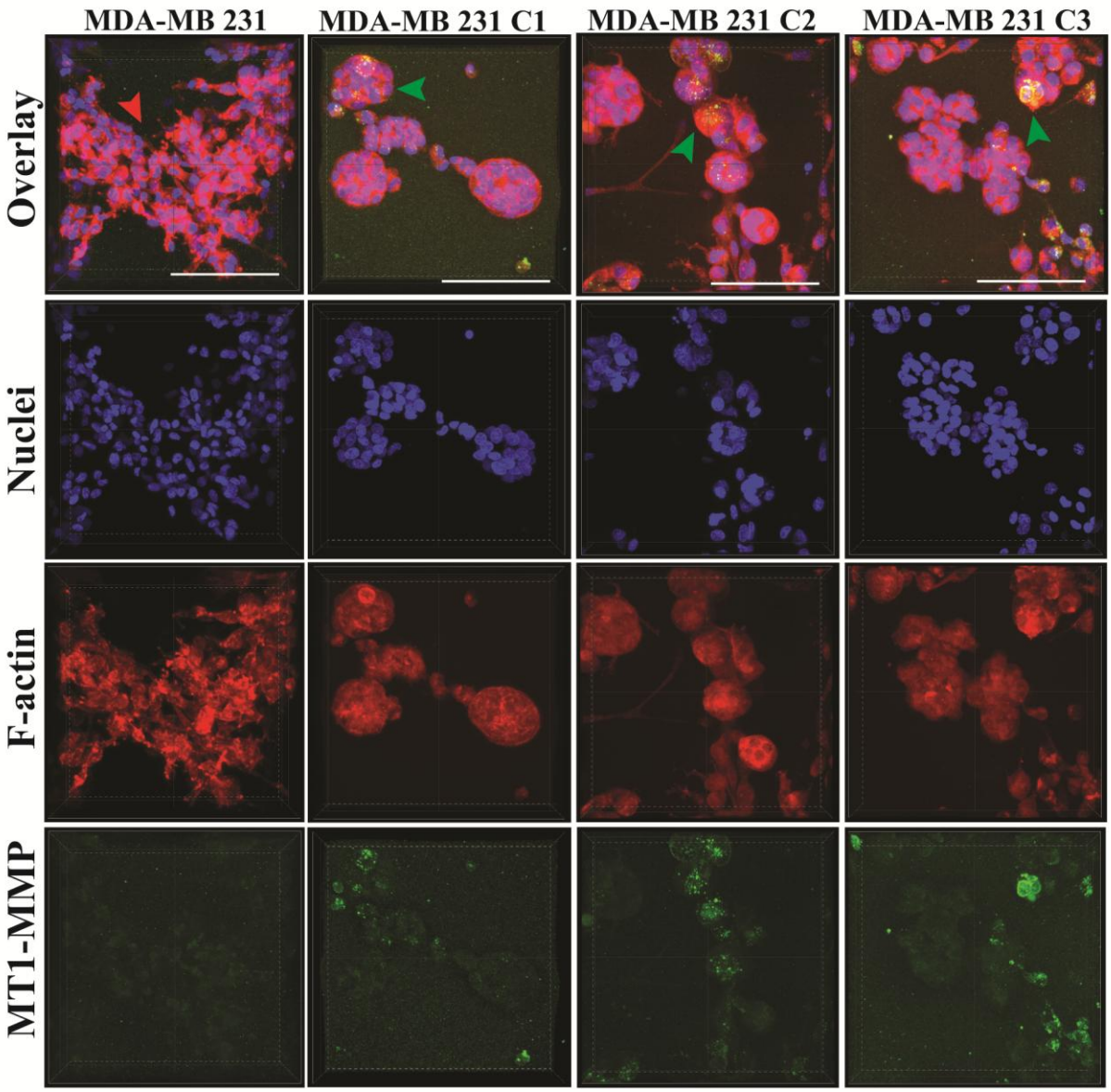
MDA-MB 231
MDA-MB 231 C1
MDA-MB 231 C2
MDA-MB 231 C3
Overlay
Nuclei
F-actin
MT1-MMP

Figure 26. High levels of MT1-MMP mediated retention of a circular morphology of MDA-MB 231 cells during 3D culture.

Representative 3D volume views of immunofluorescence analysis after MDA-MB 231 MT1-MMP cells were embedded in Matrigel for 5 days. Samples were imaged using confocal microscopy at 60x and are displayed as an overlay (top) showing nuclei (blue), F-actin (red), and MT1-MMP signal (green), and the respective individual channels below. Scale bars = 100 μm. Red arrow shows irregular network of MDA-MB 231 cells, whereas green arrows show circular colonies in MDA-MB 231 MT1-MMP cell lines that are positive for MT1-MMP protein signal. Scale bars = 100 μm.

and MDA-MB 231 cells **(fig 25)**, whereas high levels of MT1-MMP expression (C1, C2, and MDA-MB 231 MT1-MMP C1, C2, and C3 cells) inhibited the ability to form protrusive networks in 3D culture and instead resulted in abnormal release of cell fragments.

3.6 Low levels of MT1-MMP expression mediated tumour vascularization and extravasation *in vivo*

Following 3D culture analysis, the *in vivo* implications of the *in vitro* observations were examined by using *ex ovo* chicken embryos [122] and zsGreen expressing MCF-7 C1, C2, and C3 cell lines. These cells, along with zsGreen MDA-MB 231 cells, were suspended in Matrigel and implanted into the ChorioAllantoic Membrane (CAM) of day 9 *ex ovo* chicken embryos [115]. Eight days post implantation the resulting xenograft was visualized using a fluorescent stereoscope to assess vascularization of the formed tumour. No MCF-7 or C1 tumours were scored as vascularized, and only a minority (2/14) of C2 tumours demonstrated vascularization by vessels of the chicken embryo **(fig 27)**. In contrast, the majority of C3 (14/15) and MDA-MB 231 (15/16) tumours were vascularized, shown by the presence of non-fluorescent vessels present within a dissected zsGreen tumour **(fig 28, white arrow)**.

The metastatic potential of these cell lines was subsequently examined by direct intravenous injection of zsGreen MCF-7 C1, C2, and C3 cell lines into the vasculature of day 14 chicken embryos, followed by assessment of extravasation efficiency 24 hours post-injection [109]. Extravasation is a necessary step that precedes metastatic colony formation and as such has been shown to directly correlate with metastatic potential [11]. MCF-7 and C1 cells, which express the highest level of MT1-MMP, demonstrate poor extravasation efficiency, as < 5% of cells were able to extravasate after 24 hours **(fig 29).** C2 cells showed a higher but non-

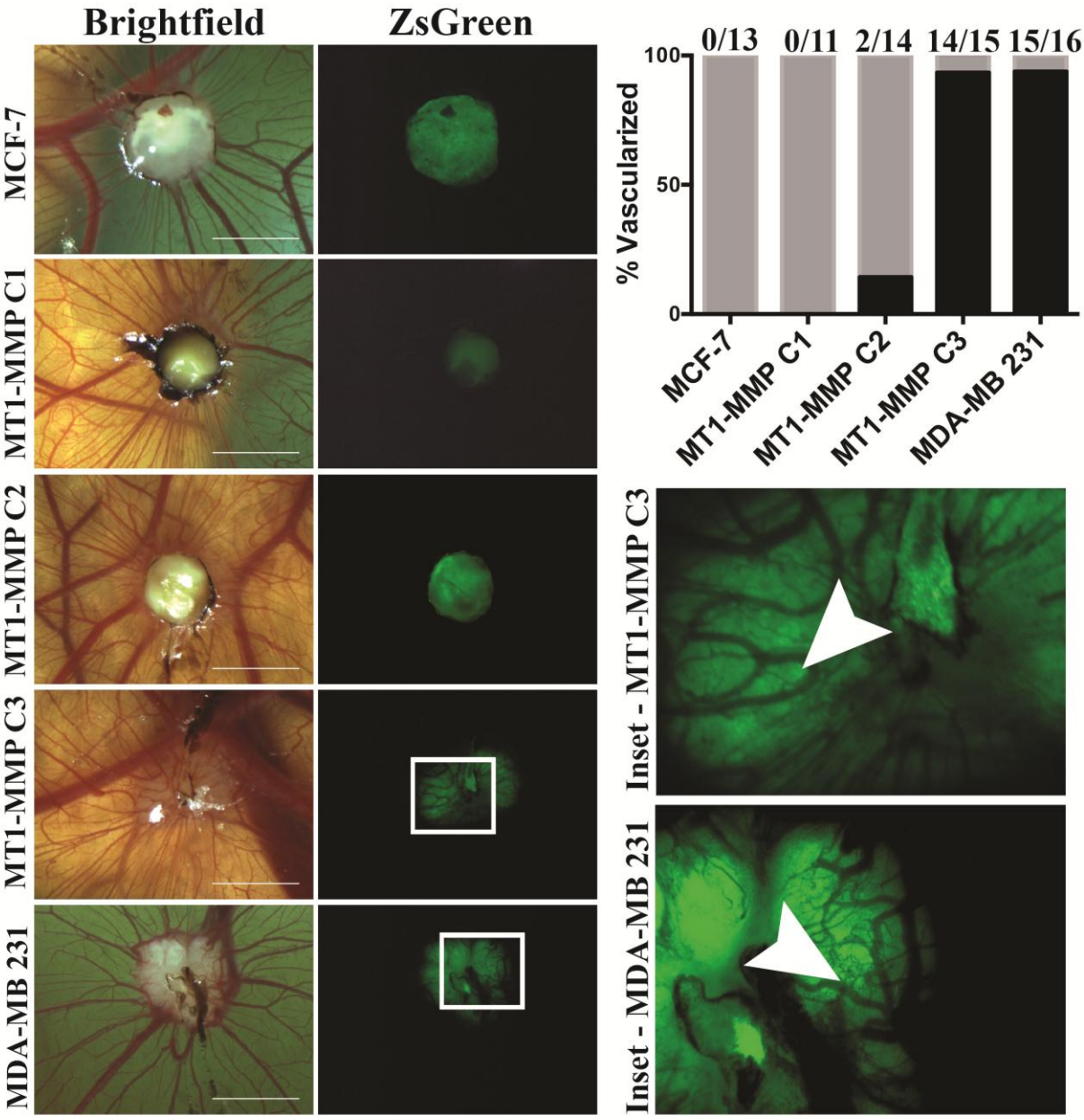
Brightfield
ZsGreen
MCF-7
MT1-MMP C1
MT1-MMP C2
MT1-MMP C3
MDA-MB 231
0/13
0/11
2/14
14/15
15/16
100
50
0
% Vascularized
MCF-7
MT1-MMP C1
MT1-MMP C2
MT1-MMP C3
MDA-MB 231
Inset - MT1-MMP C3
Inset - MDA-MB 231

Figure 27. MCF-7 MT1-MMP C3 cells formed vascularized tumors when implanted onto the avian embryo CAM.

MCF-7 MT1-MMP cell lines and MDA-MB 231 cells stably expressing zsGreen were implanted into the CAM of day 9 *ex ovo* chicken embryos and visualized 8 days post –implantation using a fluorescence stereoscope to analyze tumour vascularization. Displayed are representative bright field images showing the area of implantation on the embryo, and respective fluorescent images showing the zsGreen channel. The white boxes outline the magnified insets showing vascularization of the MT1-MMP C3 and MDA-MB 231 tumours. Bar graph shows percentage of tumours that were vascularized ($N \geq 11$). Scale bars = 2 mm.

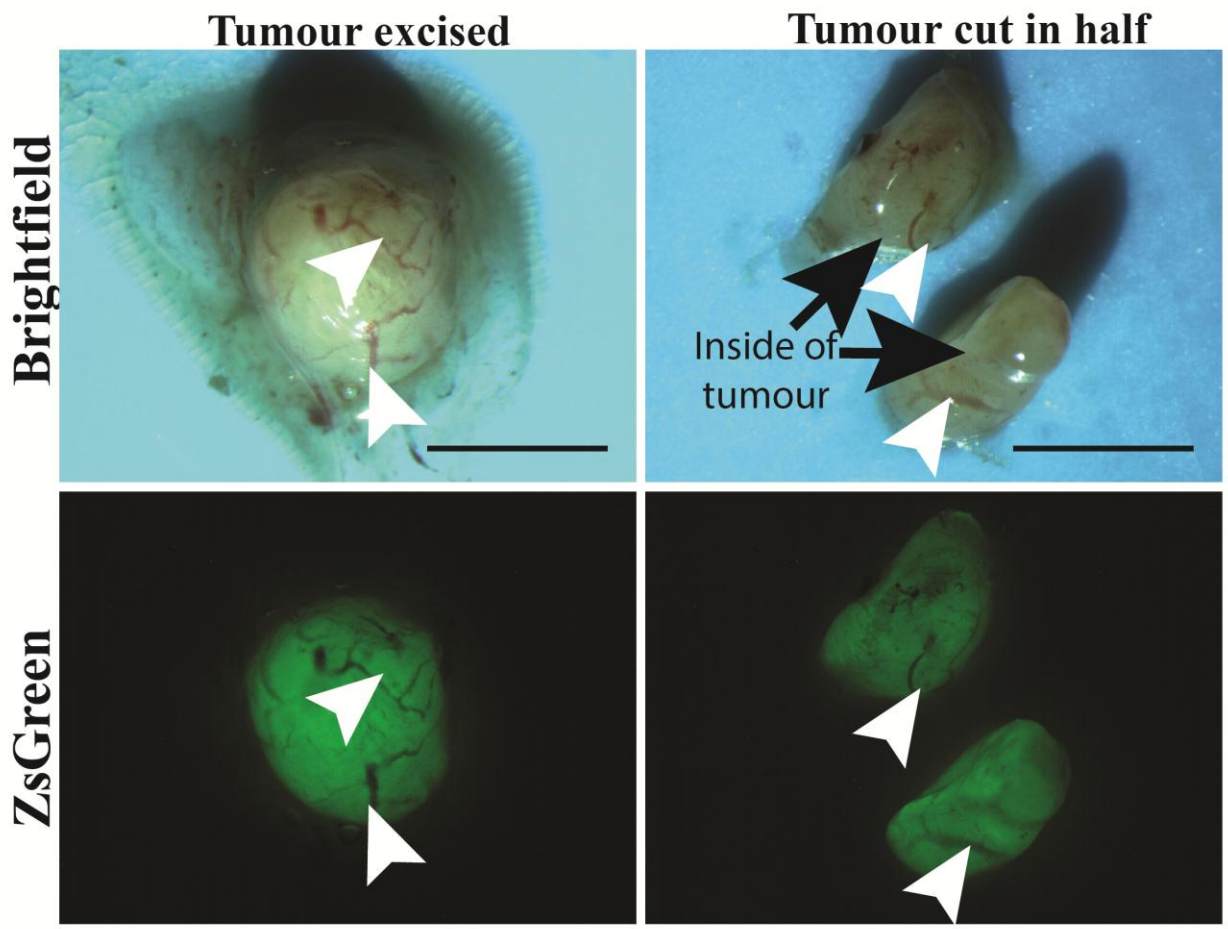
Tumour excised
Tumour cut in half
Brightfield
ZsGreen
Inside of tumour

Figure 28. Excision of vascularized tumours demonstrated internal blood vessels.

A tumour from MDA-MB 231 cells expressing zsGreen was excised from a chicken embryo 8 days post-implantation and imaged using brightfield and fluorescence microscopy. Vessels within the tumour (white arrows) can be seen by the presence of blood (brightfield) and absence of fluorescent signal (zsGreen), which indicate that these vessels originate from the chicken embryo. Cutting this tumour in half and rotating the pieces to reveal the inside of the tumour (black arrows) confirms internal vascularization. Scale bars= 2mm.

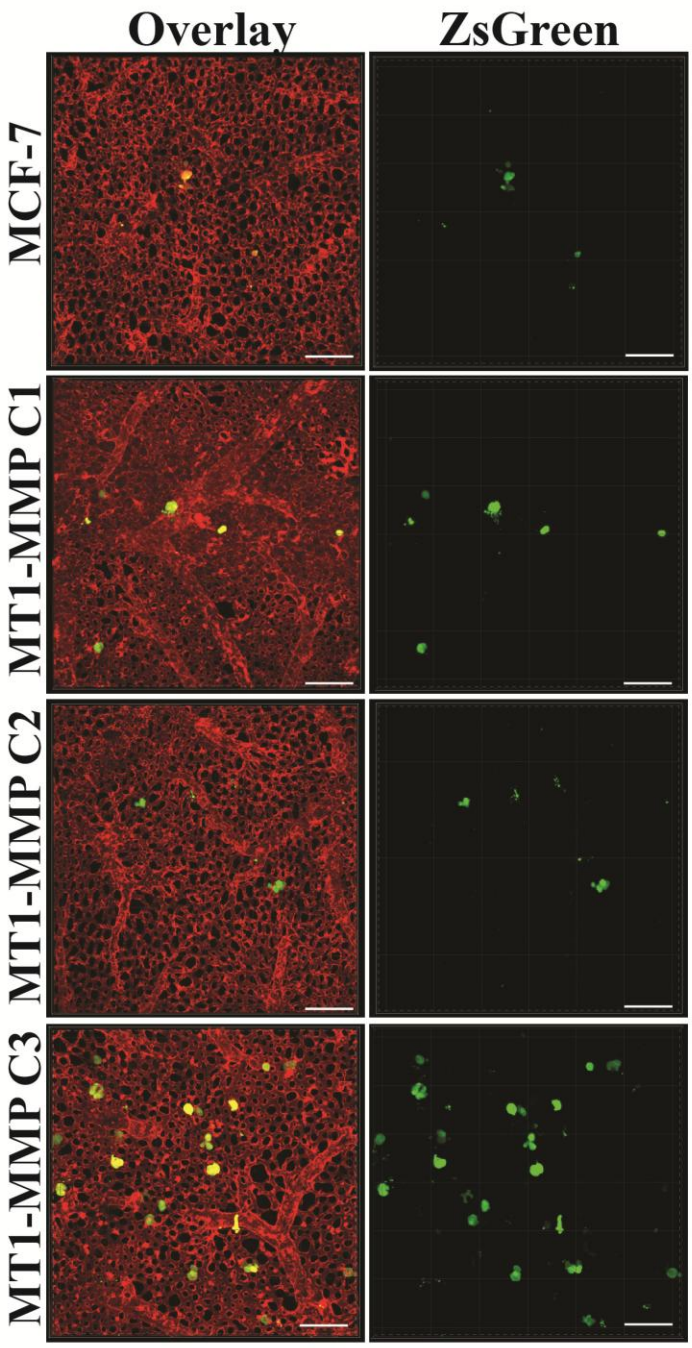
Overlay
ZsGreen
MCF-7
MT1-MMP C1
MT1-MMP C2
MT1-MMP C3

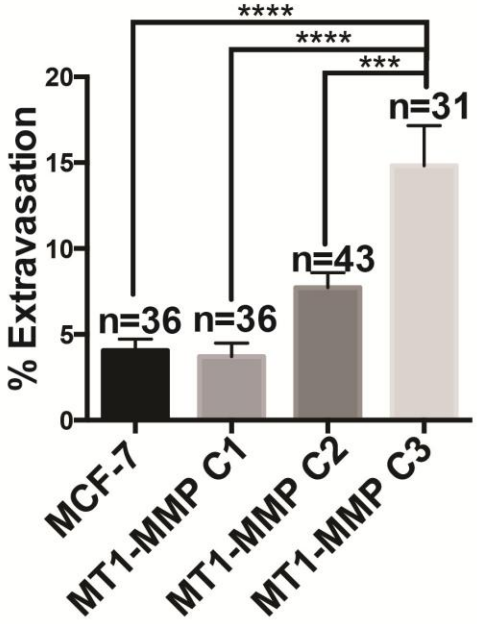
****
****
***
% Extravasation
20
15
10
5
0
n=36
n=36
n=43
n=31
MCF-7
MT1-MMP C1
MT1-MMP C2
MT1-MMP C3

Figure 29. MT1-MMP levels were inversely correlated to the extravasation efficiency of MCF-7 breast cancer cells *in vivo*.

Representative 3D volume views at 20x magnification of MCF-7 MT1-MMP cells stably expressing zsGreen 24 hours-post intravenous injection into the chicken embryo CAM vasculature. Shown is an overlay displaying the zsGreen cells (green) and CAM vasculature and underlying stromal vessels labeled using lectin-rhodamine (red), and the isolated zsGreen channel. Scale bars = 100 μm. Bar graph shows quantification of extravasation efficiency of MCF-7 MT1-MMP cell lines 24 hours post-injection ± SEM.

significant increase in percentage of extravasated cells (~8%), whereas C3 cells, which express low levels of MT1-MMP, displayed a significant increase in extravasation efficiency (~15%) compared to all other MCF-7 cell lines. Orthogonal sections of extravasated C1 and C3 cells acquired using confocal microscopy at 60x magnification showed that C1 cells are capable of extravasating out of the CAM vasculature **(fig 30)** but display membrane blebbing **(white arrow)** and cell fragment release **(green arrow)**, reminiscent of the disseminations observed in 3D culture **(fig 22)**. In contrast, C3 cells exhibited a uniform morphology as they extravasated into the stromal space **(blue arrows)** and contained cell protrusions trailing from the CAM capillary bed into the stroma **(red arrow, video 10)**, suggesting that these cells formed invadopodia *in vivo.*

3.8 Metastatic 21T breast epithelial cell line produces undetectable levels of MT1-MMP protein

To extend and corroborate the observations that low levels of MT1-MMP are optimal to promote metastatic features in 3D culture and *in vivo,* the level of MT1-MMP protein in the 21T series cell lines was assayed via immunoblot **(fig 31)**. These cells were isolated from a single patient and represent a mammary tumour progression series that mimic specific and progressive stages of breast cancer progression [111, 123], from atypical ductal hyperplasia (21PT-ADH), to ductal carcinoma *in situ* (21NT – DCIS) to an invasive mammary carcinoma (21MT-1- IMC). Assaying MT1-MMP protein levels in these cell lines demonstrated that ADH and DCIS variants produced active MT1-MMP, with the non-invasive DCIS cells producing higher levels of MT1-MMP protein. Direct comparison to the MCF-7 MT1-MMP cell lines showed that C1 and C2 cells produced more active MT1-MMP than 21T ADH or DCIS cells. In contrast, 21T MT-1

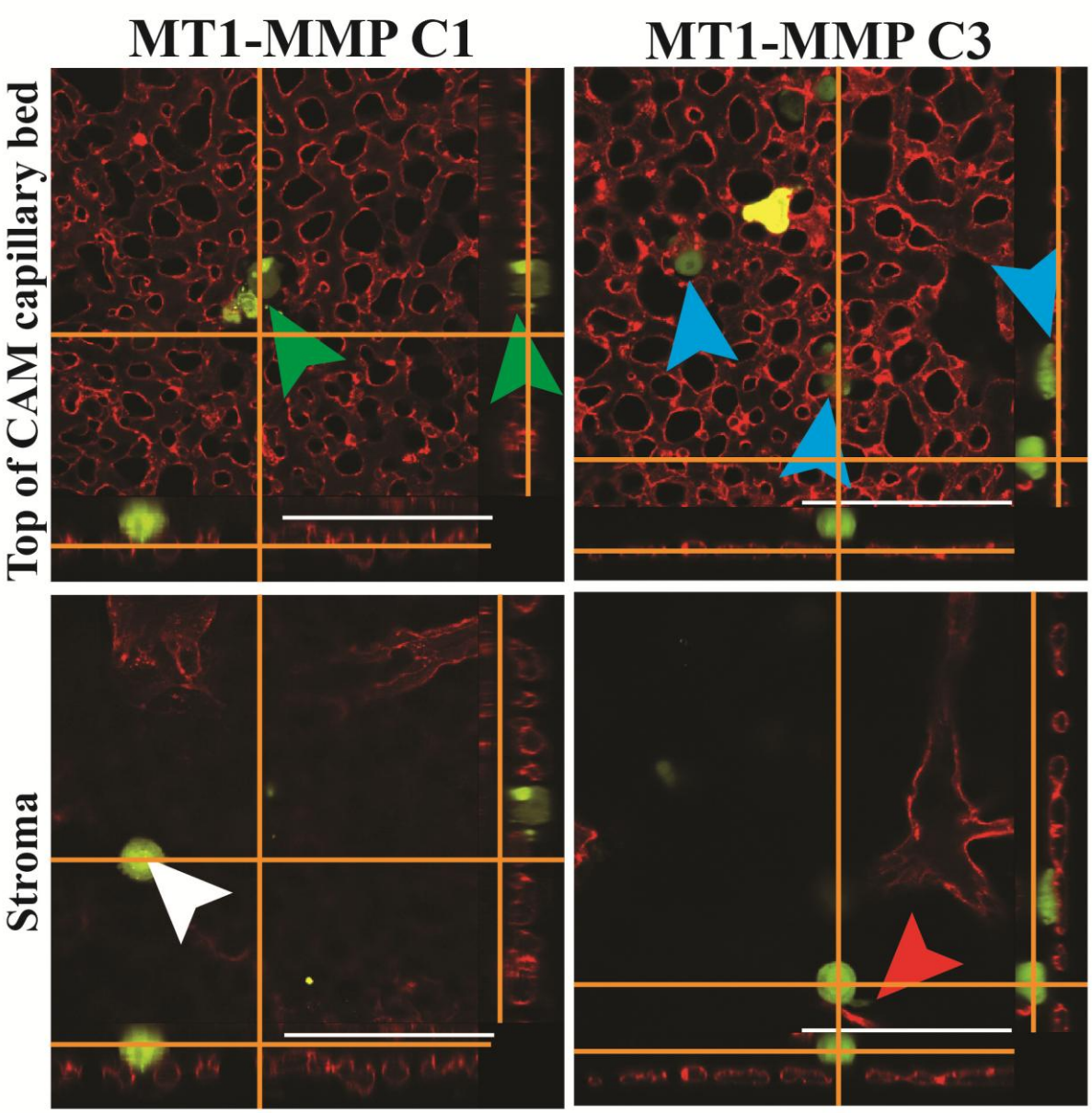
MT1-MMP C1
MT1-MMP C3
Top of CAM capillary bed
Stroma

Figure 30. MCF-7 cells expressing low levels of MT1-MMP demonstrated a uniform protrusive morphology when extravasating *in vivo*.

Orthogonal views of Z-stacks acquired using confocal microscopy at 60x of MT1-MMP C1 and C3 cells 24 hours post-injection showing the top of the CAM capillary bed (top) and the underlying stroma (bottom). Extravasated MT1-MMP C1 cells display cell fragmentation (green arrows) and membrane blebbing (white arrow), whereas MT1-MMP C3 cells extravasate to below the CAM with uniform morphology (blue arrows) and are capable of forming discrete invasive protrusions in the stroma (red arrow). Scale bars = 100 μm.

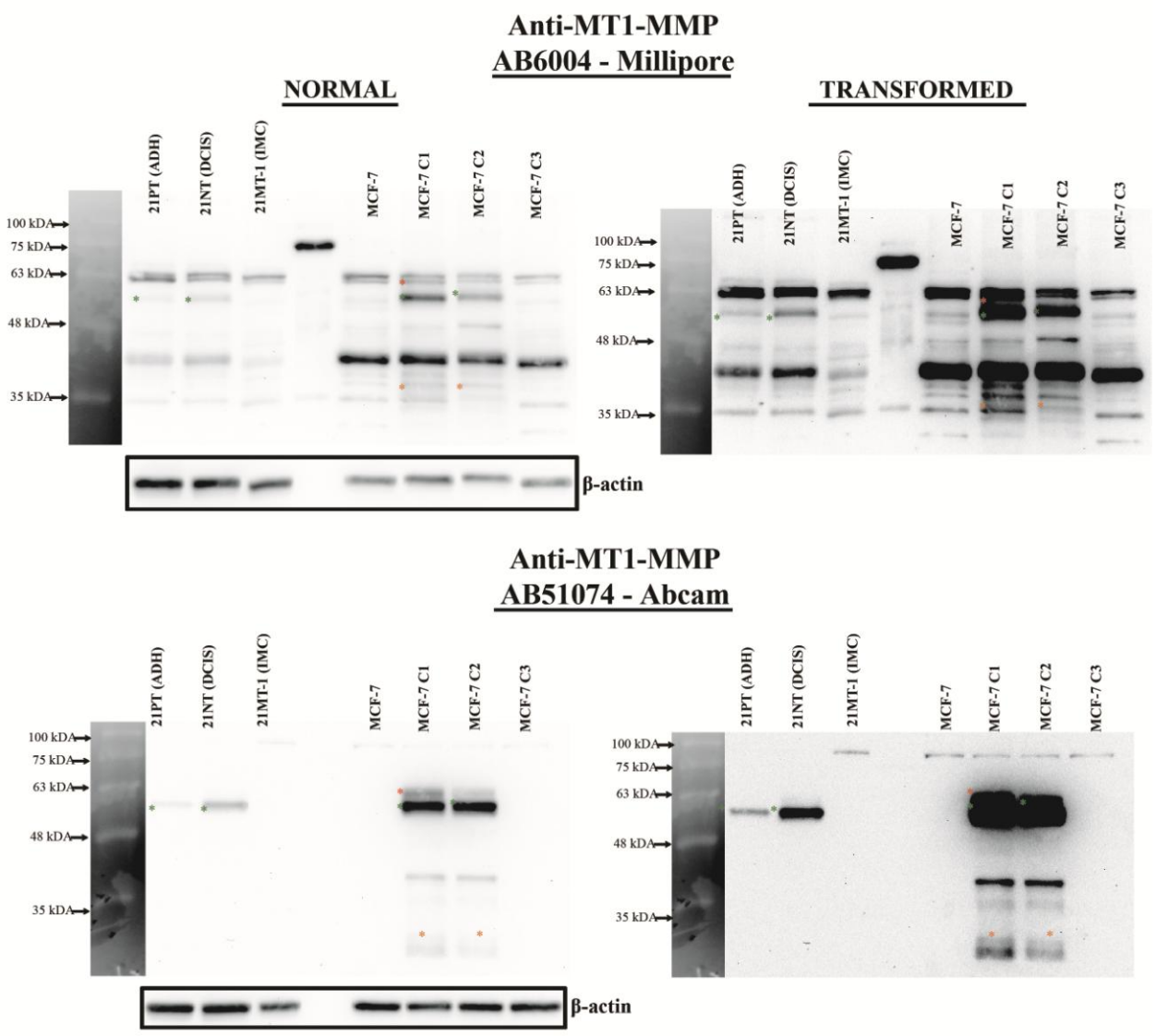
Anti-MT1-MMP
AB6004 - Millipore
NORMAL
TRANSFORMED
21PT (ADH)
21NT (DCIS)
21MT-1 (IMC)
MCF-7
MCF-7 C1
MCF-7 C2
MCF-7 C3
100 kDA
75 kDA
63 kDA
48 kDA
35 kDA
β-actin
Anti-MT1-MMP
AB51074 - Abcam

Figure 31. Metastatic human 21T breast cancer cells showed undetectable levels of MT1-MMP protein similar to MCF-7 C3 cells.

Protein lysate from human 21T breast cancer cell lines, which represent a progression series from atypical ductal hyperplasia (21PT-ADH), to ductal carcinoma *in situ* (21NT – DCIS), to invasive mammary carcinoma (21MT-1- IMC), were analyzed via immunoblot for MT1-MMP protein levels along with the MCF-7 MT1-MMP cell lines. The blots were probed with either AB6004 (top) or AB51074 (bottom) antibody and shown as the normal exposure and as transformed versions to clearly show banding pattern. Asterisks indicate MT1-MMP isoforms (green – pro- form, red- active form, orange – degradation forms). β-actin was used as a loading control.

cells, which represent an invasive mammary carcinoma, produced undetectable levels of MT1-MMP protein as determined by immunoblot, similar to C3 cells. The 21MT-1 IMC cells have been show to possess metastatic qualities in 3D culture and *in vivo* when compared to the non-invasive variants [111], consistent with my observations that low levels of MT1-MMP are representative of metastatic breast cancer.

Taken together, the observations in my study demonstrate that low levels of MT1-MMP expression are optimal for tumourigenicity and metastatic potential *in vivo*, and importantly, that abnormally high MT1-MMP overexpression correlated with a decrease, rather than enhancement of tumorigenic features **(see schematic representation fig. 32)**.

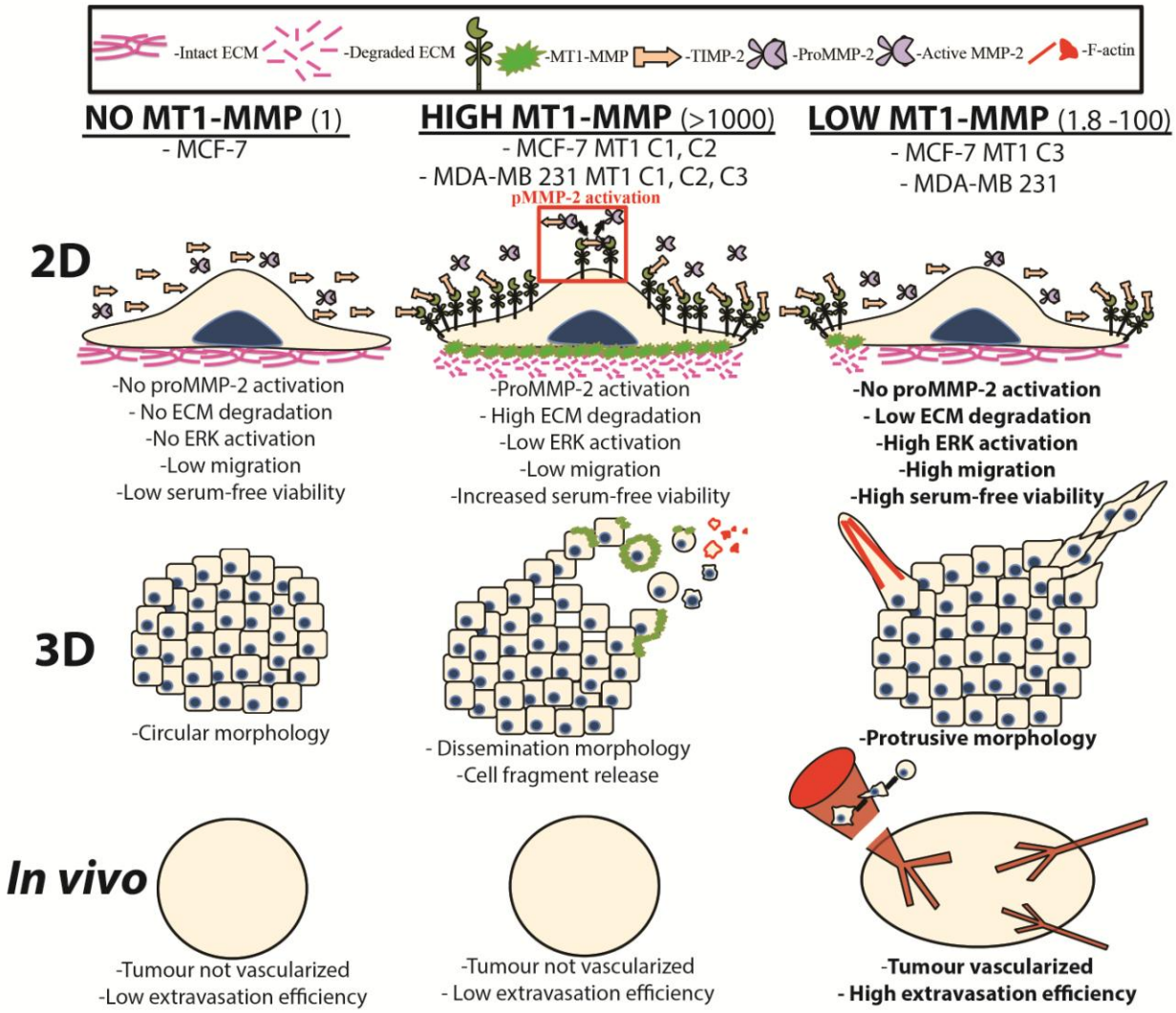
-Intact ECM
-Degraded ECM
-MT1-MMP
-TIMP-2
-ProMMP-2
-Active MMP-2
-F-actin
NO MT1-MMP (1)
- MCF-7
HIGH MT1-MMP (>1000)
- MCF-7 MT1 C1, C2
- MDA-MB 231 MT1 C1, C2, C3
LOW MT1-MMP (1.8 -100)
- MCF-7 MT1 C3
- MDA-MB 231
pMMP-2 activation
2D
-No proMMP-2 activation
- No ECM degradation
-No ERK activation
-Low migration
-Low serum-free viability
-ProMMP-2 activation
- High ECM degradation
-Low ERK activation
-Low migration
-Increased serum-free viability
-No proMMP-2 activation
- Low ECM degradation
-High ERK activation
-High migration
-High serum-free viability
3D
-Circular morphology
- Dissemination morphology
-Cell fragment release
-Protrusive morphology
In vivo
-Tumour not vascularized
-Low extravasation efficiency
-Tumour not vascularized
- Low extravasation efficiency
-Tumour vascularized
- High extravasation efficiency

Figure 32. Schematic overview of MT1-MMP expression levels and associated changes in substrate degradation and cell migration in 2D culture, phenotypes in 3D culture, and tumourigenesis *in vivo*.

Schematic representation of the findings of this study showing cell phenotypes across 2D and 3D culture platforms and *in vivo*. Legend describing molecular components in diagrams is shown at the top, and fold change relative to MCF-7 parental cells is in the brackets to the right of the bolded titles. MT1-MMP deficient breast cancer cells, such as MCF-7 cells, are incapable of proMMP-2 activation or ECM degradation, and show low migration and viability during serum-free incubation. These cells retain a circular morphology in 3D culture, and do not form vascularized tumours nor display high extravasation efficiency *in vivo*. Cells expressing high levels of MT1-MMP are capable of proMMP-2 activation and widespread ECM degradation, have increased survivability to serum-free stress, but do not demonstrate increased migration in 2D experiments. In 3D culture, these cells demonstrate a dissemination morphology and cell fragment release mediated by MT1-MMP. Despite MT1-MMP protein production and associated substrate degradation, these cells are unable to form vascularized tumours or increase their extravasation efficiency *in vivo*. Cells expressing low levels of MT1-MMP do not demonstrate proMMP-2 activation or widespread ECM degradation, but do show increased migratory potential, and high viability during serum-free incubation. These cells demonstrate a protrusive morphology in 3D culture, form vascularized tumours *in vivo*, and have significantly increased extravasation efficiency, which are representative features of a metastatic phenotype.

Chapter 4

4 Discussion

4.1 Low levels of MT1-MMP are optimal to mediate a metastatic phenotype across various experimental platforms

In this study, I utilized overexpression of functional MT1-MMP in MCF-7 and MDA-MB 231 breast cancer cells and demonstrated how high overexpression corresponds to proMMP-2 activation and ECM degradation, but inversely correlates to migration and viability in 2D culture, protrusive phenotype in 3D culture, and tumorigenic features *in vivo*. Instead I showed that high overexpression of MT1-MMP negatively affects cell viability, and causes an abnormal loss of colony structure and cell fragment release in 3D culture that translates to decreased tumorigenic potential *in vivo*. I also demonstrated using the human 21T cell lines mammary tumour progression series that breast cancer cells which mimic an invasive mammary carcinoma (IMC) are better represented by low, rather than high, levels of MT1-MMP protein. My data is at odds with the notion that high MT1-MMP expression is crucial for tumour progression, as numerous studies report that MT1-MMP overexpression is associated with enhanced migratory ability and tumourigenicity [40, 41, 49, 70, 95, 98], including increased cell migration [98], metastatic potential [40, 41], and tumor/metastasis volume [49]; although there is also evidence in agreement with my study which shows that high MT1-MMP overexpression is insufficient to increase metastasis of human cancer cells [124]. Here, using MCF-7 clonal cell lines stably expressing untagged MT1-MMP, I showed that migration, as shown by a scratch closure assay and by time-lapse microscopy of cells on fluorescent substrate, is dependent on levels of MT1-

MMP, with high levels decreasing migratory ability and low levels promoting it. I also demonstrated that MT1-MMP-mediated migration changes seen using transwell assays involve a substantial cell viability component, where high MT1-MMP overexpression negatively affects viability and low levels enhances it. This viability difference likely contributed to the magnitude of migration augmentation between transwell and other assays. Studies that show an increase in cancer cell migration as a result of MT1-MMP overexpression demonstrate migration enhancement ranging from 50 -500% [31, 49, 98], whereas others show a requirement of TIMP-2 for MT1-MMP mediated migration enhancement [99, 116]. These reports do not agree on a specific mechanism, except general ERK activation. In contrast, there are studies demonstrating that MT1-MMP overexpression does not increase migration of breast cancer cells [73], and also that MT1-MMP overexpression decreases ERK activation in cancer cells [96]. In the latter study, the authors demonstrated that MT1-MMP overexpression in various cancer cell lines, including MCF-7 cells, downregulates ERK activation and migration in response to FGF-2, which is consistent with my findings using cells that express high levels of MT1-MMP. Other studies have provided strong mechanistic evidence that MT1-MMP is involved in apoptosis protection [100] and viability enhancement via HIF1α stabilization [50, 104], which are in line with my observations that MT1-MMP enhances viability during serum-free incubation.

In this study I also discovered a novel inverse transcriptional relationship between MMP-2 and -9 mediated by the ERK pathway in MT1-MMP expressing cancer cells. Using the MCF-7 and MDA-MB231 MT1-MMP stable cell lines, and MDA-MB 231 and HS578t parental cells, I showed that ERK phosphorylation in MT1-MMP positive breast cancer cells correlates with an increase in MMP-9 levels and concomitant decrease in MMP-2 levels. An important aspect of this relationship is that regardless of the level of ERK phosphorylation, one of these gelatinases

is elevated in breast cancer cells that produce MT1-MMP. Myself and recently graduated MSc Caitlin Evered used MDA-MB 231 cells to show that ERK inhibition causes changes in *MMP-2* and -*9* transcription as shown by luciferase reporter assays, and also decreased the migration of these cells in 2D culture, and inhibited a protrusive phenotype in 3D culture, despite increased expression of MMP-2 [125]. These data are consistent with my study in that increased MMP expression, which is assumed to be accompanied by increased MMP activity, does not always correlate with the promotion of metastatic features.

Despite the mounting evidence demonstrating that MMPs have a direct role in basement membrane degradation *in vitro,* there is no evidence to date that shows this is the case *in vivo* during cancer progression, or during development where MMPs are thought to be critical for ECM remodeling and embryo patterning [19]. During *C. elegans* larval development, the uterine and vulval tissues are initially separated by epidermal basement membranes, which needs to be breached by a specialized cell, the anchor cell, for development to progress normally [126]. A gene necessary for anchor cell invasion is the *C. elegans* Fos transcription factor orthologue, *fos-1a*, for which mutations results in invadopodia that fail to breach the basement membrane [127]. One of the genes regulated by FOS-1A is *zmp-1,* a member of the MMP family in *C. elegans*, implying a role for MMPs in anchor cell invasion [128]. However, animals that contain a mutation in *zmp-1* do not have defects in anchor cell invasion, which shows that ZMP-1 may not be necessary for this particular process during *C. elegans* development [127, 128]. Follow-up work demonstrated that during anchor cell invasion, the basement membrane was moved aside by the invasive protrusion of the anchor cells, rather than being dissolved [129]. During mouse development, the maternal uterus spatially restricts the growing embryo, causing an increase in mechanical stress at the distal tip of the forming embryo, where basement membrane breaching

occurs [130]. These breaches allow early epiblast cells to migrate through the gaps in the basement membrane and form the distal visceral endoderm, a group of cells that are necessary to establish the anterior-posterior axis during development [130, 131]. During this basement membrane breaching process, it has been shown that MMPs are not expressed at the distal tip of the embryo and fluorescent protease reporters were not active, demonstrating that MMPs are not required for basement membrane disruption during mouse embryo development, and instead suggests a predominant role for mechanical force in basement membrane breaching during this process [131].

The *Drosophila* developmental model is also a useful platform to study MMP function as it contains only two MMPs, *Mmp1* and *Mmp2,* one which is secreted and the other is membrane bound, and that contain the canonical MMP structure but have no direct human MMP orthologues [132, 133]. During *Drosophila* development, cells of the outer squamous peripodial epithelium and stalk (PS) invade the underlying larval epidermis by breaking through the basement membrane [134]. This invasive process clears a path through the larval epidermis for disc eversion and formation of adult structures, such as the wing. Hypomorphic mutants in both *Mmp1* and *Mmp2* leads to maintenance of type IV collagen in the *Drosophila* embryo [135], indicating that MMPs promote basement membrane removal during eversion, thereby establishing a role for MMPs in basement membrane loss. However, whether the MMPs remove basement membrane through bulk dissolution, limited proteolysis, or other mechanisms, remains unclear. In disc eversion as in tumour development, where MMPS are thought to function as ECM remodelers, the interactions between cells and the matrix that lead to basement membrane removal have not yet been visualized, and recent observations suggest that the role of MMPs

during basement membrane traversion may be related to proteolysis of non-ECM components or induction of mechanical force, rather than solely the degradation of the ECM.

Consistent with aforementioned observations that basement membrane traversion may not require ECM degradation mediated by MMPs are the observations seen in my physiologically relevant *ex vivo* and *in vivo* experiments. In these experimental platforms I showed that MCF-7 cells expressing low levels of MT1-MMP (C3) demonstrated metastatic qualities in Matrigel 3D culture and *in vivo*, despite not demonstrating ability for proMMP-2 activation and widespread ECM degradation. C3 cells have increased protrusive morphology in 3D culture and this is contrasted with MCF-7 cells overexpressing high levels of MT1-MMP which show reduced protrusive ability and increased cell fragmentation. Similarly, C3 cells were tumorigenic and showed metastatic potential *in vivo*, unlike C1 and C2 cells, which is consistent with studies that knock down MT1-MMP expression and show inhibited tumourigenesis and metastasis. Importantly, I demonstrated that C3 cells have high extravasation efficiency *in vivo* after direct injection into the CAM vessels of day 13 chicken embryos when the vasculature has developed a basement membrane [136]. During extravasation, cells need to traverse the basement membrane, and my results show that C3 cells (low MT1-MMP levels and activity), rather than C1 or C2 cells (high MT1-MMP levels and activity), demonstrated increased ability to extravasate, which shows that ECM degradation is not correlated to basement membrane traversion and instead may be inhibitory if excessive. Furthermore, high magnification confocal analysis **(fig 30)** and real time imaging **(video 10)** showed that C3 cells formed cellular protrusions when extravasating *in vivo*, consistent with the protrusive morphology in 3D culture, and suggesting that MT1-MMP may instead generate invasive protrusions that breach the basement membrane via mechanical force.

Analysis of MT1-MMP protein levels in the 21T cell lines mammary tumour progression series demonstrated that breast cancer cells which represent early stage ADH and DCIS mammary tumours produce high levels of active MT1-MMP protein, whereas invasive 21MT-1 IMC cells produce undetectable levels of MT1-MMP, an observation that is consistent with my findings using MCF-7 C3 cells and my overall conclusion that low levels of MT1-MMP may better represent metastatic cancer. A similar study using the HMT-3522 epithelial cell series yielded results consistent with my analysis of MT1-MMP levels in 21T cells, as these authors analyzed microarray data to show that MMP-9, -13,-15 and -17, but not MT1-MMP, were functionally significant in the acquisition of invasiveness [137].

Interestingly, the observation that DCIS 21T cells produced high levels of active MT1-MMP in comparison to their IMC counterparts is similar to the 3D culture phenotype of the MDA-MB 231 cells overexpressing MT1-MMP. In this study, parental MDA-MB 231 cells, which are naturally invasive, readily form irregular networks in 3D culture in contrast to non-invasive cell lines that partially maintain polarity and form acini similar to the TDLU in the human breast (eg MCF-7 cells). It was surprising that overexpression of MT1-MMP in invasive MDA-MB 231 cells reverted their phenotype in 3D culture towards a DCIS-like morphology where the ability to form networks in matrigel 3D culture was restricted and a higher proportion of these cells retain acini-like colonies. The reversion of MDA-MB 231 cells to a DCIS-like phenotype in 3D culture as a result of MT1-MMP overexpression is consistent with the analysis of MT1-MMP protein levels in the 21T cell lines, whereby DCIS (21NT) cells produce more active MT1-MMP and predominantly form acini in 3D culture, and IMC (21MT-1) cells produce less MT1-MMP protein and display invasive 3D behavior [111], similar to MT1-MMP MDA-MB 231 cells and parental MDA-MB 231 cells, respectively.

4.2 Inhibited MT1-MMP correlates with increased cell migration and viability in 2D culture

A striking finding of my *in vitro* analysis regarding the relationship between MT1-MMP expression and migration was that the most migratory cells were the ones which had a low MT1-MMP:high TIMP-2 ratio. Of the MCF-7 MT1-MMP cell lines used, C3 and C3 SH 1 cells displayed low MT1-MMP levels (11 and 1.8 fold change vs parental MCF-7 cells, respectively), and their migration ability was greatly enhanced when the levels of TIMP-2 increased, especially C3 SH 1 cells. MDA-MB 231 MT1-MMP cell lines displayed the same trend whereby MT1-MMP overexpression with no change in TIMP-2 expression (data not shown) shifted the ratio in favor of excess MT1-MMP, leading to uncontrolled proMMP-2 activation and ECM degradation, and thereby causing a decrease in migratory potential and viability. Similarly, analysis of the natural migration potential of MCF-7, MDA-MB 231, and HS578t cells is consistent with this relationship to TIMP-2, as HS578t cells were the most migratory and displayed the highest level of TIMP-2 expression relative to MT1-MMP. Noteworthy in this analysis was also the observation that MDA-MB 231 cells displayed the highest ERK activation, but were not the most migratory. This was consistent with the comparison of MCF-7 C2 and C3 cells, whereby C2 cells showed the highest ERK activation but were less migratory than C3 cells, which displayed comparatively lower ERK activation even in the presence of high levels of TIMP-2.

Although TIMP-2 is a natural MMP inhibitor and as such has attracted therapeutic interest along with synthetic MMP inhibitors [87-89, 94, 138, 139], neither have shown value in clinical trials [93]. Instead, some have suggested that high TIMP-2 levels may promote tumourigenicity [37, 99, 140], which has been strengthened by the association of high TIMP-2

levels with poor prognosis in various human cancers, including breast [44, 45, 47, 141-143]. Although this association between an MMP inhibitor and poor cancer prognosis may be paradoxical, I describe here that while TIMP-2 regulation of MT1-MMP activity is complex, as exemplified by MDA-MB 231 and HS578t cells, high TIMP-2:low MT1-MMP ratios in these cells correlate with their migratory potential, and also with their low proMMP activation ability and lack of gelatin degradation. Despite the fact that MDA-MB 231 and HS578t cells naturally express MT1-MMP, MMP-2, and -9, the extracellular gelatinases are predominantly found in their pro-forms yet to be activated. As MT1-MMP activity is pivotal in gelatinase activation [85], this indicates that MT1-MMP present in these cells is inhibited, likely by TIMP-2. This is consistent with lack of gelatinase activity of C3 cells, and in stark contrast to C1 and C2 cells, suggesting that cells with non-physiologically high MT1-MMP levels but low TIMP-2 levels (which is not typical of cancers) exhibit excessive proteolysis which may be counterproductive to migration and cell viability. This is corroborated both with the rescued serum free viability and migration of C1 cells as a result of BB94 treatment, and with the role of TIMP-2 in mediating survivability under serum free conditions as shown by others [100]. Since MT1-MMP is a proteolytic enzyme that can cleave and alter the function of many ECM and non-ECM proteins crucial for proper cell behavior [22], it is logical that such a potent protease with wide substrate specificity would be under tight control by TIMP-2 to appropriately mediate cell behaviour.

4.3 Immunological detection of human MMPs is unreliable

Recently Maden and Bugge (2015) analyzed the last two decades of literature to examine if there was a consensus regarding the cellular source of MMPs (including MT1-MMP) in human cancers and whether they were predominantly stromal or cancer cell derived [78]. These authors

noted that publications were widely inconsistent in regards to the cellular source of MMPs, particularly when immunodetection was involved. Only when *in situ* hybridization was used was there a consensus seen that MMPs were likely stromal cell derived. The authors proposed reasons for these difficulties, one being that there is likely inherently low expression of MMPs in cancer cells compared to stromal cells making immunodetection technically challenging.

I believe that unreliable immunodetection reagents (discussed in [144]) is a major contributing reason as to why there is such inconsistency when assessing the abundance of MMPs in human cancers and their value as prognostic markers. In this study, I initially experienced difficulties assessing immunoblots for MT1-MMP, which could only be correctly interpreted after examining the immunological banding pattern for MT1-MMP expressing MCF-7 and MDAMB-231 cell lines, and probing with two different primary antibodies against human MT1-MMP **(fig 33)**. To strengthen the idea that improper immunodetection of MT1-MMP protein can lead to incorrect conclusions, I highlight my (lack of) immunodetection of MT1-MMP in MCF-7 breast cancer cells. I strongly believe, as supported by my data, and as suggested by others, that MCF-7 cells are MT1-MMP deficient [40, 99], particularly because it has been shown that the MT1-MMP promoter in these cells is hypermethylated and thus transcriptionally repressed [106]. Yet despite this observation, published studies claim to detect both pro- and active MT1-MMP protein via immunoblot in MCF-7 cells [41, 145], which could be due to incorrect identification of the cell line used for experimentation, or lack of stringency when conducting immunodetection. As can be seen from my immunoblot data, usage of a polyclonal antibody against MT1-MMP resulted in a non-specific signal that could easily be misinterpreted as pro- and active MT1-MMP in MCF-7 cells **(fig 33, AB6004)**. Furthermore, in

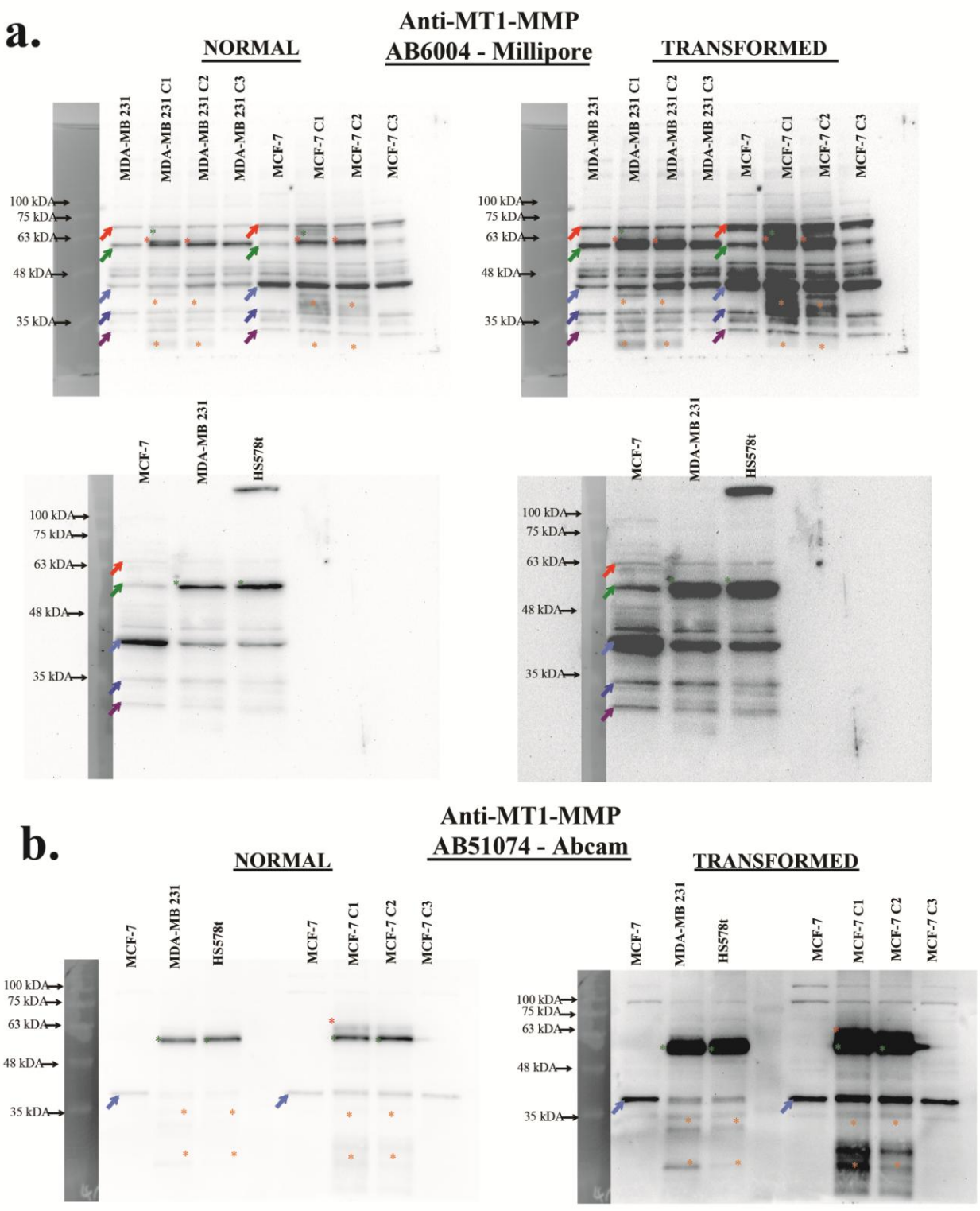
a.
Anti-MT1-MMP
AB6004 - Millipore
NORMAL
TRANSFORMED
MDA-MB 231
MDA-MB 231 C1
MDA-MB 231 C2
MDA-MB 231 C3
MCF-7
MCF-7 C1
MCF-7 C2
MCF-7 C3
100 kDA
75 kDA
63 kDA
48 kDA
35 kDA
MCF-7
MDA-MB 231
HS578t
b.
Anti-MT1-MMP
AB51074 - Abcam
NORMAL
TRANSFORMED
MCF-7
MDA-MB 231
HS578t
MCF-7
MCF-7 C1
MCF-7 C2
MCF-7 C3
100 kDA
75 kDA
63 kDA
48 kDA
35 kDA

Figure 33. Immunological detection of MT1-MMP protein can be confounding depending on antibody utilized.

(a) Immunoblot analysis of MCF-7 and MDA-MB 231 MT1-MMP cell lines (top), or MCF-7, MDA-MB 231 and HS578t breast cancer cell lines (bottom) using a polyclonal anti-MT1-MMP rabbit antibody (AB6004 – Millipore). **(b)** Immunoblot analysis of MCF-7, MDA-MB 231, and HS578t breast cancer cells, along with the MCF-7 MT1-MMP cell lines, using a monoclonal rabbit antibody (AB51075- Abcam). These blots were ran for 6 hours at 140 volts on a 15% acrylamide gel to ensure optimal band separation. On the left is a normal exposure of each blot and on the left is transformed version to clearly demonstrate banding pattern. Arrows indicate non-specific signal, whereas asterisks indicate specific signal pertaining to MT1-MMP isoforms (green – pro- form, red- active form, orange – degradation forms). Note the substantial amount of non-specific signal obtained when using AB6004 compared to AB51074, despite both antibodies being able to specifically detect multiple isoforms of MT1-MMP. Of particular interest are the red and green non-specific bands obtained using AB6004, which could be misinterpreted as pro- and active forms of MT1-MMP, respectively (see banding pattern for MT1-MMP deficient MCF-7 cells).

the study done by Köhrmann et al. (2009), although the authors reported MT1-MMP protein in MCF-7 cells, they were not able to detect MT1-MMP protein from tumour samples via immunoblot, despite showing increased MT1-MMP mRNA in these samples compared to normal breast tissue [41]. However, these authors were able to detect MT1-MMP protein using histology in tissue sections from tumour samples and not from normal tissues. Studies such as this that are internally inconsistent regarding MT1-MMP protein detection, and when containing clinical samples, can create confounding conclusions regarding the role of MMPs in cancer. This is in agreement with the observations of Madsen and Bugge regarding the discrepancies of the source of MMPs in human cancer, and the potential role of unreliable immunodetection when examining MMPs, including MT1-MMP, in different human cancer tissue.

Additionally, visualizing MT1-MMP protein localization at a cellular level using immunofluorescence may also lead to similar immunodetection problems. Lodillinsky et al. (2016) recently implicated the p63/MT1-MMP axis in the transition from ductal carcinoma *in situ* to metastatic breast cancer, reporting that MT1-MMP protein is present during BM invasion of MCF10DCIS.com xenografts [59]. However, with the knowledge that MT1-MMP should be localized to distinct specialized regions of the cell membrane to initiate invasion (invadopodia), I question such immunofluorescence data that show MT1-MMP protein is present throughout the cell membrane of every cell in the xenograft, regardless of whether it is in physical proximity to invade the BM.

4.4 Modest increase in MT1-MMP expression is physiologically relevant in human cancer

To assess the physiological relevance of observed levels of MT1-MMP expression in this study, I searched the literature for recently reported MT1-MMP mRNA levels in malignant human breast tissue compared to non-malignant tissue. The reported increase in MT1-MMP mRNA levels in malignant breast tissue compared to normal tissue ranged between ~1.7 to ~3.2 fold [48, 59, 64]. Similarly, a pioneering study used MDA-MB 231 variants that produced constitutively active scr kinase, which is known to be upregulated during cancer progression [66]. These MDA-MB 231 variants generated significantly more MT1-MMP containing invadopodia. Analysis of MT1-MMP mRNA changes between control and constitutively active src kinase cells demonstrated a ~1.8 fold change increase in MT1-MMP mRNA, which the authors describe as a mechanistically meaningful increase in MT1-MMP expression level. Therefore, the physiological relevance of extreme changes in expression levels, such as ~17,000 fold change in MT1-MMP mRNA seen in transient transfectants, or ~1500 fold change in stable cell lines, would be difficult to reconcile with primary human breast cancers which have a ~1.7 to 3.2 fold change in MT1-MMP mRNA compared to normal tissue. Additionally, in line with the idea that immunological reagents of MT1-MMP may be unreliable, if normal non-malignant tissues do not contain detectable levels of MT1-MMP [41, 70] and cancerous tissues demonstrate only a ~1.7 to 3.2 fold increase in MT1-MMP mRNA, then is it reasonable that a transcriptional increase of that magnitude would be difficult to immunodetect at the protein level.

Taken together, my study shows that a physiologically relevant increase in MT1-MMP levels during metastatic breast cancer is a best represented by a 1.8 to 11-fold change compared to normal tissue. Additionally, although abnormally high levels of MT1-MMP overexpression

may not reflect those seen in primary breast cancers, there is still mechanistic value in this approach, as utilized in this study to demonstrate the constancy of the TIMP-2 mediated activation of proMMP-2 by MT1-MMP. With this work I challenge the long-standing view that MMPs, particularly MT1-MMP, exert their role in cancer progression as proteases that predominantly degrade ECM components to allow cancer cell invasion, and instead suggest a subtle role for MT1-MMP in tumour progression as metastatic cancer appears to be better represented by low levels of TIMP-2-inhibited MT1-MMP protein.

Chapter 5

Conclusions

MT1-MMP is a multifunctional protease that can affect cell function via proteolytic and non-proteolytic mechanisms, and it was presumed that high levels of MT1-MMP mediate metastatic progression via ECM degradation. My findings that low levels of MT1-MMP are physiologically relevant and correlate with a metastatic phenotype suggest that very high levels MT1-MMP overexpression represents a non-relevant level of MT1-MMP expression during cancer progression. Excessive ECM degradation mediated by high levels of MT1-MMP is not permissive to cell migration and tumourigenesis, while low levels of MT1-MMP promote extravasation and vascularization *in vivo* via increased cell migration and viability.

Future work could focus on the examination of the binding partners of MT1-MMP, and their role in mediating the phenotypes of the cells utilized in this study. As well, an in-depth analysis of changes in cell signaling cascades in cell overexpressing MT1-MMP should be conducted to determine the mechanisms responsible for the phenotype of these cells. Additionally, MT1-MMP expression should be knocked down in the cell lines overexpressing high levels of MT1-MMP to determine if an invasive phenotype is rescued when the level of MT1-MMP expression is reduced.

Video Legends

Videos 1-4. Time-lapse analysis of ECM degradation and cell migration of MCF-7 MT1-MMP cells. Parental MCF-7 (Video 1), and MT1-MMP C1, C2, and C3 (Videos 2, 3, 4, respectively) cells stably expressing zsGreen (green) were seeded on Alexa594 gelatin coated coverslips (red) and incubated in a live imaging chamber at 37^0C, 5 % CO_2. Images were acquired using a Leica DM16000 B fluorescent microscope. Frames were taken every 10 minutes for 20 hours and compiled into time-lapse movies using ImageJ. Representative stills of each cell line at time 0 and 20 hours are shown in Figure 16a. Scale bars = 100 μm.

Videos 5. ADAPT workflow for automated analysis of cell migration. Shown is an example of the ADAPT plugin and associated trajectory visualization of the MCF-7 MT1-MMP C2 video (Video 3). Video 3 is shown as the overlay of zsGreen cells (green) and Alexa594 gelatin coating (red), as well as the individual channels (top). The zsGreen channel was used for the ADAPT analysis (bottom, left) to yield a trajectory visualization of individual cells from initial point of tracking (bottom, right). Three videos from independent experiments were analyzed in this manner and the trajectory visualization from each was used to quantify individual cell migration after 20 hours. Cell migration data is compiled in Figure 16b. Scale bars = 100 μm.

Videos 6-9. Time-lapse analysis of 3D culture dynamics of MCF-7 MT1-MMP cells. Parental MCF-7 (Video 6), and MT1-MMP C1, C2, and C3 (Videos 7, 8, 9, respectively) cells were embedded in 50% matrigel and incubated in a live imaging chamber at 37^0C, 5 % CO_2. Z-stacks (100 μm, 5 μm slices) were acquired using a Leica DM16000 B microscope. Frames were taken every 30 minutes for 72 hours and focal planes showing colony features with the greatest clarity

were compiled into time-lapse movies using ImageJ. Representative stills of each cell line at three different time points are shown in fig 19. Scale bars = 100 μm.

Video 10. Real-time intravital imaging of extravasated MCF-7 MT1-MMP C3 cells. MCF-7 MT1-MMP C3 cells stably expressing zsGreen (green) were injected intravenously into the CAM vasculature of day 13 chicken embryos and imaged 24 hours post-injection after labeling the vessels with lectin rhodamine (red). A movie in real-time was acquired using the resonant scanner of a Nikon A1R+ confocal microscope. The focus of the microscope was moved manually to show that a single C3 cells has extravasated from the CAM vasculature and shows a protrusion into the stroma (devoid of lectin-rhodamine signal). Scale bar = 100 μm

References

1. **American Cancer Society. *Global Cancer Facts & Figures* 3rd Edition.** *Atlanta: American Cancer Society* 2015.
2. **Statistics Canada. Leading Causes of Death in Canada, 2011.** *Ottawa: Statistics Canada* 2014.
3. **Canadian Cancer Society. Canadian Cancer Society's Advisory Committee on Cancer Statistics.** *Canadian Cancer Statistics 2015 Toronto, ON* 2015.
4. **Public Health Agency of Canada 2014. Economic Burden of Illness in Canada, 2005–2008.** *Ottawa Available at:* http://wwwphac-aspcgcca/ebic-femc/index-engphp 2014.
5. Weigelt B, Peterse JL, van 't Veer LJ: **Breast cancer metastasis: markers and models**. *Nature reviews Cancer* 2005, **5**(8):591-602.
6. Nguyen DX, Bos PD, Massague J: **Metastasis: from dissemination to organ-specific colonization**. *Nature reviews Cancer* 2009, **9**(4):274-284.
7. Valastyan S, Weinberg RA: **Tumor metastasis: molecular insights and evolving paradigms**. *Cell* 2011, **147**(2):275-292.
8. Chambers AF, Groom AC, MacDonald IC: **Dissemination and growth of cancer cells in metastatic sites**. *Nature reviews Cancer* 2002, **2**(8):563-572.
9. Chiang AC, Massague J: **Molecular basis of metastasis**. *The New England journal of medicine* 2008, **359**(26):2814-2823.
10. Christofori G: **New signals from the invasive front**. *Nature* 2006, **441**(7092):444-450.
11. Leong HS, Robertson AE, Stoletov K, Leith SJ, Chin CA, Chien AE, Hague MN, Ablack A, Carmine-Simmen K, McPherson VA *et al*: **Invadopodia are required for cancer cell extravasation and are a therapeutic target for metastasis**. *Cell reports* 2014, **8**(5):1558-1570.
12. Rowe RG, Weiss SJ: **Breaching the basement membrane: who, when and how?** *Trends in cell biology* 2008, **18**(11):560-574.
13. Hynes RO: **Integrins: bidirectional, allosteric signaling machines**. *Cell* 2002, **110**(6):673-687.
14. Berrier AL, Yamada KM: **Cell-matrix adhesion**. *Journal of cellular physiology* 2007, **213**(3):565-573.
15. Geiger B, Spatz JP, Bershadsky AD: **Environmental sensing through focal adhesions**. *Nature reviews Molecular cell biology* 2009, **10**(1):21-33.
16. Legate KR, Wickstrom SA, Fassler R: **Genetic and cell biological analysis of integrin outside-in signaling**. *Genes & development* 2009, **23**(4):397-418.
17. Discher DE, Mooney DJ, Zandstra PW: **Growth factors, matrices, and forces combine and control stem cells**. *Science* 2009, **324**(5935):1673-1677.
18. Hynes RO: **The extracellular matrix: not just pretty fibrils**. *Science* 2009, **326**(5957):1216-1219.
19. Kelley LC, Lohmer LL, Hagedorn EJ, Sherwood DR: **Traversing the basement membrane in vivo: a diversity of strategies**. *The Journal of cell biology* 2014, **204**(3):291-302.
20. Stocker W, Grams F, Baumann U, Reinemer P, Gomis-Ruth FX, McKay DB, Bode W: **The metzincins--topological and sequential relations between the astacins,**

adamalysins, serralysins, and matrixins (collagenases) define a superfamily of zinc-peptidases. *Protein science : a publication of the Protein Society* 1995, **4**(5):823-840.
21. Clark IM, Swingler TE, Sampieri CL, Edwards DR: **The regulation of matrix metalloproteinases and their inhibitors**. *Int J Biochem Cell Biol* 2008, **40**(6-7):1362-1378.
22. Kukreja M, Shiryaev SA, Cieplak P, Muranaka N, Routenberg DA, Chernov AV, Kumar S, Remacle AG, Smith JW, Kozlov IA *et al*: **High-Throughput Multiplexed Peptide-Centric Profiling Illustrates Both Substrate Cleavage Redundancy and Specificity in the MMP Family**. *Chemistry & biology* 2015, **22**(8):1122-1133.
23. Egeblad M, Werb Z: **New functions for the matrix metalloproteinases in cancer progression**. *Nature reviews Cancer* 2002, **2**(3):161-174.
24. Belkin AM, Akimov SS, Zaritskaya LS, Ratnikov BI, Deryugina EI, Strongin AY: **Matrix-dependent proteolysis of surface transglutaminase by membrane-type metalloproteinase regulates cancer cell adhesion and locomotion**. *The Journal of biological chemistry* 2001, **276**(21):18415-18422.
25. Ra HJ, Parks WC: **Control of matrix metalloproteinase catalytic activity**. *Matrix Biol* 2007, **26**(8):587-596.
26. Chakraborti S, Mandal M, Das S, Mandal A, Chakraborti T: **Regulation of matrix metalloproteinases: an overview**. *Mol Cell Biochem* 2003, **253**(1-2):269-285.
27. Nagase H: **Activation mechanisms of matrix metalloproteinases**. *Biological chemistry* 1997, **378**(3-4):151-160.
28. Illman SA, Keski-Oja J, Parks WC, Lohi J: **The mouse matrix metalloproteinase, epilysin (MMP-28), is alternatively spliced and processed by a furin-like proprotein convertase**. *The Biochemical journal* 2003, **375**(Pt 1):191-197.
29. Kang T, Nagase H, Pei D: **Activation of membrane-type matrix metalloproteinase 3 zymogen by the proprotein convertase furin in the trans-Golgi network**. *Cancer research* 2002, **62**(3):675-681.
30. Iyer RP, Patterson NL, Fields GB, Lindsey ML: **The history of matrix metalloproteinases: milestones, myths, and misperceptions**. *American journal of physiology Heart and circulatory physiology* 2012, **303**(8):H919-930.
31. Rozanov DV, Deryugina EI, Ratnikov BI, Monosov EZ, Marchenko GN, Quigley JP, Strongin AY: **Mutation analysis of membrane type-1 matrix metalloproteinase (MT1-MMP). The role of the cytoplasmic tail Cys(574), the active site Glu(240), and furin cleavage motifs in oligomerization, processing, and self-proteolysis of MT1-MMP expressed in breast carcinoma cells**. *The Journal of biological chemistry* 2001, **276**(28):25705-25714.
32. Gomez DE, Alonso DF, Yoshiji H, Thorgeirsson UP: **Tissue inhibitors of metalloproteinases: structure, regulation and biological functions**. *European journal of cell biology* 1997, **74**(2):111-122.
33. Lambert E, Dasse E, Haye B, Petitfrere E: **TIMPs as multifacial proteins**. *Crit Rev Oncol Hematol* 2004, **49**(3):187-198.
34. Greene J, Wang M, Liu YE, Raymond LA, Rosen C, Shi YE: **Molecular cloning and characterization of human tissue inhibitor of metalloproteinase 4**. *The Journal of biological chemistry* 1996, **271**(48):30375-30380.

35. Leco KJ, Apte SS, Taniguchi GT, Hawkes SP, Khokha R, Schultz GA, Edwards DR: **Murine tissue inhibitor of metalloproteinases-4 (Timp-4): cDNA isolation and expression in adult mouse tissues**. *FEBS letters* 1997, **401**(2-3):213-217.
36. Stetler-Stevenson WG: **Tissue inhibitors of metalloproteinases in cell signaling: metalloproteinase-independent biological activities**. *Sci Signal* 2008, **1**(27):re6.
37. Stetler-Stevenson WG: **The tumor microenvironment: regulation by MMP-independent effects of tissue inhibitor of metalloproteinases-2**. *Cancer metastasis reviews* 2008, **27**(1):57-66.
38. Hayakawa T, Yamashita K, Ohuchi E, Shinagawa A: **Cell growth-promoting activity of tissue inhibitor of metalloproteinases-2 (TIMP-2)**. *Journal of cell science* 1994, **107 (Pt 9)**:2373-2379.
39. Duffy MJ, Maguire TM, Hill A, McDermott E, O'Higgins N: **Metalloproteinases: role in breast carcinogenesis, invasion and metastasis**. *Breast Cancer Res* 2000, **2**(4):252-257.
40. Figueira RC, Gomes LR, Neto JS, Silva FC, Silva ID, Sogayar MC: **Correlation between MMPs and their inhibitors in breast cancer tumor tissue specimens and in cell lines with different metastatic potential**. *BMC Cancer* 2009, **9**:20.
41. Kohrmann A, Kammerer U, Kapp M, Dietl J, Anacker J: **Expression of matrix metalloproteinases (MMPs) in primary human breast cancer and breast cancer cell lines: New findings and review of the literature**. *BMC Cancer* 2009, **9**:188.
42. Nawrocki B, Polette M, Marchand V, Monteau M, Gillery P, Tournier JM, Birembaut P: **Expression of matrix metalloproteinases and their inhibitors in human bronchopulmonary carcinomas: quantificative and morphological analyses**. *International journal of cancer* 1997, **72**(4):556-564.
43. Kousidou OC, Roussidis AE, Theocharis AD, Karamanos NK: **Expression of MMPs and TIMPs genes in human breast cancer epithelial cells depends on cell culture conditions and is associated with their invasive potential**. *Anticancer research* 2004, **24**(6):4025-4030.
44. Ree AH, Florenes VA, Berg JP, Maelandsmo GM, Nesland JM, Fodstad O: **High levels of messenger RNAs for tissue inhibitors of metalloproteinases (TIMP-1 and TIMP-2) in primary breast carcinomas are associated with development of distant metastases**. *Clinical cancer research : an official journal of the American Association for Cancer Research* 1997, **3**(9):1623-1628.
45. Davidson B, Goldberg I, Gotlieb WH, Kopolovic J, Ben-Baruch G, Nesland JM, Berner A, Bryne M, Reich R: **High levels of MMP-2, MMP-9, MT1-MMP and TIMP-2 mRNA correlate with poor survival in ovarian carcinoma**. *Clinical & experimental metastasis* 1999, **17**(10):799-808.
46. Okada A, Bellocq JP, Rouyer N, Chenard MP, Rio MC, Chambon P, Basset P: **Membrane-type matrix metalloproteinase (MT-MMP) gene is expressed in stromal cells of human colon, breast, and head and neck carcinomas**. *Proceedings of the National Academy of Sciences of the United States of America* 1995, **92**(7):2730-2734.
47. Davidson B, Goldberg I, Kopolovic J, Lerner-Geva L, Gotlieb WH, Ben-Baruch G, Reich R: **MMP-2 and TIMP-2 expression correlates with poor prognosis in cervical carcinoma--a clinicopathologic study using immunohistochemistry and mRNA in situ hybridization**. *Gynecologic oncology* 1999, **73**(3):372-382.

48. Li Y, Cai G, Yuan S, Jun Y, Li N, Wang L, Chen F, Ling R, Yun J: **The overexpression membrane type 1 matrix metalloproteinase is associated with the progression and prognosis in breast cancer**. *American journal of translational research* 2015, **7**(1):120-127.
49. Zarrabi K, Dufour A, Li J, Kuscu C, Pulkoski-Gross A, Zhi J, Hu Y, Sampson NS, Zucker S, Cao J: **Inhibition of matrix metalloproteinase 14 (MMP-14)-mediated cancer cell migration**. *The Journal of biological chemistry* 2011, **286**(38):33167-33177.
50. Sakamoto T, Niiya D, Seiki M: **Targeting the Warburg effect that arises in tumor cells expressing membrane type-1 matrix metalloproteinase**. *The Journal of biological chemistry* 2011, **286**(16):14691-14704.
51. Hotary K, Li XY, Allen E, Stevens SL, Weiss SJ: **A cancer cell metalloprotease triad regulates the basement membrane transmigration program**. *Genes & development* 2006, **20**(19):2673-2686.
52. Lee H, Overall CM, McCulloch CA, Sodek J: **A critical role for the membrane-type 1 matrix metalloproteinase in collagen phagocytosis**. *Molecular biology of the cell* 2006, **17**(11):4812-4826.
53. Li XY, Ota I, Yana I, Sabeh F, Weiss SJ: **Molecular dissection of the structural machinery underlying the tissue-invasive activity of membrane type-1 matrix metalloproteinase**. *Molecular biology of the cell* 2008, **19**(8):3221-3233.
54. Perentes JY, Kirkpatrick ND, Nagano S, Smith EY, Shaver CM, Sgroi D, Garkavtsev I, Munn LL, Jain RK, Boucher Y: **Cancer cell-associated MT1-MMP promotes blood vessel invasion and distant metastasis in triple-negative mammary tumors**. *Cancer research* 2011, **71**(13):4527-4538.
55. Rozanov DV, Deryugina EI, Monosov EZ, Marchenko ND, Strongin AY: **Aberrant, persistent inclusion into lipid rafts limits the tumorigenic function of membrane type-1 matrix metalloproteinase in malignant cells**. *Experimental cell research* 2004, **293**(1):81-95.
56. Cao J, Chiarelli C, Richman O, Zarrabi K, Kozarekar P, Zucker S: **Membrane type 1 matrix metalloproteinase induces epithelial-to-mesenchymal transition in prostate cancer**. *The Journal of biological chemistry* 2008, **283**(10):6232-6240.
57. Golubkov VS, Chekanov AV, Savinov AY, Rozanov DV, Golubkova NV, Strongin AY: **Membrane type-1 matrix metalloproteinase confers aneuploidy and tumorigenicity on mammary epithelial cells**. *Cancer research* 2006, **66**(21):10460-10465.
58. Hotary KB, Allen ED, Brooks PC, Datta NS, Long MW, Weiss SJ: **Membrane type I matrix metalloproteinase usurps tumor growth control imposed by the three-dimensional extracellular matrix**. *Cell* 2003, **114**(1):33-45.
59. Lodillinsky C, Infante E, Guichard A, Chaligne R, Fuhrmann L, Cyrta J, Irondelle M, Lagoutte E, Vacher S, Bonsang-Kitzis H *et al*: **p63/MT1-MMP axis is required for in situ to invasive transition in basal-like breast cancer**. *Oncogene* 2016, **35**(3):344-357.
60. Riggins KS, Mernaugh G, Su Y, Quaranta V, Koshikawa N, Seiki M, Pozzi A, Zent R: **MT1-MMP-mediated basement membrane remodeling modulates renal development**. *Experimental cell research* 2010, **316**(17):2993-3005.
61. Sabeh F, Ota I, Holmbeck K, Birkedal-Hansen H, Soloway P, Balbin M, Lopez-Otin C, Shapiro S, Inada M, Krane S *et al*: **Tumor cell traffic through the extracellular matrix is controlled by the membrane-anchored collagenase MT1-MMP**. *The Journal of cell biology* 2004, **167**(4):769-781.

62. Szabova L, Chrysovergis K, Yamada SS, Holmbeck K: **MT1-MMP is required for efficient tumor dissemination in experimental metastatic disease**. *Oncogene* 2008, **27**(23):3274-3281.
63. Seals DF, Azucena EF, Jr., Pass I, Tesfay L, Gordon R, Woodrow M, Resau JH, Courtneidge SA: **The adaptor protein Tks5/Fish is required for podosome formation and function, and for the protease-driven invasion of cancer cells**. *Cancer cell* 2005, **7**(2):155-165.
64. Marchesin V, Castro-Castro A, Lodillinsky C, Castagnino A, Cyrta J, Bonsang-Kitzis H, Fuhrmann L, Irondelle M, Infante E, Montagnac G *et al*: **ARF6-JIP3/4 regulate endosomal tubules for MT1-MMP exocytosis in cancer invasion**. *The Journal of cell biology* 2015, **211**(2):339-358.
65. Uekita T, Itoh Y, Yana I, Ohno H, Seiki M: **Cytoplasmic tail-dependent internalization of membrane-type 1 matrix metalloproteinase is important for its invasion-promoting activity**. *The Journal of cell biology* 2001, **155**(7):1345-1356.
66. Artym VV, Zhang Y, Seillier-Moiseiwitsch F, Yamada KM, Mueller SC: **Dynamic interactions of cortactin and membrane type 1 matrix metalloproteinase at invadopodia: defining the stages of invadopodia formation and function**. *Cancer research* 2006, **66**(6):3034-3043.
67. Mantuano E, Inoue G, Li X, Takahashi K, Gaultier A, Gonias SL, Campana WM: **The hemopexin domain of matrix metalloproteinase-9 activates cell signaling and promotes migration of schwann cells by binding to low-density lipoprotein receptor-related protein**. *J Neurosci* 2008, **28**(45):11571-11582.
68. Sternlicht MD, Werb Z: **How matrix metalloproteinases regulate cell behavior**. *Annu Rev Cell Dev Biol* 2001, **17**:463-516.
69. Poincloux R, Lizarraga F, Chavrier P: **Matrix invasion by tumour cells: a focus on MT1-MMP trafficking to invadopodia**. *Journal of cell science* 2009, **122**(Pt 17):3015-3024.
70. Seiki M: **Membrane-type 1 matrix metalloproteinase: a key enzyme for tumor invasion**. *Cancer Lett* 2003, **194**(1):1-11.
71. Marchant DJ, Bellac CL, Moraes TJ, Wadsworth SJ, Dufour A, Butler GS, Bilawchuk LM, Hendry RG, Robertson AG, Cheung CT *et al*: **A new transcriptional role for matrix metalloproteinase-12 in antiviral immunity**. *Nature medicine* 2014, **20**(5):493-502.
72. Lehti K, Lohi J, Juntunen MM, Pei D, Keski-Oja J: **Oligomerization through hemopexin and cytoplasmic domains regulates the activity and turnover of membrane-type 1 matrix metalloproteinase**. *The Journal of biological chemistry* 2002, **277**(10):8440-8448.
73. Williams KC, Coppolino MG: **Phosphorylation of membrane type 1-matrix metalloproteinase (MT1-MMP) and its vesicle-associated membrane protein 7 (VAMP7)-dependent trafficking facilitate cell invasion and migration**. *The Journal of biological chemistry* 2011, **286**(50):43405-43416.
74. Stetler-Stevenson WG, Yu AE: **Proteases in invasion: matrix metalloproteinases**. *Seminars in cancer biology* 2001, **11**(2):143-152.
75. Hadler-Olsen E, Fadnes B, Sylte I, Uhlin-Hansen L, Winberg JO: **Regulation of matrix metalloproteinase activity in health and disease**. *The FEBS journal* 2011, **278**(1):28-45.

76. Kuo L, Chang HC, Leu TH, Maa MC, Hung WC: **Src oncogene activates MMP-2 expression via the ERK/Sp1 pathway**. *Journal of cellular physiology* 2006, **207**(3):729-734.
77. Burger KL, Learman BS, Boucherle AK, Sirintrapun SJ, Isom S, Diaz B, Courtneidge SA, Seals DF: **Src-dependent Tks5 phosphorylation regulates invadopodia-associated invasion in prostate cancer cells**. *The Prostate* 2014, **74**(2):134-148.
78. Madsen DH, Bugge TH: **The source of matrix-degrading enzymes in human cancer: Problems of research reproducibility and possible solutions**. *The Journal of cell biology* 2015, **209**(2):195-198.
79. Bourboulia D, Stetler-Stevenson WG: **Matrix metalloproteinases (MMPs) and tissue inhibitors of metalloproteinases (TIMPs): Positive and negative regulators in tumor cell adhesion**. *Seminars in cancer biology* 2010, **20**(3):161-168.
80. Hawkes SP, Li H, Taniguchi GT: **Zymography and reverse zymography for detecting MMPs and TIMPs**. *Methods in molecular biology* 2010, **622**:257-269.
81. Lindsey ML, Zamilpa R: **Temporal and spatial expression of matrix metalloproteinases and tissue inhibitors of metalloproteinases following myocardial infarction**. *Cardiovascular therapeutics* 2012, **30**(1):31-41.
82. Strongin AY, Collier I, Bannikov G, Marmer BL, Grant GA, Goldberg GI: **Mechanism of cell surface activation of 72-kDa type IV collagenase. Isolation of the activated form of the membrane metalloprotease**. *The Journal of biological chemistry* 1995, **270**(10):5331-5338.
83. Stetler-Stevenson WG, Seo DW: **TIMP-2: an endogenous inhibitor of angiogenesis**. *Trends in molecular medicine* 2005, **11**(3):97-103.
84. Hernandez-Barrantes S, Toth M, Bernardo MM, Yurkova M, Gervasi DC, Raz Y, Sang QA, Fridman R: **Binding of active (57 kDa) membrane type 1-matrix metalloproteinase (MT1-MMP) to tissue inhibitor of metalloproteinase (TIMP)-2 regulates MT1-MMP processing and pro-MMP-2 activation**. *The Journal of biological chemistry* 2000, **275**(16):12080-12089.
85. Itoh Y, Takamura A, Ito N, Maru Y, Sato H, Suenaga N, Aoki T, Seiki M: **Homophilic complex formation of MT1-MMP facilitates proMMP-2 activation on the cell surface and promotes tumor cell invasion**. *The EMBO journal* 2001, **20**(17):4782-4793.
86. Zucker S, Cao J, Chen WT: **Critical appraisal of the use of matrix metalloproteinase inhibitors in cancer treatment**. *Oncogene* 2000, **19**(56):6642-6650.
87. Bramhall SR, Hallissey MT, Whiting J, Scholefield J, Tierney G, Stuart RC, Hawkins RE, McCulloch P, Maughan T, Brown PD *et al*: **Marimastat as maintenance therapy for patients with advanced gastric cancer: a randomised trial**. *Br J Cancer* 2002, **86**(12):1864-1870.
88. Pavlaki M, Zucker S: **Matrix metalloproteinase inhibitors (MMPIs): the beginning of phase I or the termination of phase III clinical trials**. *Cancer metastasis reviews* 2003, **22**(2-3):177-203.
89. Coussens LM, Fingleton B, Matrisian LM: **Matrix metalloproteinase inhibitors and cancer: trials and tribulations**. *Science* 2002, **295**(5564):2387-2392.
90. Baker AH, Edwards DR, Murphy G: **Metalloproteinase inhibitors: biological actions and therapeutic opportunities**. *Journal of cell science* 2002, **115**(Pt 19):3719-3727.

91. Steeg PS, Anderson RL, Bar-Eli M, Chambers AF, Eccles SA, Hunter K, Itoh K, Kang Y, Matrisian LM, Sleeman JP *et al*: **An open letter to the FDA and other regulatory agencies: Preclinical drug development must consider the impact on metastasis**. *Clinical cancer research : an official journal of the American Association for Cancer Research* 2009, **15**:4529.
92. Overall CM, Lopez-Otin C: **Strategies for MMP inhibition in cancer: innovations for the post-trial era**. *Nature reviews Cancer* 2002, **2**(9):657-672.
93. Cathcart J, Pulkoski-Gross A, Cao J: **Targeting Matrix Metalloproteinases in Cancer: Bringing New Life to Old Ideas**. *Genes & Diseases* 2015, **2**(`1):26-34.
94. Chambers AF, Matrisian LM: **Changing views of the role of matrix metalloproteinases in metastasis**. *Journal of the National Cancer Institute* 1997, **89**(17):1260-1270.
95. Sounni NE, Noel A: **Membrane type-matrix metalloproteinases and tumor progression**. *Biochimie* 2005, **87**(3-4):329-342.
96. Tassone E, Valacca C, Mignatti P: **Membrane-Type 1 Matrix Metalloproteinase Downregulates Fibroblast Growth Factor-2 Binding to the Cell Surface and Intracellular Signaling**. *Journal of cellular physiology* 2015, **230**(2):366-377.
97. Gingras D, Bousquet-Gagnon N, Langlois S, Lachambre MP, Annabi B, Beliveau R: **Activation of the extracellular signal-regulated protein kinase (ERK) cascade by membrane-type-1 matrix metalloproteinase (MT1-MMP)**. *FEBS letters* 2001, **507**(2):231-236.
98. Mori H, Tomari T, Koshikawa N, Kajita M, Itoh Y, Sato H, Tojo H, Yana I, Seiki M: **CD44 directs membrane-type 1 matrix metalloproteinase to lamellipodia by associating with its hemopexin-like domain**. *The EMBO journal* 2002, **21**(15):3949-3959.
99. D'Alessio S, Ferrari G, Cinnante K, Scheerer W, Galloway AC, Roses DF, Rozanov DV, Remacle AG, Oh ES, Shiryaev SA *et al*: **Tissue inhibitor of metalloproteinases-2 binding to membrane-type 1 matrix metalloproteinase induces MAPK activation and cell growth by a non-proteolytic mechanism**. *The Journal of biological chemistry* 2008, **283**(1):87-99.
100. Valacca C, Tassone E, Mignatti P: **TIMP-2 Interaction with MT1-MMP Activates the AKT Pathway and Protects Tumor Cells from Apoptosis**. *PloS one* 2015, **10**(9):e0136797.
101. Warburg O: **On the origin of cancer cells**. *Science* 1956, **123**(3191):309-314.
102. Semenza GL: **HIF-1: upstream and downstream of cancer metabolism**. *Current opinion in genetics & development* 2010, **20**(1):51-56.
103. Vander Heiden MG, Cantley LC, Thompson CB: **Understanding the Warburg effect: the metabolic requirements of cell proliferation**. *Science* 2009, **324**(5930):1029-1033.
104. Sakamoto T, Seiki M: **A membrane protease regulates energy production in macrophages by activating hypoxia-inducible factor-1 via a non-proteolytic mechanism**. *The Journal of biological chemistry* 2010, **285**(39):29951-29964.
105. Shiryaev SA, Remacle AG, Golubkov VS, Ingvarsen S, Porse A, Behrendt N, Cieplak P, Strongin AY: **A monoclonal antibody interferes with TIMP-2 binding and incapacitates the MMP-2-activating function of multifunctional, pro-tumorigenic MMP-14/MT1-MMP**. *Oncogenesis* 2013, **2**:e80.

106. Chernov AV, Sounni NE, Remacle AG, Strongin AY: **Epigenetic control of the invasion-promoting MT1-MMP/MMP-2/TIMP-2 axis in cancer cells**. *The Journal of biological chemistry* 2009, **284**(19):12727-12734.
107. Cvetkovic D, Goertzen CG, Bhattacharya M: **Quantification of breast cancer cell invasiveness using a three-dimensional (3D) model**. *Journal of visualized experiments : JoVE* 2014(88).
108. Tran TA, Leong HS, Pavia-Jimenez A, Fedyshyn S, Yang J, Kucejova B, Sivanand S, Spence P, Xie XJ, Pena-Llopis S *et al*: **Fibroblast Growth Factor Receptor-Dependent and -Independent Paracrine Signaling by Sunitinib-Resistant Renal Cell Carcinoma**. *Molecular and cellular biology* 2016, **36**(13):1836-1855.
109. Kim Y, Williams KC, Gavin CT, Jardine E, Chambers AF, Leong HS: **Quantification of cancer cell extravasation in vivo**. *Nature protocols* 2016, **11**(5):937-948.
110. Walsh LA, Cepeda MA, Damjanovski S: **Analysis of the MMP-dependent and independent functions of tissue inhibitor of metalloproteinase-2 on the invasiveness of breast cancer cells**. *Journal of cell communication and signaling* 2012, **6**(2):87-95.
111. Souter LH, Andrews JD, Zhang G, Cook AC, Postenka CO, Al-Katib W, Leong HS, Rodenhiser DI, Chambers AF, Tuck AB: **Human 21T breast epithelial cell lines mimic breast cancer progression in vivo and in vitro and show stage-specific gene expression patterns**. *Laboratory investigation; a journal of technical methods and pathology* 2010, **90**(8):1247-1258.
112. Marshall J: **Transwell((R)) invasion assays**. *Methods in molecular biology* 2011, **769**:97-110.
113. Martin KH, Hayes KE, Walk EL, Ammer AG, Markwell SM, Weed SA: **Quantitative measurement of invadopodia-mediated extracellular matrix proteolysis in single and multicellular contexts**. *Journal of visualized experiments : JoVE* 2012(66):e4119.
114. Barry DJ, Durkin CH, Abella JV, Way M: **Open source software for quantification of cell migration, protrusions, and fluorescence intensities**. *The Journal of cell biology* 2015, **209**(1):163-180.
115. Tran TA, Leong HS, Pavia-Jimenez A, Fedyshyn S, Yang J, Kucejova B, Sivanand S, Spence P, Xie XJ, Pena-Llopis S *et al*: **FGFR-Dependent and -Independent Paracrine Signaling by Sunitinib-Resistant RCC**. *Molecular and cellular biology* 2016.
116. Sounni NE, Rozanov DV, Remacle AG, Golubkov VS, Noel A, Strongin AY: **Timp-2 binding with cellular MT1-MMP stimulates invasion-promoting MEK/ERK signaling in cancer cells**. *International journal of cancer* 2010, **126**(5):1067-1078.
117. Wingfield PT, Sax JK, Stahl SJ, Kaufman J, Palmer I, Chung V, Corcoran ML, Kleiner DE, Stetler-Stevenson WG: **Biophysical and functional characterization of full-length, recombinant human tissue inhibitor of metalloproteinases-2 (TIMP-2) produced in Escherichia coli. Comparison of wild type and amino-terminal alanine appended variant with implications for the mechanism of TIMP functions**. *The Journal of biological chemistry* 1999, **274**(30):21362-21368.
118. Worley JR, Thompkins PB, Lee MH, Hutton M, Soloway P, Edwards DR, Murphy G, Knauper V: **Sequence motifs of tissue inhibitor of metalloproteinases 2 (TIMP-2) determining progelatinase A (proMMP-2) binding and activation by membrane-type metalloproteinase 1 (MT1-MMP)**. *The Biochemical journal* 2003, **372**(Pt 3):799-809.

119. Maquoi E, Frankenne F, Noel A, Krell HW, Grams F, Foidart JM: **Type IV collagen induces matrix metalloproteinase 2 activation in HT1080 fibrosarcoma cells**. *Experimental cell research* 2000, **261**(2):348-359.
120. Inman JL, Bissell MJ: **Apical polarity in three-dimensional culture systems: where to now?** *Journal of biology* 2010, **9**(1):2.
121. Weigelt B, Bissell MJ: **Unraveling the microenvironmental influences on the normal mammary gland and breast cancer**. *Seminars in cancer biology* 2008, **18**(5):311-321.
122. Ribatti D: **The chick embryo chorioallantoic membrane as a model for tumor biology**. *Experimental cell research* 2014, **328**(2):314-324.
123. Band V, Zajchowski D, Swisshelm K, Trask D, Kulesa V, Cohen C, Connolly J, Sager R: **Tumor progression in four mammary epithelial cell lines derived from the same patient**. *Cancer research* 1990, **50**(22):7351-7357.
124. Yamamoto H, Noura S, Okami J, Uemura M, Takemasa I, Ikeda M, Ishii H, Sekimoto M, Matsuura N, Monden M *et al*: **Overexpression of MT1-MMP is insufficient to increase experimental liver metastasis of human colon cancer cells**. *International journal of molecular medicine* 2008, **22**(6):757-761.
125. Cepeda MA, Evered CL, Pelling JJ, Damjanovski S: **Inhibition of MT1-MMP proteolytic function and ERK1/2 signalling influences cell migration and invasion through changes in MMP-2 and MMP-9 levels**. *Journal of cell communication and signaling* 2017.
126. Sherwood DR, Sternberg PW: **Anchor cell invasion into the vulval epithelium in C. elegans**. *Developmental cell* 2003, **5**(1):21-31.
127. Sherwood DR, Butler JA, Kramer JM, Sternberg PW: **FOS-1 promotes basement-membrane removal during anchor-cell invasion in C. elegans**. *Cell* 2005, **121**(6):951-962.
128. Altincicek B, Fischer M, Fischer M, Luersen K, Boll M, Wenzel U, Vilcinskas A: **Role of matrix metalloproteinase ZMP-2 in pathogen resistance and development in Caenorhabditis elegans**. *Developmental and comparative immunology* 2010, **34**(11):1160-1169.
129. Hagedorn EJ, Ziel JW, Morrissey MA, Linden LM, Wang Z, Chi Q, Johnson SA, Sherwood DR: **The netrin receptor DCC focuses invadopodia-driven basement membrane transmigration in vivo**. *The Journal of cell biology* 2013, **201**(6):903-913.
130. Rossant J, Tam PP: **Blastocyst lineage formation, early embryonic asymmetries and axis patterning in the mouse**. *Development* 2009, **136**(5):701-713.
131. Hiramatsu R, Matsuoka T, Kimura-Yoshida C, Han SW, Mochida K, Adachi T, Takayama S, Matsuo I: **External mechanical cues trigger the establishment of the anterior-posterior axis in early mouse embryos**. *Developmental cell* 2013, **27**(2):131-144.
132. Page-McCaw A: **Remodeling the model organism: matrix metalloproteinase functions in invertebrates**. *Seminars in cell & developmental biology* 2008, **19**(1):14-23.
133. Page-McCaw A, Ewald AJ, Werb Z: **Matrix metalloproteinases and the regulation of tissue remodelling**. *Nature reviews Molecular cell biology* 2007, **8**(3):221-233.
134. Pastor-Pareja JC, Grawe F, Martin-Blanco E, Garcia-Bellido A: **Invasive cell behavior during Drosophila imaginal disc eversion is mediated by the JNK signaling cascade**. *Developmental cell* 2004, **7**(3):387-399.

135. Srivastava A, Pastor-Pareja JC, Igaki T, Pagliarini R, Xu T: **Basement membrane remodeling is essential for Drosophila disc eversion and tumor invasion**. *Proceedings of the National Academy of Sciences of the United States of America* 2007, **104**(8):2721-2726.
136. Yuan YJ, Xu K, Wu W, Luo Q, Yu JL: **Application of the chick embryo chorioallantoic membrane in neurosurgery disease**. *Int J Med Sci* 2014, **11**(12):1275-1281.
137. Rizki A, Weaver VM, Lee SY, Rozenberg GI, Chin K, Myers CA, Bascom JL, Mott JD, Semeiks JR, Grate LR *et al*: **A human breast cell model of preinvasive to invasive transition**. *Cancer research* 2008, **68**(5):1378-1387.
138. Albini A, Melchiori A, Santi L, Liotta LA, Brown PD, Stetler-Stevenson WG: **Tumor cell invasion inhibited by TIMP-2**. *Journal of the National Cancer Institute* 1991, **83**(11):775-779.
139. Alvarez OA, Carmichael DF, DeClerck YA: **Inhibition of collagenolytic activity and metastasis of tumor cells by a recombinant human tissue inhibitor of metalloproteinases**. *Journal of the National Cancer Institute* 1990, **82**(7):589-595.
140. Sounni NE, Janssen M, Foidart JM, Noel A: **Membrane type-1 matrix metalloproteinase and TIMP-2 in tumor angiogenesis**. *Matrix Biol* 2003, **22**(1):55-61.
141. Wood M, Fudge K, Mohler JL, Frost AR, Garcia F, Wang M, Stearns ME: **In situ hybridization studies of metalloproteinases 2 and 9 and TIMP-1 and TIMP-2 expression in human prostate cancer**. *Clinical & experimental metastasis* 1997, **15**(3):246-258.
142. Visscher DW, Hoyhtya M, Ottosen SK, Liang CM, Sarkar FH, Crissman JD, Fridman R: **Enhanced expression of tissue inhibitor of metalloproteinase-2 (TIMP-2) in the stroma of breast carcinomas correlates with tumor recurrence**. *International journal of cancer* 1994, **59**(3):339-344.
143. Remacle A, McCarthy K, Noel A, Maguire T, McDermott E, O'Higgins N, Foidart JM, Duffy MJ: **High levels of TIMP-2 correlate with adverse prognosis in breast cancer**. *International journal of cancer* 2000, **89**(2):118-121.
144. Bradbury A, Pluckthun A: **Reproducibility: Standardize antibodies used in research**. *Nature* 2015, **518**(7537):27-29.
145. Albrechtsen R, Kveiborg M, Stautz D, Vikesa J, Noer JB, Kotzsh A, Nielsen FC, Wewer UM, Frohlich C: **ADAM12 redistributes and activates MMP-14, resulting in gelatin degradation, reduced apoptosis and increased tumor growth**. *Journal of cell science* 2013, **126**(Pt 20):4707-4720.

Curriculum Vitae

Mario Cepeda

Education

2012-Current	**Doctorate in Biology,** Department of Biology, Western University, London, ON
2010-2012	**Master's of Science,** Department of Biology, Western University, London, ON
2006-2010	**B.Sc. Honors Specialization in Biology with Distinction,** Western University, London, ON

Awards and Scholarships

2013-2016	**NSERC Canada Graduate Scholarship-Doctorate,** Western University, London, ON ($17500/a year for three years)
2011-2012	**NSERC Canada Graduate Scholarship-Master's,** Western University, London, ON ($17500/a year for one year)
2011-2012	**Ontario Graduate Scholarship,** Western University, London, ON ($15000/a year for one year) *Declined
2010-2011	**Ontario Graduate Scholarship,** Western University, London, ON ($15000/a year for one year)
2010	**NSERC Undergraduate Student Research Award**, Western University, London, ON ($5625/May-August)
2009	**NSERC Undergraduate Student Research Award**, Western University, London, ON ($5625/May-August)
2008	**NSERC Undergraduate Student Research Award**, Western University, London, ON ($5625/May-August)
2006	**Western Scholarship of Excellence**, Western University, London, ON ($2000)

Research Experience

2015-Current **Part-time Research Technician,** Lawson Health Research Institute, London, ON

- Maintenance of the avian embryo facility at Dr. Hon Leong's lab

2010-Current **Graduate Research**, Department of Biology, Western University, London, ON

- M.Sc. Thesis: TIMP-2 decreases the invasive potential of MCF-7 and MDAMB-231 cells independent of MMP inhibition
- PhD Thesis: MT1-MMP Mediates the Migratory and Tumourigenic Potential of Breast Cancer Cells via Non-Proteolytic Mechanisms

2009-2010 **Undergraduate Research**, Department of Biology, Western University, London, ON

- Honours thesis: The effect of increased levels of tissue inhibitor of metalloproteinase-2 (TIMP-2) on the invasiveness of MCF-7 breast cancer cells

2008-2010 **NSERC Undergraduate Student Research Award program,** Department of Biology, Western University, London, ON

Contributions to Research

Peer Reviewed Publication

- **Cepeda M.A.**, Evered C.L., Pelling J.J., Damjanovski S. (2016) Inhibition of MT1-MMP proteolytic function and ERK1/2 signalling influences breast cancer cell migration and invasion through changes in MMP-2 and MMP-9 expression. Journal of Cell Communication and Signalling. DOI: 10.1007/s12079-016-0373-3.
- **Cepeda M.A**., Pelling J.J., Evered C.L., Leong H.S., Damjanovski S. (2016) The Cytoplasmic Domain of MT1-MMP is Dispensable for Migration Augmentation But Necessary to Mediate Viability of MCF-7 Breast Cancer Cells. Experimental cell research. DOI: 10.1016/j.yexcr.2016.11.019
- **Cepeda M.A**., Pelling J.J., Evered C.L., Williams K.C., Freedman Z., Stan I., Willson J.A., Leong H.S., Damjanovski S. (2016) Less is more: low expression of MT1-MMP is optimal to promote migration and tumourigenesis of breast cancer cells. Molecular cancer. DOI:10.1186/s12943-016-0547-x
- Willson, J.A., Nieuwesteeg, M.A., **Cepeda, M.A**., Damjanovski, S. (2015) Analysis of *Xenopus laevis* RECK and its relationship to other vertebrate RECK sequences. Journal of Scientific Research and Reports. 6(7): 504-513, 2015. DOI 10.9734/JSRR/2015/17044
- Nieuwesteeg, M.A., Willson, J.A., **Cepeda, M.A**., Damjanovski, S. (2014) Analysis of the effects of Tissue Inhibitor of Metalloproteinases-1, -2 and -3 N- and C-terminal domains on signalling markers during *X. laevis* development. All Res. J. Biol. 5(4):30-36. ISSN:2172-4784.
- Nieuwesteeg, M., Willson, J.A., **Cepeda, M.A.,** Fox, A.M., and Damjanovski, S. (2014) Functional Characterization of Tissue Inhibitor of Metalloproteinase-1 (TIMP-1) N- and C-Terminal Domains during Xenopus laevis Development. The Scientific World Journal. DOI:10.1155/2014/467907
- Fox, A.M., Nieuwesteeg, M., Willson, J.A., **Cepeda, M.A.,** and Damjanovski, S. (2013) Knockdown of Pex11B reveals its pivotal role in regulation peroxisomal genes, numbers and ROS levels in Xenopus laevis A6 cells. In vitro Cellular & Developmental Biology-Animal. DOI: 10.1007/s11626-013-9710-5
- Walsh, L.A., **Cepeda, M.A.** and Damjanovski, S. (2012). Analysis of MMP-dependent and independent functions of tissue inhibitor of metalloproteinase-2 on the invasiveness of breast cancer cells. J. Cell. Comm. Signal. DOI: 10.1007/s12079-011-0157-8

Invited Talks at Professional Conferences

- Breast Cancer Cells Producing Only Active MT-1 MMP Protein Have Increased Invasive Potential Via MAPK Activation. (2015). Collaborative Graduate Program in Developmental Biology 7th Annual Research Day. London. Ontario.

Poster Presentations at Professional Conferences

- Evered, C.E., **Cepeda, M.A.**, Pelling, J, Damjanovski, S. "Inhibiting MMP proteolytic activity and MAPK signalling causes changes in cell migration and invasion". Collaborative Graduate Program in Developmental Biology 8th Annual Research Day. London. Ontario. 2016. (Institutional)
- Pelling, J, **Cepeda, M.A.**, Evered, C.E., Damjanovski, S. "Alteration to the cytoplasmic domain of MT1-MMP increases MCF-7 cell invasion and migration". Collaborative Graduate Program in Developmental Biology 8th Annual Research Day. London. Ontario. 2016. (Institutional)
- **Cepeda, M.A.**, Pelling, J, Evered, C.E., Damjanovski, S. "Breast cancer cells producing only active MT1-MMP have increased invasive potential via MAPK activation." The 12th Annual Oncology Research & Education Day Oncology. London. Ontario. 2015. (Institutional)
- **Cepeda, M.A.**, Jessica Willson, Damjanovski, S. "Low Levels of MT1-MMP enhance the migration and proliferation of cells". Collaborative Graduate Program in Developmental Biology 7th Annual Research Day. London. Ontario. 2015. (Institutional)
- **Cepeda, M.A.**, Jessica Willson, Damjanovski, S. "MT-1 MMP protein levels affect how this multifunctional protease changes the behaviour of breast cancer cells". Society for Developmental Biology 73rd Annual Meeting Univ. of Washington, Seattle, WA. 2014 (International)
- Willson, J.A., **Cepeda, M.A.,** Damjanovski, S. 2014. "Developmental effects of knocking downRECK expression in early *Xenopus laevis* embryos". Society for Developmental Biology 73rd Annual Meeting Univ. of Washington, Seattle, WA. 2014 (International)
- **Cepeda, M.A.,** Nieuwesteeg, M., Willson, J.A., and Damjanovski, S. "TIMP-2 interacts with MT-1 MMP to modulate migration and invasion of MCF-7 cells independent of MMP inhibition". The international Society of Developmental Biologists, Cancun Mexico, 2013. (International)
- Nieuwesteeg, M., Willson, J.A., **Cepeda, M.A.,** and Damjanovski, S. "Analysis of the effects of TIMP-2 -2 and -3 and N- and C-terminal domain overexpression during early Xenopus laevis development using immunohistochemistry". The international Society of Developmental Biologists, Cancun Mexico, 2013. (International)
- Willson, J.A., Nieuwesteeg, M., **Cepeda, M.A.,** and Damjanovski, S. "Analysis of RECK expression during Xenopus laevis development and its colocalization with MT-1 MMP during neurulation". The international Society of Developmental Biologists, Cancun Mexico, 2013. (International)
- **Cepeda, M.A.,** Nieuwesteeg, M.A., Willson, J.A., and Damjanovski, S. "Tissue inhibitor of metalloproteinase-2 (TIMP-2) with a non-functional C-terminal domain decreases the

invasiveness of MCF-7 and MDAMB-231 breast cancer cells". The American Society for Cell Biology Annual Meeting, San Francisco, CA, 2012. (International).

- Willson, J.A., **Cepeda, M.A.,** Nieuwesteeg, M.A., and Damjanovski, S."Analysis of RECK expression in dorsalized and ventralized Xenopus laevis embryos". The American Society for Cell Biology Annual Meeting", San Francisco, CA, 2012. (International).
- Nieuwesteeg, M.A., Willson, J.A., **Cepeda, M.A.,** and Damjanovski, S. "Functional characterization of tissue inhibitor of metalloproteinase 1 (TIMP-1) N- and C- terminal domains during early Xenopus laevis development". The American Society for Cell Biology Annual Meeting, San Francisco, CA, 2012. (International).
- **Cepeda, M.A.** and Damjanovski, S. "Effects of increased levels of TIMP-2 and ALA+TIMP-2 in MCF-7 breast cancer cells". The American Society for Cell Biology 50th Annual Meeting. Philadelphia, PA, 2010. (International).

Teaching Experience

2010-present **Graduate Teaching Assistant,** Western University, London, ON
- Biology 2581b Genetics, Biology 3338a Developmental

2010-present **Mentor Honor Thesis Students,** Western University, London, ON
- Gregory Golenia, Jason Parnes, Kathleen Dickson, Jillian Watson, Nicole Edmonds, Sarah Jean Robinson, Nicole Van-Camp, Jacob Pelling, Caitlin Evered, Zoey Freedman, Ioana Stan, Carlie Muir.

2009-present **Exam Proctor,** Western University, London, ON

Community Involvement

2011-present Big Brother Big Sister of London and area
- Mentor little brother
- Spend 3-4 hours per week with little brother